The Characteristics of the CAT to CAD to Rapid Prototyping System

by

RUDOLF SCHENKER

Dissertation submitted in fulfillment of the requirements for the degree

Magister Technologiae: Engineering: Mechanical

in the

Department of Mechanical Engineering

FACULTY OF ENGINEERING

at the

TECHNIKON FREE STATE

March 2001

Supervisor: Mr D.J. de Beer (Technikon Free State)

Co-Supervisor: Dr W.B. Du Preez (C.S.I.R.)

Declaration of Independent Work

I, Rudolf Schenker, do hereby declare that this research project submitted to comply with the requirements of the degree MAGISTER TECHNOLOGIAE: ENGINEERING: MECHANICAL, is my own independent work and has not been submitted to any institution by me as part of any qualification in the past.

Signature of Student

16.03.01

Date

Acknowledgements

Dr A. Ackerman, B.Ch.D., M.Ch.D. (Pret), Prostodontist

Bernard Price Institute (WITS Paleontology)
Ms Marion Duncan
Mr Joseph Fink
(Dr Rubidge, Ph.D.)
Dr Mike Raath, Ph.D

C.S.I.R.
Dr W.B. du Preez, - Project Co- Supervisor
Dr S. Hart, Ph.D.
Dr I. Le Roux Strydom, Ph.D.
Mr. J. Scheepbouwer, MSc
Dr A.N. Kirkbride, PhD.
Mrs J. Leita
Mr F. Mosweu - Student
Ms P.S. Maswanganye - Student
Mrs B. Van Rooyen
Mr S. Yates, B.Sc. Chemistry
Mrs G. v.d. Merwe

Dr I.D. Dymond, Orthopaedic Surgeon
M.B.B.CH.(WITS), F.R.C.S. (Ed.), F.C.S. (S.A.)(ORTH.), M.MED. (ORTH. SURG.) WITS

Hydromed Hospital
Dr A.vanDyk, M.B.Ch.B. (Pret), M.Med.Rad.D. (UOVS)
Dr J.H. Lamprecht, M.B.Ch.B. (Pret), M.Med.Rad.D. (UOVS)
Dr D.J. Gouws M.B.Ch.B. (Pret), M.Med.Rad.D. (UOVS)
Mrs Sonia Myburgh and the radiology team.

General Electric CT/MRI Support
Mr Martin Bothma 082 568 5195 (Cell)
Mr Robert Beyer 082 566 2263 (Cell)

Intertech Systems
Mr Russel Oosterlaak
Mr Trevor Berry

Krugersdorp Private Hospital
Dr Diers and Partners
Dr Tobi Rossouw, the radiology team, Pam, Karen

Materialise NV, Belgium
Mr Bart Swaelens
Ms Lieve Boeykens

Matra Datavision
Mr Martin Venter
Mr John Kitchingman UK
Mr Steven Fletcher UK

Morningside Clinic
Drs Bloch, Luntz, Spiro, Rosenberg, Gouws, Schmaman, Miller, Jaffe, Dubowitz, Parert, Hurwitz, & Friedman.
The radiology team, Janice, Helen,

National Museum Bloemfontein
Mr James Brink -
Mr Leoyd Rossouw - Florisbad

Pretoria East Hospital
Dr Louise Weir and Partners,

S.A.A.F.
Sergeant Major Floris van der Walt

Silicon Graphics Computer Systems
Mr E. van Zyl

Siemens CT/MRI Support
Dr Peter Kingma
Mr Lothar Nuths

Tekor
Mr Jaco Steyn

TECHMED
Mr Martin Fox

Technikon Free State
Mr D.J. de Beer, M.DIP.TECH. Mech. Eng. - Project Supervisor

Prof. G.D. Jordaan D.Tech.
Prof. G. Prinsloo, Ph.D.

Transvaal Museum
Dr Francis Thackeray

Universitas Academic
Bio-Physics Department
Prof. Charles Herbst
Prof. Thys Lotter
Mrs Ann Sweetlove
Mr Geoffrey Gert
Mr Frikkie Beeslaar

University of Pretoria
Faculty of Dentistry
Department of Maxillo-, Cranio- and Facial Surgery
Prof. Kurt W Butow, Chief Specialist and Head of Surgery
Dr Werner B Koepp

University of the Witwatersrand (WITS)
Mr Alan Machet - Student
Mr Lyle Peters - Student

Abstract

Computer Aided Design (CAD), Rapid Prototyping (RP) and Computer Aided Tomography (CAT) technologies were researched. The project entails a unique combination of the abovementioned technologies, which had to be mastered by the author, on local and international terms.

Nine software packages were evaluated to determine the modus operandi, required input and final output results. Fifty Rapid Prototyping systems were investigated to determine the strong and weak areas of the various systems, which showed that prototype materials, machine cost and growing time play an essential role. Thirty Reverse Engineering systems were also researched. Six different RE methods were recorded with several commercial systems available. Nineteen case studies were completed by using several different Computer Aided Tomography (CAT) and Magnetic Resonance Imaging (MRI) centers. Each scanning centre has different apparatus and is discussed in detail in the various case studies.

The focus of this project is the data transfer of two dimensional CAT scanning data to three-dimensional prototypes by using Reverse Engineering (RE) and Rapid Prototyping (RP). It is therefore of cardinal importance that one is familiar and understands the various fields of interest namely Reverse Engineering, Computer Aided Tomography and Rapid Prototyping. Each of these fields will be discussed in detail, with the latest developments in these fields covered as well. Case studies and research performed in the medical field should gain the medical industry's confidence. Constant marketing and publications will ensure that the technology is applied and transferred to the industry. Commercialisation of the technology is of utmost importance.

Uittreksel

Navorsing is gedoen in Rekenaar Gesteunde Ontwerp (RGO), Snel Prototipe Vervaardiging (SPV) en Rekenaar Tomografie (RT). Die projek behels die unike kombinasie van bogenoemde tegnologieë. Dit is dus van belang om b.g. tegnologieë te bemeester op lokale vlak sowel as in die intenasionale arena.

Nege sagteware pakkette is ondersoek om te bepaal hoe dit werk, wat die insette behels en watter uitsette dit kan oplewer. Vyftig Snel Prototipe Vervaardiging (SPV) metodes is ondersoek om die sterk en swak punte van elke sisteem vas te stel. Materiaalkeuse, masjienkoste en groeityd het ook 'n belangrike rol gespeel. Ses Truwaartse Ingenieurswese (TI) metodes word gestaaf.

Negentien gevallestudies was voltooi deur van verskye Rekenaar Tomografie (RT) en Magnetiese Resonansie Afbeelding (MR) sentrums gebruik te maak. Elke sentrum het verskillende apparaat en word breedvoerig in die gevallestudies bespreek.

Die projek is op die omskakeling van twee-dimensionele RT data in drie-dimensionele prototipes gefokus. Dit is dus van kardinale belang om 'n oorkoepelende insig in die relevante velde naamlik Truwaartse Ingenieurswese (TI) en Snel Prototipe Vervaardiging (SPV) te hê. Elke tegnologie word afsonderlik beskryf. Daar word van die nuutse verwikkelinge melding gemaak.

Die mediese industrie se vertroue behoort met die gevallestudies en navorsing gewen te kan word. Konstante bemarking en publikasies sal verseker dat die tegnologie toegepas en aan die industrie oorgedra word. Kommersialisasie van die tegnologie is van kardinale belang.

Table of Contents:

1 INTRODUCTION 1

1.1 Basic Work Procedure: 3

2 STUDY MATERIALS AND RESEARCH METHODS USED 5

2.1 Applications 6

2.1.1 Medical Applications 6

2.1.2 Anthropological Applications 7

2.1.3 Industrial Applications 8

2.2 Local and International Studies 9

2.2.1 Local 9

2.2.1.1 Primate Fossil Vertebrae 10

2.2.2 International Research and Applications 11

2.2.2.1 Medical 11

2.2.2.2 *Thrinaxodon* Fossil at the University of Texas 11

2.2.2.3 Other Case Studies 15

2.3 Software Evaluation 17

2.3.1 Materialise 17

2.3.1.1 Mimics 18

2.3.1.2 CTM 18

2.3.1.3 Magics Viewer 19

2.3.2 Velocity TM V2.0 19

2.3.3 Surfacer - Imageware 21

2.3.4 Strim - Matra Datavision 21

2.3.5 Cosmos - VRML 22

2.3.6 Raindrop Geometry 22

2.3.7 Desk Artes ... 22

2.3.8 Solid View ... 23

2.3.9 MPEG Generators ... 23

2.4 Rapid Prototyping Technologies ... 24

2.4.1 Background ... 24

2.4.2 Fused Deposition Modelling ... 31

2.4.2.1 Costing Methods ... 33

2.4.2.2 Material Update ... 35

2.4.3 Stereo Lithography ... 37

2.4.3.1 Material Update ... 39

2.5 Reverse Engineering Technologies ... 40

2.5.1 Co-ordinate Measurement Machine method ... 43

2.5.2 Robot arm type method ... 43

2.5.2.1 FaroArm ... 43

2.5.2.2 Kreon Handscan - Versa Scan ... 44

2.5.3 Laser scanner methods ... 44

2.5.3.1 Digibotics - Digibot II ... 45

2.5.3.2 Laser Design Inc. ... 45

2.5.3.3 Sharnoa ... 46

2.5.3.4 Kreon 24- Versa Scan ... 47

2.5.4 Computer-aided Tomography ... 47

2.5.4.1 Scientific Measurement Systems (SMS) ... 47

2.5.4.2 Aaroflex Inc. ... 48

2.5.4.3 ARACOR ... 48

2.5.5 Destructive Methods: CGI - RE1000 ... 49

2.5.6 Optical methods ... 50

2.5.6.1 Steinbichler - Comet 50

2.5.6.2 Atos - Newport 51

2.5.7 Summary of the World's Reverse Engineering Systems 51

2.6 Computer-aided Tomography Technologies 52

2.6.1 History of CAT 53

2.6.1.1 Roentgen and the "Invisible Light" 53

2.6.1.2 Marie Curie's Research 53

2.6.1.3 The New Elements: Amazing but Dangerous 54

2.6.1.4 Francis Williams (1852 - 1936) 55

2.6.2 How X-rays are produced 55

2.6.3 Basic Principles of CAT 57

2.6.4 Magnetic Resonance Imaging (MRI) 60

2.6.5 Hounsfield Units 61

2.7 Industrial CAT Apparatus of the C.S.I.R 62

2.7.1 Data Collection Procedure 65

2.7.2 Data-processing Procedure 69

2.7.3 The Accuracy Testing Procedure 73

2.7.4 Finding the Optimum Conditions 74

2.8 Medical Apparatus 85

2.8.1 Krugersdorp Private Hospital 85

2.8.1.1 Data Collection Procedure 85

2.8.1.2 Data-processing Procedure 85

2.8.2 Hydromed Hospital 86

2.8.2.1 Data Collection Procedure 86

2.8.2.2 Data Processing Procedure 87

2.8.3 Morningside Clinic and Pretoria East Hospital 87

2.8.3.1 Data Collection Procedure 87

2.8.3.2 Data-processing Procedure 88

2.8.4 Medical Apparatus Summary: 88

2.8.5 Other Potential Medical Apparatus 89

3 ANTHROPOLOGICAL CASE STUDIES 90

3.1 Lystrosaurus Skull - Anthropological 90

3.1.1 Background 90

3.1.2 Images 92

3.1.3 Lystrosaurus Data Sheet: 93

3.2 Thrinaxodon - Anthropological 94

3.2.1 Background 94

3.2.2 Images 96

3.2.3 *Thrinaxodon* Data Sheet: 97

3.3 Cango Cave Buck - Anthropological 98

3.3.1 Background 98

3.3.2 Images 99

3.3.3 Cango Cave Buck Data Sheet: 100

3.4 Sea-horse - Anthropological 101

3.4.1 Background 101

3.4.2 Images 102

3.4.3 Sea-horse Data Sheet: 103

3.5 Meerkat Skull - Anthropological 104

3.5.1 Background 104

3.5.2 Images 105

3.5.3 Meerkat Skull Data Sheet: 106

3.6 Taung Child Skull - Anthropological 107

3.6.1 Background ... 107

3.6.2 Images ... 109

3.6.3 Taung Child Skull Data Sheet: ... 110

3.7 Discussion of Anthropological Case Studies ... 111

3.7.1 Advantages ... 111

3.7.1.1 Non-destructive Analysis ... 111

3.7.1.2 Geometric Complexity ... 112

3.7.1.3 The Digital Format ... 112

3.7.2 Process Limitations ... 113

3.7.2.1 Slice Interval ... 113

3.7.2.2 Data Storage and Processing ... 113

3.7.2.3 Storage Media ... 114

3.7.2.4 Material Properties ... 115

4 MEDICAL CASE STUDIES ... 116

4.1 Human Maxilla and Mandible - Medical ... 116

4.1.1 Background ... 117

4.1.2 Images ... 118

4.1.3 Maxilla and Mandible Data Sheet: ... 119

4.2 Human Pelvis - Medical ... 120

4.2.1 Background ... 121

4.2.2 Images ... 123

4.2.3 Pelvis Data Sheet: ... 124

4.3 Human Brain - Medical ... 125

5.3.1 Background ... 125

4.3.2 Images ... 126

4.3.3 Brain Data Sheet: ... 127

4.4 Maxilla Cranio Facial – Medical 128
4.4.1 Background 128
4.4.2 Images 130
4.4.3 Maxilla Cranio Facial Data Sheet: 132
4.5 Discussion of Medical Case Studies 133
4.5.1 Advantages 133
4.5.1.1 Pre-operative Planning 133
4.5.1.2 Virtual Reality Interface 134
4.5.2 Process Limitations 135
4.5.2.1 Cost and Delivery 135
4.5.2.2 Dimensional Verification 135
5 INDUSTRIAL CASE STUDIES 137
5.1 Internal Combustion Engine Piston - Industrial 137
5.1.1 Background 137
5.1.2 I.C.E. Piston Data Sheet: 140
5.2 Motor Car Door Mirror Rubber Seal - Industrial 141
5.2.1 Background 141
5.2.2 Images 142
5.2.3 Rubber Seal Data Sheet: 143
5.3 Gearbox Housing - Industrial 144
5.3.1 Background 144
5.3.2 Images 145
5.3.3 Gearbox Housing Data Sheet: 146
5.4 Aluminium Foam - Industrial 147
5.4.1 Background 147
5.4.2 Images 149

5.4.3 Aluminium Foam Data Sheet: 150
5.5 Oxygen Face Mask - Industrial 151
5.5.1 Background 151
5.5.2 Images 152
5.5.3 Oxygen Face Mask Data Sheet: 153
5.6 Discussion of Industrial Case Studies 154
5.6.1 Advantages 154
5.6.1.1 Geometric Complexity 154
5.6.2 Process Limitations 155
5.6.2.1 RE Process Selection 155
5.6.2.2 Material Properties 156
5.6.2.3 Software & Hardware 157
5.6.2.4 CAT-scanning Settings 158
6 BIOLOGICAL CASE STUDIES 159
6.1 Avocados - Industrial/Biological 159
6.1.1 Background 159
6.1.2 Conclusion 160
6.1.3 Images 161
6.1.4 Avocado Data Sheet: 162
7 FUTURE APPLICATIONS AND RECOMMENDATIONS 163
7.1 Technology Transfer to Industry 163
7.2 Commercialisation 164
8 REFERENCES 165

List of Figures

Figure 2.1 Combined Bone & Fibre 16

Figure 2.2 Water Bottle 16

Figure 2.3 Multiple Pelvic Bones 16

Figure 2.4 Jaw Bone 16

Figure 2.5 Soft Tissue 16

Figure 2.6 Multiple Wrist Bones 16

Figure 2.7 Development vs. Profit costs 25

Figure 2.8 The Product Development Shortcoming 26

Figure 2.9 Software Segments 28

Figure 2.10 The Fused Deposition Modelling Process 32

Figure 2.11 Costing Methods 34

Figure 2.12 The SLA process 38

Figure 2.13 The CAT scanning equipment 62

Figure 2.14 Explanation of fan angle 63

Figure 2.15 CAT image of a fossil 70

Figure 2.16 An X-Ray image of STS 2426, the antelope vertebra 75

Figure 2.17 A CAT scan showing circular rings 76

Figure 2.18 The image without rings using copper filters 79

Figure 2.19 The problem of saturating the detectors 81

Figure 2.20 Comparing the same image using different filters 83

Figure 2.21 Confirmation of final parameters 84

Figure 3.1 The Lystrosaurus. 92

Figure 3.2 The Lystrosaurus encapsulated in rock. 92

Figure 3.3 2D CAT-scanned slice No. 138 92

Figure 3.4 3D rendering of the top twenty slices 92

Figure 3.5 3D rendering of the skull, top-righthand view of skull. 92

Figure 3.6 3D rendering of the skull, top-lefthand view of skull. 92

Figure 3.7 The Thrinaxodon Fossil (grey) and ABS Plastic Prototype (red) 96

Figure 3.8 An artistic impression of the Thrinaxodon 96

Figure 3.9 3D Reconstruction-1mm thick slices 99

Figure 3.10 3D Reconstruction-3mm thick slices 99

Figure 3.11 Frontal left hand view of the 3D reconstructed Sea-horse. 102

Figure 3.12 Left hand view of the 3D reconstructed Sea-horse. 102

Figure 3.13 Bottom view of the 3D reconstructed Sea-horse. 102

Figure 3.14 FDM Prototype of the Sea-horse 102

Figure 3.15 Meerkat Skull mounted onto the Aluminium fixture. 105

Figure 3.16 Representation of the Australopithecus Africanus 109

Figure 3.17 3D Image of the Taung Child fossil's skull 109

Figure 3.18 The three parts of the Taung Child fossil, side view. 109

Figure 3.19 CAT-scanned 3D reconstructed image, frontal top view. 109

Figure 3.20 3D image of the complete reconstructed skull, frontal side view. 109

Figure 3.21 Another representation of the reconstructed skull, frontal top view 109

Figure 4.1 The Human Maxilla and Mandible. 118

Figure 4.2 The Human Mandible, front view 118

Figure 4.3 The Human Mandible, side view. 118

Figure 4.4 The patient's reconstructed Maxilla 118

Figure 4.5 The patient's reconstructed Mandible 118

Figure 4.6 FDM Prototypes 118

Figure 4.7 The Human Pelvis and Femur. 123

Figure 4.8 The Human Pelvis. 123

Figure 4.9 3D reconstruction of the patient's Pelvis. 123

Figure 4.10 3D reconstruction of the patient's Pelvis. 123

Figure 4.11 FDM prototype of the patient's Pelvis with prosthesis fitted. 123

Figure 4.12 FDM prototype of the patient's Pelvis with prosthesis fitted. 123

Figure 4.13 Human Brain artery network, top view. 126

Figure 4.14 Human Brain artery network, top right hand view. 126

Figure 4.15 Human Brain artery network, frontal left hand view. 126

Figure 4.16 Human Brain artery network, frontal view. 126

Figure 4.17 2D CAT scan slice at the 1100 position. 130

Figure 4.18 2D CAT scan slice at the 1080 position. 130

Figure 4.19 SLS skull prototype in GF nylon. 130

Figure 4.20 Bronze casting of the skull. 130

Figure 4.21 FDM skull prototype in ICW06 wax. 131

Figure 4.22 Surgical Reconstructed SLS prototype. 131

Figure 4.23 3D Image of skull, combines soft and hard tissue. 131

Figure 4.24 3D Image of skull, bone structure only. 131

Figure 4.25 Skull sections already cut and removed. 131

Figure 4.26 The metal brace fitted. 131

Figure 5.1 Motorcar door window rubber seal, rear view. 142

Figure 5.2 Motorcar door window rubber seal, frontal-right-hand view. 142

Figure 5.3 Motorcar door window rubber seal, frontal-left-hand view. 142

Figure 5.4 Motorcar door window rubber seal, frontal-top view. 142

Figure 5.5 Gearbox housing, bottom view. 145

Figure 5.6 Gearbox housing, elevated frontal view. 145

Figure 5.7 Gearbox housing, elevated rear view. 145

Figure 5.8 Aluminium foam suspended in a tube. 149

Figure 5.9 2D CAT-scanned image of Aluminium foam. 149

Figure 5.10 Image of the cubical Aluminium foam. 149

Figure 5.11 Image of the cubical Aluminium foam. 149

Figure 5.12 Cross sections of the mask. 152

Figure 5.13 CAT-scanned 3D reconstruction. 152

Figure 5.14 2D CAT-scanned Slice 119 of the face mask (yellow section).. 152

Figure 5.15 2D CAT-scanned Slice 89 of the face mask (yellow section).. 152

Figure 5.16 Face mask undercut section.. 152

Figure 6.1 Isometric view of several avocados' water-rich areas. 161

Figure 6.2 Front view of several avocados' water-rich areas. 161

List of Tables

Table 1 Project Flow Chart: 2

Table 1.1 Basic Works Procedure 4

Table 2.1 Significant RP events 27

Table 2.2 Summary of the World's Rapid Prototyping Systems 29

Table 2.3 Elastomer Material Properties 36

Table 2.4 Summary of the World's Reverse Engineering Systems 51

Table 2.5 Hounsfield Units of Materials 61

Table 2.6 Parameter Variation, Power 77

Table 2.7 Parameter Variation, SOD and SID 78

Table 2.8 Parameter Variation, Filter Thickness 79

Table 2.9 Parameter Variation, Filter Thickness at New SOD and SID 80

Table 2.10 Parameter Variation, Integration Time 82

Table 2.11 Summary of the Medical CAT Scanners used in this study 88

Table 2.12 Summary of the Medical Apparatus 89

Table 6.1 Avocado Mass & Volumetric Data 161

List of Acronyms:

2D - Two Dimensional, usually in x and y axis

3D - Three Dimensional, usually x, y and z axis

ABS - Acrylonitrile-Butadyne-Styrene

ASCII - American Standard Code for Information Interchange

AVI - Animated Video Image, Microsoft Media

CAD - Computer Aided Design

CAE - Computer Aided Engineering

CAM - Computer Aided Machining

CAT - Computer Aided Tomography

CCD - Charged Coupled Diode

CD - Compact Disk

CMM - Co-ordinate Measurement Machine

CNC - Computerised Numeric Control

CT - Computer Tomography

Cu - Copper

DAT - Digital Audio Tape

DR - Digital Radiograph

DXF - Data Exchange File

EM - Electro Magnetic

FDM - Fused Deposition Control

FEM - Finite Element Modeling

FOR - Field Of Region

FOV - Field Of View

List of Acronyms cont.

FTP - File Transfer Protocol

GE - General Electric

HP - Hewlett Packard

HTML - Hypertext Markup Language

ICE - Internal Combustion Engine

ICW - Investment Casting Wax

IGES - Initial Graphics Exchange Specification

LAN - Local Area Network

LASER - Light Amplification by Stimulated Emission of Radiation

LOM - Layer Object Manufacturing

MOD - Magnetic Optical Disk

MPEG - Moving Pictures Experts Group

MRI - Magnetic Resonance Imaging

Pb - Lead

PC - Personal Computer

RAM - Random Access Memory

RE - Reverse Engineering

RGB - Red, Green, Blue

ROI - Region Of Interest

ROM - Read Only Memory

RP - Rapid Prototyping

RTV - Room Temperature Vulcanizing

SCSI - Small Computer Systems Interface

SGI - Silicon Graphics Inc.

List of Acronyms cont.

SID - Source Image Distance

SLA - Stereo Lithography Apparatus

SLS - Selective Laser Sintering

SML - Stratasys Modeling Language

SOD - Source Object Distance

SQ - Square

SSL - Stratasys Slice Language

STL - Structured Triangular Language

VRML - Virtual Reality Modelling Language

1. INTRODUCTION

The aim of this project was to investigate the characteristics of a system to link three unique technologies, Computer Aided Tomography (CAT), Computer-aided Design (CAD) and Rapid Prototyping (RP). This technology can be considered as one of many Reverse Engineering (RE) methods to be practiced in the South African industry.

Local and international research were included and compared in this study in order to evaluate the feasibility and previous success achieved with the application of these technologies. The evaluation of various software packages related to this field of study also played a critical and integral role.

An in-depth literature study was performed that went beyond this project. Only two of the more than 50 rapid prototyping methods investigated are included in this thesis. This study can also be used to assist the South African market to become aware of the variety of available systems. Every system has a unique niche that could assist technologists in solving a specific problem more easily.

The various RE methods, of which more than 31 systems have been investigated, can be divided in two groups, namely contact and non-contact methods. The contact group consists of touch probe and destructive methods. The non-contact group consists of laser, CAT (X-ray), optical and ultrasonic methods.

A more in-depth study of specifically CAT (X-ray) methods was conducted, as very little work in this field has been performed in South Africa. Various systems and approaches were investigated in several case studies in order to become familiar with various systems, as well as to set up a small national infrastructure within which this technology can be practiced in future. Several prototypes were created to prove the success of the process by using two different Rapid Prototyping (RP) Systems. The application of CAT, CAD and RP - a unique combination - will solve many problems in a wide field in the industry. Table 1 shows the project process.

Table 1 Project Flow Chart:

Step 1 - Research		**Step 2**
More than 30 R.E. Methods & Systems. 1. Contact 2. Non-contact		Reverse Engineering Methodologies.
Step 3 - Research		**Step 4**
1. Basic Principles of CAT. 2. History of CAT. 3. Industrial X-ray applications		Computer Aided Tomography.
Step 5 - Research		**Step 6**
Various Local Systems. 1. C.S.I.R.. 2. Hydromed Hospital. 3. Morningside Clinic. 4. Krugersdorp Private Hospital. 5. Pretoria East Hospital		The Data Conversion Methods of Local CAT Systems.
Step 7 - Research		**Step 8**
More than 50 R.P. Systems Investigated.		Rapid Prototyping.
Step 9		**Step 10**
Physical Prototypes.		More than sixteen case studies in the following fields: 1. Medical related. 2. Industrial related. 3. Biological related 4. Anthropological related.

1.1 Basic Work Procedure:

The need to produce functional prototypes rapidly in various materials is constantly increasing [4]. To convert CAT and MRI to Rapid Prototyping is one of the requirements found in the industry. Various materials can already be used with different systems. Since 1985, Rapid Prototyping (RP) Systems have been developed with constant quality improvements, as well as a reduction in prototype growing times. The RP process normally starts with a three-dimensional solid or surface Computer-aided Design (CAD) model [28]. This model is then converted to a Stereolithography (STL) type file. This STL file is a triangulate surface wire mesh of the CAD model and the standard RP interface. The STL model is then sliced into horizontal layers, and these layers are parameterised. Some of the parameters used for Fused Deposition Modelling (FDM) are road widths, slice intervals or thickness fill types, start and end positions [31].

The CAT and MRI to Rapid Prototyping process starts at the scanning device. The Materialise Software is used to convert the scanned data to a 3D STL file [5]. The selected rapid prototyping software is subsequently used to process the STL file. The rapid prototyping machine uses the data to produce a physical model.

The following table describes the six step work procedure:

Table 1.1 Basic Work Procedure

1. CAT-SCANNING –DATA-CAPTURING 1.1. OUTPUT - 2D CT IMAGES 1.2. OUTPUT - 3D CT RECONSTRUCTION
2. CAT IMAGE CONVERSION 2.1. OUTPUT - 2D MIMICS IMAGES 2.2. OUTPUT - 2D BITMAP IMAGES
3. 3D IMAGING 3.1. OUTPUT - 3D IMAGE RECONSTRUCTION 3.2. OUTPUT - 2D BITMAP IMAGES
4. MODEL GENERATION 4.1. OUTPUT - 3D DATA IN IGES, STL, VRML FORMATS
5. RAPID PROTOTYPING 5.1. OUTPUT - 3D PROTOTYPES
6. CAD MODIFICATION 6.1. OUTPUT - VARIOUS CAD FORMATS

2 Study Materials and RESEARCH Methods used

Various methods and materials regarding the CAT to CAD to RP technology exist locally and internationally. Computer-aided design (CAD), rapid prototyping (RP) and computer aided tomography (CAT) technologies were researched. This project constitutes a unique combination of the above-mentioned technologies and had to be mastered by the author, on local and international terms. The combination of these technologies forms one of various reverse engineering systems available.

More than nine software packages were investigated to determine the modus operandi, required input and final output results. Approximately 50 rapid prototyping systems were investigated to determine the strong and weak areas of the various systems. Prototype materials play an essential role. Various reverse engineering systems were also researched. About thirty different RE methods were recorded with several commercial systems available. Computer Aided Tomography (CAT) and Magnetic Resonance Imaging (MRI) Centres assisted in completing more than sixteen case studies.

The focus of this project is the data transfer of two-dimensional CAT-scanning data to three-dimensional prototypes by using Reverse Engineering (RE) and Rapid Prototyping (RP). It is therefore of cardinal importance that one is familiar with and understands the various fields of interest, namely reverse engineering, computerised tomography and rapid prototyping. Each of these fields will be discussed in detail. The latest developments in these fields are covered, and international contact persons' details since 1995 are listed.

Case studies and research performed in the medical field will easily gain credibility in the industry. All that is required is proper publications and advertisements as part of the commercialisation strategy. Commercialisation is of cardinal importance in order to apply and transfer the technology in and to the industry.

2.1 Applications

The main areas in which this unique combination of technologies are used are medical-, industrial-, anthropological- and biological-related.

2.1.1 Medical Applications

Two-dimensional CAT scan images allow a surgeon to accurately measure bone structures. Rulers can be used to measure from life-size scanned images. A series of scanned images at different intersections along the axis of the body allows a physician to form a global picture of the patient's internal condition [6], [40].

The advantage of this technology is that the two-dimensional images can be converted into images of three-dimensional reconstruction. By means of the combination of RP, it also enables the surgeon to have a physical three-dimensional model of a bone structure. The fibre section can be added to the rapidly produced prototypes to view and plan an operation. The risk involved in any medical operation can be greatly reduced [7]. This technology can also be applied in reconstructive surgery. Existing bone structures can be used to model and replace damaged sections [36]. This technology can also be used to rapidly produce an artificial limb [8]. The application of this technology can also be of assistance in the case of bio-mechanical analysis applications [9] & [19].

Anatomical areas in which this technology has been successfully applied at international level are the following: [27]

- Maxillofacial reconstruction
- Knee Surgery
- Pelvic Fractures
- Hip dysplasia, aseptic necrosis and epiphysiolysis
- Spinal trauma
- Congenital and degenerative spinal disease
- Skull plasticities
- Craniosynostosis
- Skull and maxillo-facial tumours
- Orthodontic surgery
- Nose reconstruction
- Deformities of the distal radio-lunar joint
- Foot malformations
- Models of soft tissue structures, e.g. cardiovascular systems

2.1.2 Anthropological Applications

Rare, precious and fragile fossils are not available for public and educational purposes. These fossils are normally kept behind closed doors. Very often, only photos or sometimes very poor replicas of these fossils are available to the public and industry. Replicas cannot be made of the fragile fossils, as they may be damaged during the replication process.

The advantage of this technology is that the two-dimensional CAT-scanned images are converted to three-dimensional images. To view these 3D- models of rare fossils, one can also use a simple software package. It enables the student to have a physical three-dimensional model of a bone structure in his hand to look at. Multiple prototypes can be made and will be accessible to more people interested in the anthropological field. [21]

2.1.3 Industrial Applications

CAT scanning is becoming a very attractive method of reverse engineering. Non-destructive measurements of 6" thick super alloy parts can be performed with the aid of high-powered CAT scanners. Other companies also use this approach to reverse engineer parts on a bigger scale. [10]

This technology enables one to reverse engineer bigger parts. Underutilised or older CAT scanners can be used to scan industrial parts cost-effectively. Smaller parts can be scanned by means of high-resolution CAT scanners. The C.S.I.R. is constantly researching reverse engineering applications and methods. This is first-world technology and the impact of this process will be tremendous. This technology has a great potential market in South Africa as the medical CAT-scanning infrastructure already exists.

This technology will be used in collaboration with the researchers at the TECHNIKON FREE STATE. Bloemfontein has a leading medical school and facilities, and the TECHNIKON FREE STATE is a key role-player, interacting with the medical school and utilising these facilities.

2.2 Local and International Studies

2.2.1 Local

As part of a preliminary project, data from hospitals where radiologists were keen to assist in demonstrating this technology were firstly sampled. An immature baboon skull was CAT-scanned at the C.S.I.R.. A prototype was produced by using the Stratasys FDM RP Technology. The ABS plastic prototype was finished by hand. Finer CAT slices had to be taken to produce a more detailed final product.

The human skull, vertebrae and feet data sets were collected from the Krugersdorp Private Hospital. It was one of the first data sets collected to evaluate the conversion process. The CAT scan slice thickness was not ideal and caused the staircase surface effect, but the results were still acceptable.

2.2.1.1 Primate Fossil Vertebrae

This project dealt with the replication of the vertebral column of STS14. It is a fossil set aged at between 2.5 and 2.8 million years of the hominid species Australopithecus Africanis. The main objective of the project was to successfully replicate the spinal column by first CAT-scanning the fossil vertebra, converting the CAT-scanned images to CAD solid models, and then growing rapid prototypes of these models by using Stereolithograpy. Further objectives included the following: investigating the accuracy of the process, as well as an investigation into the many data conversion issues that surround this technique.

A thorough literature survey into all aspects of the work was conducted. Topics included traditional replication techniques, basic stereolithography and digital image processing. The procedure used for the CAT-scanning of fossils was given, as well as the data conversion procedures used.

Also included was a detailed account of the CAT- scanning parameter selection tests and a final set of the parameters that gave the best images. A full account of all observations made with respect to the problems encountered in CAT-scanning, data conversion, stereolithography growing, molding and casting processes followed. This account included problems found with the particular software used for this project. Conclusions were drawn up, commenting on the progress made with the realisation of the objectives. Recommendations were made based on the results and conclusions of the project. Similar applications for the technologies used in this project were also mentioned. Finally, a blueprint was provided, giving a set of standard parameters and suggestions for similar work to be done in fossil replication and other related areas. [18]

2.2.2 International Research and Applications

2.2.2.1 Medical

The Rapid Prototyping Association of the Society of Manufacturing Engineering (RPA/SME) was founded in 1993 to communicate the vision and direction of rapid prototyping technology users. They recently published a book with 34 case studies, mainly craniofacial, Maxillofacial, pelvic, and spinal type applications. [27]

2.2.2.2 *Thrinaxodon* Fossil at the University of Texas

Background

One of the UT research programmes is aimed at testing a wide range of analytical technologies for problems experienced in mineralogy and petrology tests performed during 1992. The other is directed at exploring various digital technologies useful for the study of skeletal tissue in modern and extinct vertebrates. [30]

One of the Texas Industrial Research and Development efforts is conducted in the field of computed X- ray tomographic (CT or CAT) scanning. CT scanning is a standard medical diagnostic tool that has been used for more than two decades to image the human skeleton and other dense tissues. For nearly a decade, medical scanners have been periodically applied to examine fossils. Considerable success was achieved during 1984 in the case of tests with human-sized (and somewhat larger) vertebrates. Scientific Measurement Systems (SMS) of Austin recently developed a CT scanner that can achieve two orders of magnitude, better resolution than what was previously possible with medical scanners, while also successfully imaging a much wider range of materials. This opened the door for the for imaging both modern and fossilised bone that lie within the smallest order of vertebrate size magnitudes.

This remarkable new technology forms a basis for the reanalysis of the fossil *Thrinaxodon*, an extinct relative of modern mammals, that played an important role in the understanding of the early history of mammals, as discovered during tests performed in 1993. [30]

Another form of technology central to this research is CD-ROM technology. A major goal of modern digital technologies in Earth Sciences has been to evaluate potential methods for distributing the data generated by these new tools. In the two decades that CT-scanning has been applied to skeletal tissues, only a tiny fraction of the expensive data generated has been archived or distributed for general use by the research and educational communities. Most of what has been distributed, was recorded on film instead of in its native digital format. Until now the visualisation of original digital CT imagery has required powerful, expensive computational facilities with large volumes of storage space. Typically, suitable equipment was found only on-site with the CT scanner itself, usually at a medical imaging centre. CT-scanning has to fulfil its revolutionising research potential. In the absence of a feasible method to disseminate and archive the large volumes of digital data produced by this technology, it served the purposes of only a small fraction of the interested scientist community. As the cost of compact discs dropped dramatically and computers capable of visualising CT-imagery and using CD-ROMs became widely affordable, CD-ROM technology became a practical method for publishing large volumes of digital data.

The ability of Scientific Measurement Systems to provide imagery in easily exportable file formats was another key component ensuring the success of this project. The entire spectrum of results obtained by means of CT analysis, a total of 767 separate CT images plus several thousand images that animate visual passage through the skull, was presented on this disc in formats designed to facilitate rapid inspection and comparison. This combination of technologies provides a tool of unprecedented power and information for anthropological studies. Other biologists interested in hard tissue and models can use this data to generate images that can be used for other scientific studies as well.

The collaboration of the University of Texas Press was a last key element in this project. The UT Press solved a host of publication issues relating to the copyright pertaining to digital media, reproduction permission for older literature than that which is included on the disc, and the distribution of the disc. Without their assistance, the publication of this unique data set and the accompanying research library on CD-ROM would not have been possible.

Thrinaxodon

Thrinaxodon was an ideal test of ultra-high resolution CT scanning utilised to image small fossils, because it was already comparatively well-known. For more than a century it has played a significant role in the understanding of the evolution of mammals from more primitive cynodonts, and the full range of techniques available to paleontologists has been applied to achieve it. *Thrinaxodon* has been studied in great detail from mechanically sectioned specimens, also from acid and mechanically prepared whole specimens that represent a range of ontogenetic stages. The study was particularly thorough. Based on serial sections of an entire specimen made at 200-micron intervals in the coronal (vertical) plane, it provided an exceptionally detailed control mechanism for evaluating the CT imagery of *Thrinaxodon* provided on this disc. [30]

An excellent adult specimen was kindly made available by the Museum of Paleontology and the University of California, Berkeley (UCMP 40466). The SMS scanner was able to image the specimen at 200-micron slice thickness, duplicating or exceeding the resolution of earlier studies using mechanical techniques according to work done.

The SMS scanner also provided substantially greater precision in the measurement and calibration of successive sections than was possible with the mechanical techniques.

Two groups of articles are included on this disc to assist readers in interpreting CT imagery and in understanding the anatomy and importance of *Thrinaxodon*. The first group describes some technological aspects of this disc. In "A Brief Introduction to Computed X-ray Tomography", William Carlson presents discussions on the fundamentals of X-ray CT imaging, what a CT image shows, and some complexities and limitations of CT imaging. A short overview of how this data was converted and transferred onto CD-ROM is presented below, as part of this Introduction to the Digital Atlas.

As an additional aid to readers in evaluating the capabilities of this technology, the study of *Thrinaxodon* is truly comprehensive and takes full advantage of the large storage volume of CD-ROM. A reference library of digital editions of the classic literature on the anatomy of *Thrinaxodon* is also included. The republished works include a classic monograph on "The Origin of Mammals Based on Cranial Morphology of the Therapsid Suborders", in which Thrinaxodon was among a number of fossils serially sectioned in one of the most extensive comparative studies ever to use mechanical sectioning techniques. Also included are a detailed study of *Thrinaxodon* based on serial sections and a study of a growth series of *Thrinaxodon* that includes the specimen imaged on this disc. [30]

2.2.2.3 Other Case Studies

Other case studies performed by Materialise and Velocity software distributors show the benefits that can be obtained by applying these technologies. Note that mainly 3D-reconstructed images are displayed here.

Fig. 2.1 shows the combination of bone and fibre sections. This is extremely useful to surgeons who wish to reference the bone section with the fibre in order to plan the operation and position of the first incision.[35]

Fig. 2.2 displays a plastic water bottle that was reverse engineered. The data was captured and the neck geometry was used in a new bottle design. [3]

Fig. 2.3, 2.4 and 2.6 show that multiple bones can be combined during a study. One or several of these bones can then be separated for further studies. [3]

Fig. 2.5 shows that CAT data, as well as MRI data, can be used. Several sections of a human brain were combined during this study. The outer part of the brain was made transparent with the aid of digital imaging techniques, in order to view the central section of the brain. Reference to the outer section of the brain was maintained for pre-operational planning procedures. [3]

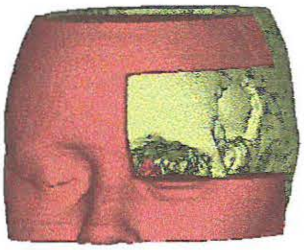

Figure 2.1 Combined Bone & Fibre [35]

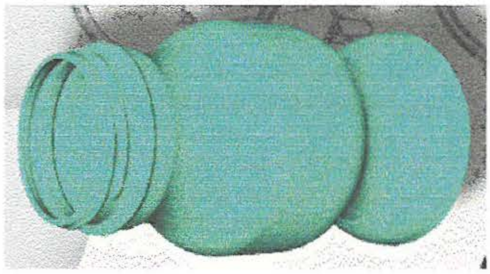

Figure 2.2 Water Bottle[3]

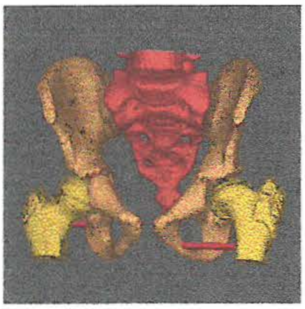

Figure 2.3 Multiple Pelvic Bones [3]

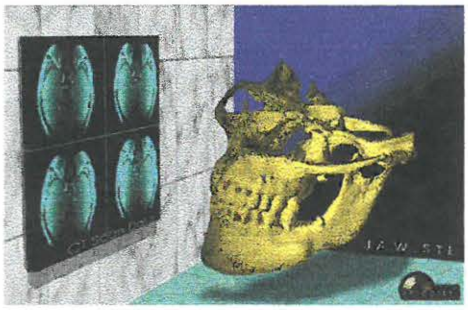

Figure 2.4 Jaw Bone [3]

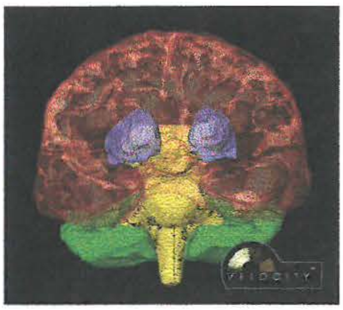

Figure 2.5 Soft Tissue [3]

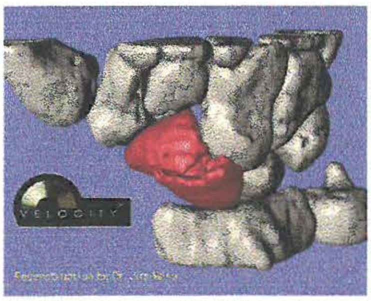

Figure 2.6 Multiple Wrist Bones [3]

2.3 Software Evaluation

The use of software was critical during the various stages of this project. The correct tools were required to perform specific tasks. The object was to investigate and evaluate the various software packages in order to determine the use and application of these packages in our environment. Another objective of this task was to determine the correct tool to be used to perform a specific task effectively and efficiently. Software actually plays a critical role in the product development stage. It is the heart of the modern product development process.

The design concept is transferred to a 3D electronic prototype. This stage of 3D prototyping is developing rapidly. The application and communication of a 3D concept is of critical importance. Virtual prototyping is one step beyond rapid prototyping. It is therefore important to use the correct software package for the right application. A large number of CAD and visualisation packages are available, ranging from low-end to high-end applications.

2.3.1 Materialise

Various software modules are available from the vendor. Only the following three packages were evaluated.

2.3.1.1 Mimics

The main application of this software is to import the data from various CAT or MRI scanners. The second application is to process the data to suit the specific requirement. The procedure starts with 2D image processing, followed by 3D visualisation. During the 2D processing stage, certain parts can be separated by using masks. The pelvis can be separated from the femur by using different masks. The correct windowing and threshold parameters can also be set to suit the application. The latest version features double threshold settings, as well as transparency. One can visualise the bone structure through the fibre or soft tissue sections.

The final phase is to export *.3dd files to be used in the CTM conversion software. [35]

2.3.1.2 CTM

The *.3dd file is used as input file. Several file types can be output, in order to suit the application. STL, IGES, VRML, SLA or FDM output files can be generated from the input file. There is not much of a graphical interface of the file to be converted, but mainly the parameters need to be set to suit the conversion.

The STL output is only available in ASCII format and does not always provide watertight surfaces [35].

2.3.1.3 Magics Viewer

The Magics Viewer software was extensively used to view STL files. The shareware version was downloaded and used successfully. Sections of parts can be made in three axes and measurements can be taken of certain dimensions. Hard copy printouts were also made for record-keeping purposes. This software can also be used to point out faulty STL files. It is Microsoft Windows-based.

2.3.2 Velocity TM V2.0

The Velocity software, distributed by Image3 LLC, can also be used to convert CAT-scanned images. A demonstration version was evaluated. The restriction pertaining to the demonstration version was that no data could be imported. A full version of Velocity includes a ToImg module that strips the common file header that contains information regarding the image and adds a Velocity header. The ToImg module accepts 8,16 or 32 bit per pixel grey value of RGB colour images and is also capable of handling byte swap data. It can only be used to process existing demo data that has already been converted.

The software seemed to be stable. The speed of outputting the STL data was very impressive. The real test would be in actually converting new data from various CAT scanners and processing it. The distributor was still preparing demo CDs in early July 1997. The strength of the process lies in SGI's excellent graphics which allow for the production of stunning images.

The Velocity software package consists of five modules, namely Image, Surfer, Display, PolyMerge and STLConvert. The modules can be managed as phases of data transfer.[3] The first, Image, is used to import an *. info file containing all the converted CAT or MRI 2D images. Parameters such as threshold, pixel size and material assignment can be set and stored in a model file called *.bin. Masks can be used to isolate a region of interest (ROI). Artifacts can also be removed with this module. Many 2D CAT and MRI images can be viewed simultaneously.

Phase two, the Surfer command, is used to generate the model file with the settings assigned in the Logic environment, during phase one.

Phase three is a 3D-verification stage. The Display module, 3D renderings can be verified. 3D Data can be rotated, scaled and translated, using the Display module to modify background, lighting, transparency and stereoscopic viewing and material assignment parameters. A new model file can then be saved if it is altered.

Phase four of the data-processing stage, called PolyMerge, involves polygon reduction and curve smoothing. It is accomplished by collecting small triangles into larger triangles in regions where surfaces are relatively flat. PolyMerge will also clean surface irregularities caused by noise. The original model file is visually compared to the modified version. A new model file can again be saved if required.

Phase five, STLConvert, is the final phase of converting 2D CAT images into 3D geometry. Both ASCII and binary STL format files can be exported. Three STL files, 6Mb, 8Mb and 34 Mb, were exported in approximately 2 seconds each during the demonstration. Compared to other STL generators, it was very impressive. The interface

The Velocity software package consists of five modules, namely Image, Surfer, Display, PolyMerge and STLConvert. The modules can be managed as phases of data transfer.[3] The first, Image, is used to import an *. info file containing all the converted CAT or MRI 2D images. Parameters such as threshold, pixel size and material assignment can be set and stored in a model file called *.bin. Masks can be used to isolate a region of interest (ROI). Artifacts can also be removed with this module. Many 2D CAT and MRI images can be viewed simultaneously.

Phase two, the Surfer command, is used to generate the model file with the settings assigned in the Logic environment, during phase one.

Phase three is a 3D-verification stage. The Display module, 3D renderings can be verified. 3D Data can be rotated, scaled and translated, using the Display module to modify background, lighting, transparency and stereoscopic viewing and material assignment parameters. A new model file can then be saved if it is altered.

Phase four of the data-processing stage, called PolyMerge, involves polygon reduction and curve smoothing. It is accomplished by collecting small triangles into larger triangles in regions where surfaces are relatively flat. PolyMerge will also clean surface irregularities caused by noise. The original model file is visually compared to the modified version. A new model file can again be saved if required.

Phase five, STLConvert, is the final phase of converting 2D CAT images into 3D geometry. Both ASCII and binary STL format files can be exported. Three STL files, 6Mb, 8Mb and 34 Mb, were exported in approximately 2 seconds each during the demonstration. Compared to other STL generators, it was very impressive. The interface is X Windows based, written in C and OpenGL, and runs on SGI work stations with IRIX version 6.

2.3.3 Surfacer - Imageware

This was the C.S.I.R.'s front-end CAD package. This software was extensively used for importing data from the CMM. This data was then manipulated to be on a CAD design level. Subsequently, the data is further used in the CAD environment. This software was also used to determine the deviation of CAT-scanned data compared to CMM data. The process is called registration. This is one of the view software packages that caters for reverse engineering.

2.3.4 Strim - Matra Datavision

This is another RE CAD software package supplied by Matra Datavision, which is one of the few software packages that caters for reverse engineering. Data is imported from various data-capturing devices. Data is then converted and surface creation follows. Several stages are required for data conversion and about 80% of the surface generation can be done automatically. Their powerful surface capabilities can generate the rest of the modelling. The RE approach used in this package is very different from existing methods of reverse engineering.

The Strim package can also be used for 3D inspection in a production environment. A 3D mapping of the surface can be displayed to view the deviation of the production part compared to the original master part. Matra Datavision launched the Euclid version 2 software packages during the last quarter of 1998. [38]

2.3.5 Cosmos - VRML

This software was used to create HTML Internet web pages. Several web pages were made to demonstrate this research project's results. It also has a VRML editor that can be used to view and create 3D objects for 3D visualisation. Special lighting effects, colours, material properties and patterns can be applied to the 3D geometry. The part can easily be rotated in 3D cyberspace. This software was supplied by SGI. It is part of the developer packages [32].

2.3.6 Raindrop Geometry

Raindrop Geometry is a software package that can be used to repair and re-mesh STL files. The limitation of the Microsoft Windows-based demo software package was that it did not allow one to save any work that was performed. It also expired after a period. Large files were processed, but could not be saved as part of the evaluation limitations. [20]

2.3.7 Desk Artes

Another software package, Desk Artes, can be used to repair and re-mesh STL files. A fair amount of 3D modelling can also be performed. Several modules are available, each addressing different areas, and can be used for various design and verification applications. [12]

2.3.8 Solid View

The Solid View software package can be used to view STL files. 3D Data visualisation and white boarding are the main applications of this package. [33]

Solid View is a very friendly Microsoft Windows-based package which was reasonably priced at US$500 in 1999. This software is available in modules and can be upgraded to perform IGES and other CAD format data conversions.

2.3.9 MPEG Generators

MPEG generators are very important in the generation of a movie or a part to view 3D data sets more easily. A 1.5Mb MPEG movie can be created from a 30Mb STL file. Such large STL data sets are not easily manageable. The MPEG movie generator is used to solve this problem. A super computer is not required to view the data. An AVI- type movie can also be made with the aid of the ALIAS software package. Two local companies offered these services. [17]

2.4 Rapid Prototyping Technologies

2.4.1 Background

The applications of rapid prototyping are constantly growing. Many industries are implementing this new technology. Benefits of rapid prototyping include enhanced "visualization capability, decreases in cost and cycle time associated with the fabrication of prototype parts, increased ability to calculate mass properties and detect design flaws before hardware fabrication, and increased part optimization and development prior to prototyping." [19]

Rapid prototyping technologies considerably reduce the time used to market products. This model making technology uses no tooling to manufacture prototypes. CAD easily accommodates engineering changes. A company can keep up with the changing market by using the latest Concurrent Engineering (CE) technologies. Objects with shapes that are more complex and intricate can be built with the aid of RP, with less potential for human error. A single rapid prototyping (RP) system can overcome the complexity and expense of using multiple machine tools.

The reduction in time to market of a product provides a reduction in consumer product costs. The potential to reduce development costs can reduce the final product cost for the consumer, providing the possibility of an even stronger market share. Inventory decreases can also be achieved because the object can be produced on a need-only basis. Cost, delivery and time to market are still critical issues. Figure 3.7 shows it is actually more important to get a new product on the market as soon as possible than to stick to the budget. The new product will generate an income as soon as it is introduced to the market. If the product appears 6 months late on the market, 33% of the profit could be lost. If the product is 9% overpriced, 22% of the profit could be lost. If the development budget is 50% overspent, but the product is on the market in time, only 3.5% of the profit could be lost, according to the McKinsey & Company (USA electronics industry) study. [22] p16-22.

Thus, if the new product appears six months too late on the market, up to 33% of the gross profit could be lost according to the Gallup study. RP technology and concurrent engineering could insure that the product is marketed just in time.

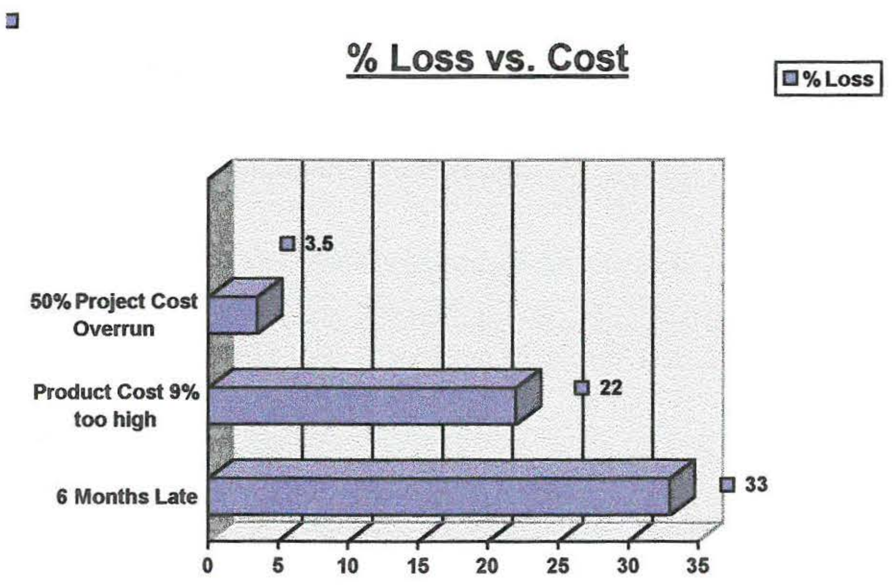

Figure 2.7 Development vs. Profit costs [22]

The chart in Fig. 2.8 shows the results of a survey that indicates the top three reasons for slippages in product development schedules, or time-to-market delays. [23] p12-19

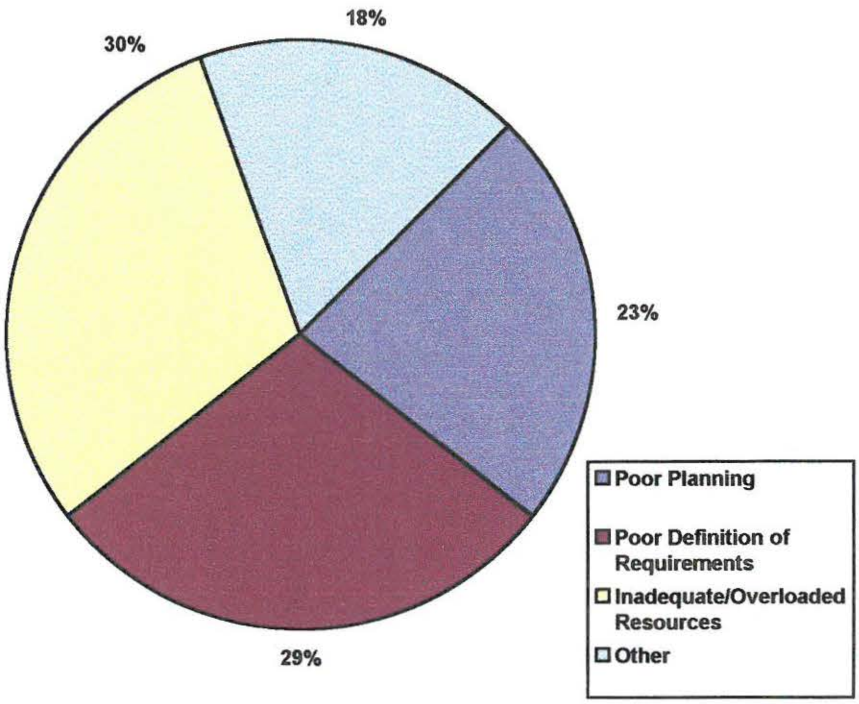

Figure 2.8 The Product Development Shortcoming [23]

The process requirements for rapid time-to-market results are:

- A clear understanding of the customer needs at the start of the project and stability in product requirements or specifications.
- A characterised and optimised product development process.
- A realistic project plan based on the best and most cost-effective technological solution.
- The availability of resources to support the project and use of full-time dedicated personnel.
- Concurrent engineering principles
- Fixed goal posts, to minimise the design content of the project.

Refer to reference [23] for international design centres that successfully apply these principles. Reference [24]p21 can be used to view schematic drawings that explains some of the RP processes.

The most significant industry events regarding the main rapid prototyping systems are listed in the following table.

Table 2.1 Significant RP events

1987	3D Systems introduced to the market.
1988	Stratasys market launch
1989	DTM market launch
1990	100th RP unit shipped
1991	Helysis introduced to the market
1993	BPM introduction.
1994	Sanders, IBM Technology & 1000th RP unit shipped
1995	Stratasys purchases Genisys IBM Technology
1996	Stratasys FDM 1650 3D Systems Actua 3D printer and 257 units of Stratasys Systems sold in 1996. 175 units of 3D Systems sold and 65 Sanders Systems sold in 1996. 35 ea. DTM & Helisys 1996.
1997	Stratasys FDM 2000,8000. New Sanders system SPII 3D Systems SLA 350 Solid State Laser Tech. DTM 2500 Sinterstation
1998	Stratasys Quantum Technology 3D Systems SLA 3500 & 5000 systems

One of the main factors ensuring growth in the rapid prototyping industry is that the product must be on the market at the right time.

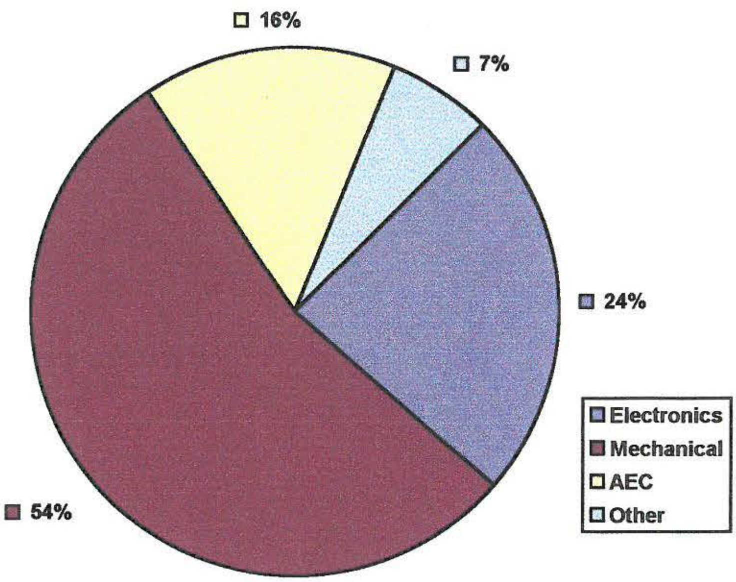

Figure 2.9 Software Segments

The Worldwide CAD/CAM/CAE software segments are displayed in Fig 2.9 above. The total revenue forecast was US$ 4 billion. In 1999 more than 2 million rapid prototype models per year were made, driven from 1.4 million CAD stations. RP systems form part of concurrent engineering technologies.

The literature study of this project covered a detailed analysis of more than 50 rapid prototyping systems. Only two of these RP systems, FDM and SLA, will be covered in detail in this study. A summary of these RP systems, not all commercially available, is listed in Table 2.2.

Table 2.2 Summary of the World's Rapid Prototyping Systems

No.	Rapid Prototype System	Manufacturer	Prototype Materials
1	Fused Deposition Modelling (FDM)	Stratasys	ABS, MABS, Nylon, Wax, Elastomer,
2	Stereo Lithography (SLA)	3D Systems	Epoxy Polyesters
3	Layer Object Manufacturing (LOM)	Helisys	Paper, Composites, Ceramics
4	Selective Laser Sintering(SLS)	DTM	ABS, Nylon, PC, TrueForm, Somos Elastomer, Sand, Metals, Ceramics
5	Solid Ground Curing(SGC)	Cubital	Poly Esther Epoxy
6	3D Plotting	Sanders	Wax & Polymer
7	Shape Melting	Babcock & Wilcox	Metals
8	3 D Printing	Z- Corporation	Starch
9	Spray Metal Mask	Carnegie Mellon Univ.	Metals
10	Photochemical Machining, Dual Laser system	Formigraphics, Battelle	Photo Polymers
11	Electrosetting	U.S. Navy, David Taylor Research Centre	Metals, Elastomers, Polymers
12	Printed Computer Tomography	Texas Instruments	Polymers
13	Stereos	Electro Optical Systems	Sand, Ceramics, Metals, Polymers, Photo Polymers
14	Computer Operator Laser Active Modelling (COLAM)	Mitsui	Photo Polymer
15	Solid Creation System(SCS)	Sony, DMEC	Photo Polymer
16	Soliform	SOMOS, DuPont Teijin, Seiki	Photo Polymer
17	Hot Plot	Sprax	Polymer
18	Layer Object Manufacturing (LOM)	Landform Topographics	Paper
19	Design-controlled Automated Fabrication(DCAF)	Light Sculpting	Photo Polymer
20	Ballistic Particle Material (BPM)	BPM	Polymer
21	Solid Object Ultraviolet Laser Plotting (SOUP)	NTT, CMET, Mitsubishi	Photo Polymer
22	Jetting Technology, Robot Arm	Visual Impact Corp.	Polymer

Table 2.2 Summary of the World's Rapid Prototyping Systems, Cont.			
No.	**Rapid Prototype System**	**Manufacturer**	**Prototype Materials**
23	Laser Modelling System(LMS)	Fokkele & Schwartze	Photo Polymer
24	Solid Laser Plotting(SLP)	Denken	Photo Polymer
25	Meiko	Meiko	Photo Polymer
26	Direct Shell Proc. Casting(DSPC)	Soligen	Ceramic
27	Stereolithography Process (SLP)	Laser 3D	Photo Polymer
28	Sheet Cut & Fold	Cybervid, Nasua	Paper
29	Fused Deposition Ceramics (FDC)	Rutgers University	Ceramics & Metals
30	Ceramic Deposition Modelling (CDM)	C.S.I.R., Pretoria	Ceramics
31	Metal Selective Laser Sintering	Centre de Transfert.	Metals
32	Electro-static Mask, Compaction & Sintering	Sintef Industrial Management	Metal Powders
33	Metal SLS	Univ. K.V. Leuven	Metals
34	SLA with Pastes	Optoform	Metals & Ceramics
35	SLA with Curtain Coating	Materialise	Photo Polymer
36	Laser of Metals	Aeromet	Metals
37	Multi-linear Type	Stratasys	Polymers
38	Laminated Paper JP5 System	Scroff & Dev. Corp.	Paper
39	Cross-sectional Prototyping (CSP)	LaserCAMM	Paper
40	Photo Lithography	USHIO	Photo Polymer
41	Selective Adhesive Manufacturing Machining	Kinergy	Paper
42	Solid Freeform Printing & 3D Printing	Prometal	Metals & Polymers
43	Cut & Fit	Charlyrobot	Sheet Materials
44	Solid Imager	Aeroflex	Polymer
45	RMPD	MicroTEC	Polymer
46	Control Metal Buildup (CMB)	Fraunhofer Institute for Laser Technology (FhG-ILT)	Metals
47	Induced Phase Transformation (IPT)	Stanford University	All Materials
48	Direct Photo Shaping	SRI International	Polymers & Ceramics
49	Selective Additive Hot Press	Kira	Paper
50	Cut-First Pattern Lamination	Ennex Corp.	Paper

2.4.2 Fused Deposition Modelling

Fused Deposition Modelling (FDM) is a non-laser-based process, developed in 1988 by Scott Crump, president of Stratasys, Inc. (Minneapolis, MN). FDM systems take CAD surface or solid models and build the parts by depositing layers of molten thermoplastic materials. FDM is a safe and affordable rapid prototyping system. [34] Figure 2.10 shows a simplified schematic of the process.

Stratasys manufactures and markets rapid prototyping systems that are used to compress the product development cycle. These rapid prototyping systems generate three-dimensional prototypes and models from 3D CAD data in an office environment. The Stratasys FDM systems use the patented, innovative Fused Deposition Modelling (FDM®) process to create prototypes. Genisys®, the 3D printer, creates 3D prints using the IBM technology acquired in January 1995.

The process begins with the input of the CAD data into the system. The UNIX-based work station will accept data in IGES format, as NC code, or in the industry standard STL format. The Quick Slice software converts the part into its layers, and the data is downloaded to the FDM machines. A spool of 0.050 inch diameter thermoplastic filament, resembling wire, is fed to the heated extruding head. The liquid thermoplastic filament is maintained at a temperature 1°F above its solidification state prior to deposition. The material then solidifies in 0.1 second upon placement by the x-y controlled extruding head. The material is deposited onto a Styrofoam slab affixed on a computer-controlled platform that controls the z-axis.

This system requires no post-curing. Layer thickness ranges from 0.001 to 0.050 in., and wall thickness ranges from 0.009 to 0.250 in. Tolerance for a 12 × 12 × 12-in. part is 0.005 in.

The non-toxic materials used include the following:

- machinable investment casting wax,
- a tough nylon-like material,
- ABS & medical ABS,
- elastomers

This system is capable of a one-hour material changeover. The process does not require elaborate supports. Any flat or near-flat overhangs should have a support structure. Stratasys has a variety of RP systems available.

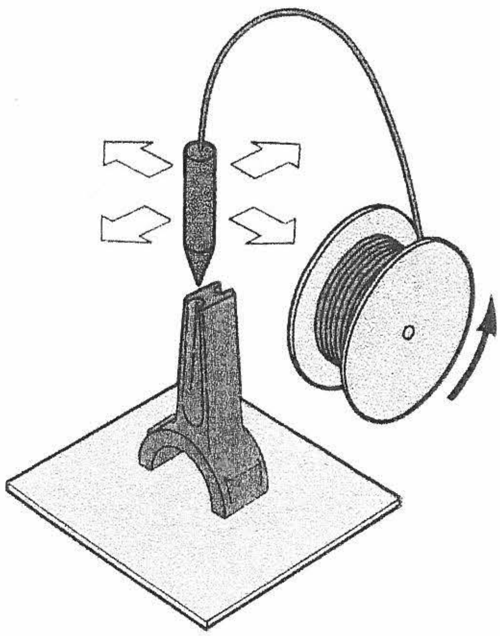

Figure 2.10 The Fused Deposition Modelling Process.

2.4.2.1 Costing Methods

The average hourly rate for FDM machines in the USA will vary from US$43-53, and in 1998, CAD rates will be US $200-400 per hour. A minimum of US$200 will be charged if the component is very small. The RP industry normally estimates the cost of a palm size model at $500. No one at the annual 1996 Stratasys User Group showed a costing method. The costing method developed by the author determines the cost by using previous deposition rates. The data was captured from previous growing parameters and comparisons were drawn to view the results. Figure 2.11 shows the deposition rates with some general combinations of tips, slice thickness and material types, the main parameters that rule the RP process. Factors that influence the cost are part orientation and amount of support generated.

The following formulae can be used to calculate the cost of manufacturing a prototype:

- Manufacturing Cost = Model Cost + Support Cost + Hand Finishing Cost + Profit
    - Model Cost = Prototype Volume x Deposition Rate
    - Support Cost = Projected Volume x Deposition Rate x 30 %
    - Hand Finishing = Labour Rate x Man-hours

This data is based on the following conditions:

- Quick Slice 1.4 software,
- FDM 1600 dual tip upgrade & hardware,
- Deposition rate unit is in thousand cubic millimeters per hour,
- Machine tariff is at R100 per hour,
- P301 - Nylon, P400 - ABS, ICW - Investment Casting Wax
- T12 - 0,012" diameter tips & T25 - 0,025" diameter tips.
- Slice thickness in 0,008"; 0,010" and 0,014" intervals.

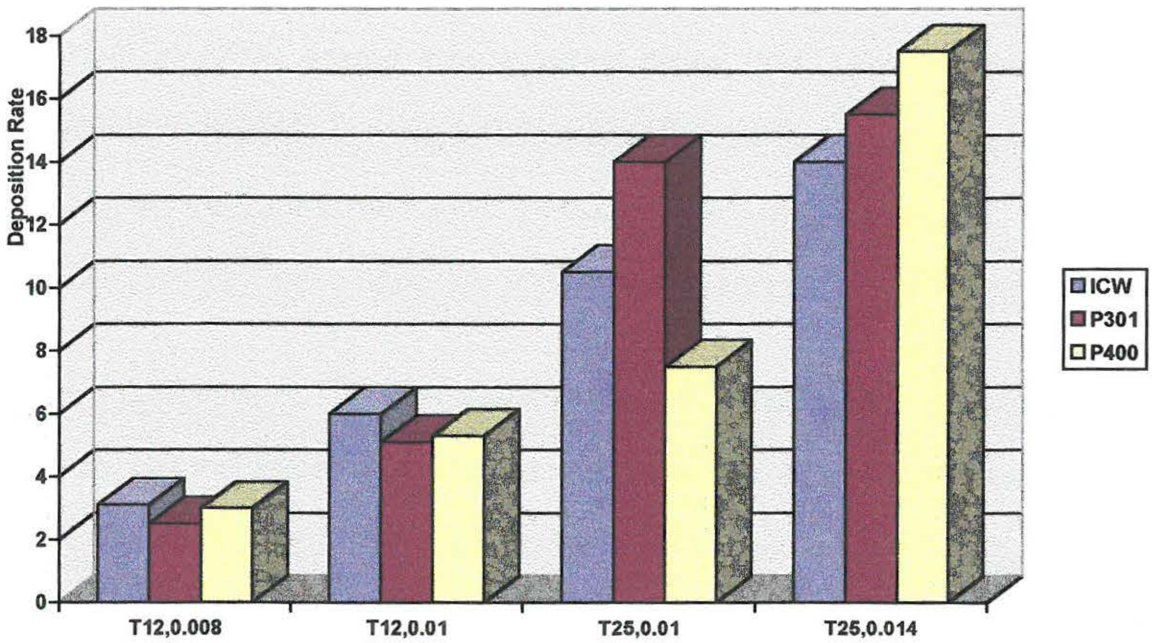

Figure 2.11 Costing Methods

For example, using P301 material and T25 tips with 0,010" slice thickness to manufacture a prototype, the FDM 1600 can grow at 14 000 mm³ per hour. Knowing the prototype volume, one can determine the total machine time and subsequently estimate the manufacturing cost.

2.4.2.2 Material Update

A new medical grade ABS is on the market called MABS. It is a methyl methacrylate ABS, and red and clear colours are available. The material will be rated a FDA CLASS 6 type. The gamma sterilisation resistance is very good and will not affect the material properties. This material will enable a prototype facility to produce a replica of a body part, allowing a physician to plan an operation and take the prototype into the theatre for visual aid. This material will have similar properties to poly-carbonate (PC). The development of soluble support material started during 1997. The material can be dissolved in ammonia and can be used with the MABS. This is very helpful, especially in the cleaning of small, hard-to-reach areas. The solution can easily be disposed of.

The normal ABS material will also be supplied in different colours, namely in white, black, red, yellow, blue and green. ABS materials can also be used in a vacuum metallisation process. The surfaces should be clean and an undercoat can be used to enhance the Aluminium bond. The vacuum metallisation takes place at 10mmHg. A top coat should be added to prevent oxidation.

During 1997 Stratasys supplied the new investment casting wax, ICW06, to their users. The author tested this material and achieved very good results. It was a great improvement on the previous material used, namely ICW05 investment casting wax.

The ceramic material created some interest as well. Rutgers University and A.C.R. have done a great deal of research.. A number of prototypes were inspected. The prototypes showed signs of problematic sintering. Warping, poor definition, poor finish, trapped air pockets and mushroom sections were some of the general defects found. Rutgers uses a polymer binder system to create the ceramic filament that is used in their old 3D modeller. A.C.R. retrofitted their FDM 1500 to extrude directly from the pressure chamber. A.C.R. is also developing another material called peek, a high-temperature polymer.

Stratasys is also looking into growing prototypes with elastomer materials (E-series). This material will be more flexible than ABS, but still maintain the toughness required. Table 2.3 shows the elastomer material's properties.

Table 2.3 Elastomer Material Properties

Properties	E50	E100	E150
Tensile Strength (MPa.)	35	28	28
Tensile Modulus (MPa.)	83	596	744
Elongation (%)	300	200	180
Flexural Modulus (MPa.)	345	689	1.034
Notched Izod, @-29 Deg. C (J/m)	1.495	748	374
Durometer (Shore D)	62	67	71
Vicat Softening Pt. (Deg C)	101	101	102
Specific Gravity	1.12	1.1	1.09

2.4.3 Stereo Lithography

Stereo Lithography is the process developed in 1984 by Charles Hull. A patent was issued for the Stereo Lithography system in 1986. Mr Hull then joined Ray Freed in forming 3D Systems, Inc. (Valencia, CA). The Stereo Lithography Apparatus (SLA) was introduced at the AutoFact trade show in November 1987. It was the only rapid prototyping system offered commercially at the time. [1]

In Stereo Lithography, a laser generates an ultraviolet beam that selectively solidifies surface areas of a photo-polymer in a vat at a point where the beam is focused. This process continues, slice by slice, until the system completes the part. 3D Systems offers three models of the SLA.

The process begins with the vat filled with the photo-polymer liquid and the elevator table set just below the surface of the liquid. The operator loads a three-dimensional CAD solid model file into the system. If needed, supports are designed to stabilise the part during building and post-curing. The translator converts the drawing into the STL file. The control unit slices the model and supports into a series of cross sections from 0.004 to 0.020 in. thick. The computer-controlled optical scanning system directs and focuses the laser beam so that it solidifies a two-dimensional cross section on the surface of the photo-polymer. The elevator table then drops enough to cover the solid polymer with another layer of the liquid. A levelling wiper moves across the surface of the polymer. The laser then draws the next layer. This process continues, building the part from the bottom up, until the system has completed the product. See Fig. 2.12, a schematic to explain the process. The part is then raised out of the vat and cleaned of excess polymer. It then proceeds to the Post-curing Apparatus for the final cure.

In the spring of 1991, 3D Systems introduced a new method of building called the "Weave". This method increased accuracy by as much as 20 times. It solidified 96% of the part in the vat before post-curing. The previous method left 40-60% of the part as liquid trapped within the walls of the cured resin. Previous distortion was primarily caused by stresses during post-curing. The Weave technique achieves very small cross-hatch spacing in each layer by making two separate passes perpendicular to each other. Post-cure time, shrinkage, and swelling are reduced with this new technique. The Weave also improves long-term dimensional stability by producing considerably fewer locked-in stresses due to post-cure. It also improves surface finish, especially on horizontal surfaces. Later, the "Star-Weave" was introduced. This technique cures the resin to 99% during the laser-drawing process. This system's accuracy is 0.002 to 0.005 in./in., depending on geometric complexity and operator skill.

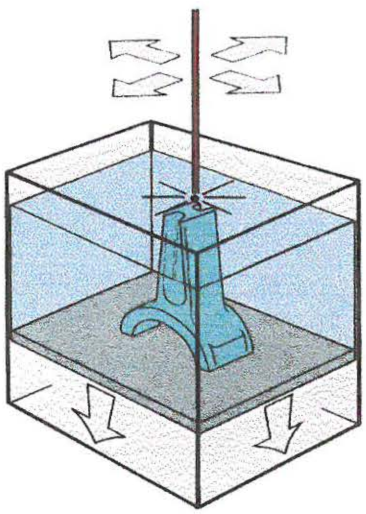

Figure 2.12 The SLA process.

2.4.3.1 Material Update

The materials used in building prototypes with Stereo Lithography are photo-curable resins. In 1999, the price of this polymer varies from US$300 to 350 per gallon. The resin in the vat not cured by the laser beam can be used again. To make a part with volume of 6 cubic inches, it would take US$25 worth of resin.

3D Systems and Ciba-Geigy Ltd. are in a joint research and development programme working on new resins. [23]p8-11 Their latest developments in 1999 were:

- CIBATOOL® SL5195, for SLA-5000
- CIBATOOL® SL5190, for SLA-3500
- CIBATOOL® SL5170, for SLA-250
- CIBATOOL® SL5149, for SLA-250

These new resins exhibit better toughness and machinability. In previous materials a problem with excessive brittleness was experienced. Allied Signal Inc. has also introduced the Exactomer 2201 resin, which demonstrates excellent material properties.

Du Pont also works in the area of liquid photo-polymer development. They have launched the following new materials:

- 2100, for argon-ion laser with high flexibility and bone-white colour material properties.
- 2110, for helium-cadmium laser with high flexibility and bone-white colour properties.

- 3100, for argon-ion laser
- SOMOS 6100, for argon-ion laser
- SOMOS 6110, for helium-cadmium laser
- SOMOS 6120, for Solid State laser

Most materials feature high-toughness and transparency. The average cost was US$ 760 per 4kg or US$ 3750 per 20kg in 1999.

Resins that can change colour as they are exposed to the laser beam have also been developed. This material is extensively used in rapid prototyping for medical applications. A tumor can be modelled and displayed in a different colour. This 3D prototype is then of great value to the surgeon.

2.5 Reverse Engineering Technologies

Projects frequently require the creation of a 3D CAD model from existing parts for further work or modifications. Various reverse engineering technologies (RE) now exist that can produce 3D CAD information from real parts. [25] There are two main stages in the RE process. The first phase is digitising or measuring and the second phase, 3D modelling and data manipulation. Some of the main applications of RE are listed below:

- making an electronic model from a handcrafted model;
- making a product that fits onto some part of the human body;
- providing 3D data when insufficient data is available;

- when the original CAD data is not usable;
- if the design changed from the initial design;
- medical applications.

Several RE methods are available. Every system has some strong and weak points. The selection of a RE system depends largely on the nature of the project, namely the final requirement. RE methods can be generally classified into two groups, namely contact and non-contact. [22]

Co-ordinate measurement machines (CMM) can be used to digitise the shape of a part. These machines normally have touch probes, but laser probes can also be fitted. CMM have either a gantry or an arm that accommodates the probe. Only a few points can be sampled per time interval, in comparison with other RE systems. Skilled meteorologists are very often required to drive the CMM systems efficiently.

Manual devices have more degrees of freedom. The user places the probe at the desired location and samples 3D co-ordinates. Manual devices are not as accurate as CMM systems.

Laser systems can measure a large number of points in a very short period of time without touching the surface of the article. Measurements are based on the reflection of a laser point or a laser line range on the surface. The system uses a charged-coupled device (CCD) camera and triangulation method to determine the co-ordinate position. The sensor (a CCD) can also be attached to a machine tool. Most laser systems are non-destructive and not as accurate as CMM equipment.

In Computer Tomography (CT) methods, penetrable X-rays are used for digitising. The part is scanned in order to produce a series of 2D slices that is used to generate 3D models. The main advantage of this method is that it is non-destructive and can capture internal geometry.

The Moiré Interferometer system is based on the projection of a grid of contrast lines onto a work piece. When the reference grid overlies the grid, interference lines are generated. The interference lines are used to calculate the geometry of the surface. A huge amount of data can be collected without making contact with the part.

The Capture Geometry Inside (CGI) slicing method is a destructive method that can measure internal as well as external geometry. [24]

Manipulation of the captured data requires computer power and proper software programs. Several software packages are available on the market. A short description of each of the RE techniques follows.

2.5.1 Co-ordinate Measurement Machine method

Co-ordinate Measurement Machine (CMM) manufacturers are LK, Mititoyo, Rennishaw (Cyclone), Mistral, D.E.A. and Okada Vigitiser, to name only a few.

Most CMMs require to be interfaced by means of a computer. Software is required to drive the CMM and to manipulate the 3D co-ordinate data. Software packages such as Surfacer, Strim RE, Surfer, Intergraph's I/CMM or other custom-designed software programs are used as front-end CAD packages to manipulate the data or to drive the CMM. Once the data have been manipulated and modified to a certain extent, it can then be used with most 3D CAD packages. Although CMM systems sample points at a much slower rate, very few reverse engineering systems can operate below a 20 micrometre tolerance. Metrology is one of the main functions of a CMM. A hole diameter, surface angle or linear dimension can quickly and easily be determined within 20 micrometre.

2.5.2 Robot arm type method

2.5.2.1 FaroArm

The FaroArm portable digitiser is distributed in S.A. by MetroCAS. It is a seven-axis arm with six degrees of freedom. The temperature-compensated, counterbalanced, articulated arm and AnthroCAM software package that caters for RE, 3D CAD and analysis can provide RE solutions on the shop floor or in the field. The probe is moved manually and points are sampled by the operator pressing the sampling button. [21] p53

2.5.2.2 Kreon Handscan - Versa Scan

The 3D hand-scan model uses a laser plane and video triangulation sensor capable of capturing 15 000 points per second and is fixed to an articulating arm. The sensor is hand-guided and can randomly be moved over complex geometry as if using a paint spray gun to collect data. Hot, fragile, flexible and soft parts can be scanned with this non-contact geometric capturing system. Data is viewed and validated dynamically during the scanning process.

2.5.3 Laser scanner methods

LASER is an acronym for Light Amplification by Simulated Emission of Radiation. The laser produces a powerful, directional monochromatic and coherent beam of electro-magnetic radiation in the infrared, visible and ultraviolet regions of the spectrum. The active medium is contained in an optically transparent cylinder with a reflecting surface at one end and a partially reflecting surface at the other end. The simulated waves make repeated passages up and down the cylinder, some of them emerging as a light through the partially reflecting end. In the ruby laser, the chromium atoms of the cylindrical-shaped ruby crystal are optically pumped to an excited state by means of a flash lamp, and can be made to emit pulses of highly coherent light. Lasers have been constructed by using a mixture of inert gases (helium and neon) to produce a beam. Another type of laser consists of a cube of specially treated gallium arsenic, which is capable of emitting infrared radiation when a current passes through it. Laser is used in eye surgery and holography, for the cutting of materials, and for printing and communications. [37] p241

2.5.3.1 Digibotics - Digibot II

The main advantage of this system is that it will always measure according to the norm of the surface. The scanner also uses the Digibot Software. It is mainly used to set up the scanner's parameters. The software is then used to incorporate the scanned data into an STL file. It can also be operated interactively. Data can be exported in IGES and DXF formats. Manual editing is required to check the slices or boundaries. The files can be modified to produce capped and closed models.

The University of Austin, Texas demonstrated the operation of the scanner at the Anthropology Department. The students there use the scanner to scan all the parts of a human skeleton. Images are then produced of the STL models and stored on CD, to be used by educational institutions and students. The demonstration model, a gearbox housing, is coated in a thin layer (0.004") of white spray to improve the accuracy and to reduce the scanning time. The model is mounted on a rotary table with the aid of a hot glue-gun. The scanning parameters are set on the 386 PC, which runs the Digibot software. The scanning continues without supervision. The equipment is very simple, user-friendly and reliable. Edge detection is still a problem for the laser scanner, and they are still improving the software and laser scanner lenses.

2.5.3.2 Laser Design Inc.

L.D.I. builds 4- to 6-axis laser scanners. Software is in-house developed specifically for their scanning equipment, called DataSculpt. This is still a front-end package for the more expensive CAD modelling system that can only handle points, poly-lines and splines. L.D.I demonstrated the software and claimed to reverse engineer a golf club in 1-3 hours of scanning and 1 hour of data manipulation.

L.D.I. claimed to be able to read CT scanned data that can be converted to slice files. This process is not automatic and requires manual editing. L.D.I demonstrated their CADCAM software. This software package can be used to machine, with the aid of CNC equipment, from 3D STL data. A golf club in 3D STL format was used to create the mould split-line, toolpaths and surface boundaries during the software demonstration. They have a generic post processor which can be set up for any CNC machine controller. The hardware, the Surveyor Scanning Series, is also in-house developed and built.

2.5.3.3 Sharnoa

Sharnoa, an Israeli-based company, manufactures machine tools which are dual tasking, and allow simultaneous machining and CAD/CAM operations. By using a PC based controller called Tiger 5, many limitations that exist in many other machine tools are reduced. A 3-axis computer numerical control (CNC) milling machine can be used as a scanner by fitting the digitising system to the machine tool. Toolpaths can be generated in any direction and is therefore not limited to machine in the same direction in which the part was scanned. Male, female and mirror image tool paths can be generated from the original scanned data. [11]

Two different laser-digitising systems can be mounted in the machine tool. The limitation of the scanning system is the standoff distance, 58 mm or 158 mm. The standoff distance is the vertical distance from the source. The sensors receive optics from the contact point and the standoff distance is proportional to the reflection angle. Laser digitising is almost 30 time faster (2 400 points per minute) than touch-probe scanners.

2.5.3.4 Kreon 24- Versa Scan

The Kreon 24 is a laser digitising system that can vectorise vertical walls and inspect production products. The Kreon 24 system can be used to retrofit CNC machines or it can also be dedicated to scanning equipment. [23] p.5

2.5.4 Computer-aided Tomography

2.5.4.1 Scientific Measurement Systems (SMS)

Scientific Measurement Systems is based in Austin, Texas. SMS manufactures Computer Tomography (CT) scanners. The CT scanners are custom-built for specific applications such as crack- or flaw-detection and reverse engineering. The accuracy varies with the CT scanning machine's specifications. SMS claims to be able to measure accurately through 6" of steel.

The cost of scanning is affected by the scanning rate. The cost of the CT scanners varies from US$ 125 000 to more than US$ 500 000.

The Materialise software was used to convert the CT-scanned data. The CT data is converted to boundary polygon data. The data had to be manually edited to remove spikes.

CADKEY and Pro Engineer CAD software packages are used to surface some of the polygon data. STL files are usually generated and supplied to the client. STL files can easily be 100Mb to 150Mb in size.

2.5.4.2 Aaroflex Inc.

The Aaroflex Solid Imager creates 3D physical models representative of CAD, CAT and MRI files by means of laser solidification of photosensitive polymer. It is one of the fastest, efficient and most accurate systems distributed in North America. The RE system includes an AccuScan scanning system, a faster scanning system than any on the market. Solid Imager rapid prototyping system also features the positive applicator blade that reduces downtime, thereby making it more effective. [26] p.39-45

2.5.4.3 ARACOR

The Advanced Research and Applications Corporation (ARACOR) is based in Ohio. ARACOR designs, manufactures, and tests inspection systems. The company's products in general address the needs of defense, aerospace, castings and electronics industries. X-ray Computer Tomography (CT) systems are being manufactured by ARACOR. The CT equipment is used for probing internal and external geometry, non-destructive testing, quality control, reverse engineering and contraband detection applications. Material type and surface finish do not affect the capturing of geometry by using the ARACOR equipment. [21] p52

2.5.5 Destructive Methods: CGI - RE1000

Capture Geometry Inside (CGI) is based in Minneapolis. The accuracy of the process is based on the scanner and the machine tolerance. One machine cycle includes a machined layer, as well as a scan that will normally take 20 seconds.

CGI has also developed their own windows-based software specifically for their system. The images will be converted to boundaries with points and lines. Every layer is then tessellated and two layers are active at once. Computer power is required if all the data needs to be handled all at once. The software seems to work well, but requires manual editing and checking.

A part is cast in a thermo-setting block of plastic that can be heated to 180°F during curing. The plastic block is then fixed into an Aluminium base. The plastic block is machined down with the component inside, capturing the internal and external geometry. CGI experienced a "rip out" situation during the machining process. The part concerned was made of a Nickel-Chrome Alloy steel material. Care should be taken when components consisting of very hard and tough materials are machined. The force required during the machining process should be substantially less than the force used to retain the component in the plastic material. The block of material is also cast into a machine base that acts as a clamping system, so that the whole block can be machined down without any clamps being in the way.

An internal combustion engine piston was sent to CGI for a benchmark exercise. The piston was reverse engineered and the data were returned from the USA within a two-week time span. The author did not have a computer available that could manage the 36Mb STL file. CGI was requested to split the file into four smaller parts, so that the data processing could be managed. The new data arrived approximately one week later. The four sections were processed separately and FDM prototypes were grown and joined after the finishing process. Another complete piston was grown on an SLA500 machine. The SLA piston was later sent to CGI as part of the reverse engineering benchmarking agreement.

2.5.6 Optical methods

Anatomy scanning devices exist that can scan a complete human head in two seconds or a complete body in less than six seconds. The CGI method can also be regarded as an optical method, as it captures an image and not 3D co-ordinate points.

2.5.6.1 Steinbichler - Comet

Comet/Optotrak, manufactured by Steinbichler Optical Technologies, is a tripod mounted solution that is claimed to have an unlimited measurement volume. The device is a combination of the Comet 400 optical 3D digitising sensor and the Optotrak optical CMM. The sensor digitises 3D objects by measuring 16 x 16 inch patches of 420 000 X-Y-Z co-ordinates in 60 seconds per view. The Comet automatically records the position and orientation of the Comet sensor as it is repositioned around the object. This information is used to seamlessly merge the digitised patches to reportedly form one very dense and accurate point cloud. [26]p.56

2.5.6.2 Atos - Newport

The new range of the ATOS measuring equipment has revolutionised non-contact measurements and has revealed the potential for new applications in surface data acquisition due to the exceptional speed (439 000 individual 3D points in a few seconds) of data acquisition. [24]

2.5.7 Summary of the World's Reverse Engineering Systems

The literature study of this project covered more than 31 reverse engineering (RE) systems in detail. Only a few of these RE systems were covered in detail in the dissertation. The residual RE systems are listed in the following table (in no particular order):

Table 2.4 Summary of the World's Reverse Engineering Systems

No.	Reverse Engineering Systems	Manufacturer
1	Cantilever Arm Type, Touch Probe	FaroArm
2	Cantilever Arm Type, Laser	Kreon
3	Machine Retrofit Type	Sharnoa
4	3D Rapid Digitiser	Virtual Technologies
5	Destructive Type	Capture Geometry Inside
6	Machine Retrofit Type	Maho
7	Laser	Digibotics
8	Laser	Laser Design Inc.
9	Laser	Cyberware

Table 2.4	Summary of the World's Reverse Engineering Systems, Cont.	
No.	**Reverse Engineering Systems**	**Manufacturer**
10	Laser	3D Scanners
11	Laser	Vitana Corporation
12	Laser	Hymarc
13	Co-ordinate Measurement Machine (CMM)	LK
14	Co-ordinate Measurement Machine	Brown & Sharpe
15	Co-ordinate Measurement Machine	Zeiss
16	CMM, Machine Retrofit Type, Touch Probe	Rennishaw
17	Co-ordinate Measurement Machine	Dea
18	Co-ordinate Measurement Machine	Mitutoyo
19	Computer Aided Tomography (CAT)	BIR
20	Computer Aided Tomography	SMS
21	Computer Aided Tomography	Elcint
22	Computer Aided Tomography	Phillips
23	Computer Aided Tomography	General Electric
24	Computer Aided Tomography	Siemens
25	Computer Aided Tomography	Toshiba
26	Computer Aided Tomography	Aracor
27	Stereo Vision, 1 Camera & 1 Fringe Projector	Steinbichler
28	New Port, 2 Camera & 1 Fringe Projector	Atos
29	Optical	Breukmann
30	Optical	Massen
31	Touch Probe	Picza-Roland

2.6 Computer-aided Tomography Technologies

Since Computer Aided Tomography (CAT) was extensively used in this study, it will now be discussed in more detail.

2.6.1 History of CAT

The word "tomography" comes from the Greek word *tomos*, which means a "section" or a "cut". It was first used in 1935. Tomography was "discovered" by at least nine people working independently in five different countries. Researchers patented it at least six times in those five countries. [39]

2.6.1.1 Roentgen and the "Invisible Light"

In 1895, a professor of physics at the University of Würzburg in Germany, was experimenting with a type of vacuum tube called a Crookes tube (named after the English physicist, William Crookes, who invented it). Scientists had known for years that when electricity runs through a Crookes tube, a light glows inside the vacuum at the other end, but they could not explain this phenomenon.

Wilhelm Roentgen discovered, through experimentation, that some kind of ray was being emitted from the Crookes tube. It could travel through a cardboard box without affecting it, speeding through the air, hitting the paper and making it glow. Since Roentgen could not identify the ray, he called it the X-ray, a name that has stuck.

2.6.1.2 Marie Curie's Research

A young woman from Poland, Manya Sklodowska (later called Marie Curie), found a way to measure the strength of X-rays. Her husband had already invented a device called an electrometer that could measure the electric charge in the air. X-rays bleed off the charge on an object and their strength was measured by how fast the charge bleeds off. Marie could thus use the invention to measure the strength of radiation emitted by a substance. She tested many different minerals and metals. The only material that radiated was uranium. It did not take her long to figure out that the strength of the rays depends on the amount of uranium in her samples. The more uranium, the stronger the rays.

Another substance that radiated was discovered and called thorium. She realised that the name she had been using, uranium rays, was not accurate; obviously, a new name had to be invented. Using her imagination, she called the rays “radioactivity”.

2.6.1.3 The New Elements: Amazing but Dangerous

The first new element the Curies named Polonium after the country of Marie’s birth. The second, however, which they called Radium, is the most radioactive substance on earth. The Curies suffered from health problems, such as fatigue, aching joints, and blood disorders known today as symptoms of radiation poisoning.

However, despite their ignorance of the dangers involved, scientists all over the world began experimenting with radium and radioactivity.

The work done by Becquerel and the Curies laid the foundation for one of the modern fields of radiology, namely the use of radiation to treat diseases, especially cancer.

2.6.1.4 Francis Williams (1852 - 1936)

Sometimes called America's first radiologist, Francis Henry Williams was born in Boston in 1852. His engineering background helped him to understand much more about the technical part of radiology than most doctors did.

Williams was a doctor at Boston City Hospital where he did his early studies on his patients. By 1896, X-ray exposures could be as short as a fifth of a second.

It was not long before doctors began to realise the dangers of X-rays, as well as their potential to help. Doctors who did a lot of X-rays, began to see changes in the skin on their hands, from peeling and shedding of the outer layer, to X-ray burns, and finally to cancers on exposed skin. Others noted their hair falling out and damage to their eyes.

In 1890, after some animal studies, a researcher, William Rollins, published safety guidelines for using X-rays in an article titled "X-Light Kills". He suggested that anyone using X-rays should:

* Wear glasses, which the rays cannot penetrate.
* Shield the X-ray tube with lead (which X-rays cannot penetrate).
* Aim the beam only at the part of the patient to be X-rayed. Cover the rest of the person's body with lead shielding.

2.6.2 How X-rays are produced

Electromagnetic radiation is energy travelling in waves; the waves are of different lengths, and the length gives each type its special properties. X-rays and gamma rays penetrate the body and can damage its tissue. Light rays enter only the eyes. Infrared rays warm every body part they touch. Radio waves pass through without the person even being aware thereof.

Other waves, such as the ultraviolet rays that tan your skin, are shorter than visible light waves. X-rays are also of this short-wave type. Short waves have more energy than long waves, and subsequently behave differently when they strike a target. The rays are produced when a stream of electrons strikes a specific material object. The atoms of the entire element emit a characteristic X-ray spectrum when bombarded by electrons. An outer electron then falls into the inner shell to replace the displaced electron while losing potential energy (ΔE). The frequency of the emitted X-rays is $\Delta E/h$ where h is the Planck constant. X-rays affect a photographic plate in a way similar to light.[39]

In order to produce X-rays, one needs three things, namely electrons, high-voltage electricity to make them move fast, and a target that is bombarded by the electrons. Electrons are not hard to produce. When something is heated to a high enough temperature, electrons "boil off". However, producing electrons and using electricity to get them moving fast, is not enough to produce X-rays.

The electrons also have to hit a target. When millions of electrons speeding through vacuum hit a metal target, they penetrate it and release X-rays. The faster the electrons are moving, the easier it is for them to penetrate the target. In an X-ray tube, a particular metal is used as the target. The speeding electrons hit the metal, interact with the metal atoms, and produce the radiation we call X-rays.

X-rays are produced in an evacuated tube. It contains an electron gun and a heavy metal target forming part of the anode. The metal emits an X-ray when electrons bombard it. The spectrum of the radiation depends on the voltage between the cathode and the anode, the temperature of the cathode and the metal target.

The first X-ray tubes were the Crookes tubes Roentgen used. They were not very effective because they did not contain a complete vacuum, and there was no way to focus the electrons on a target. Tubes became more efficient as scientists bent them to target the electrons more closely and found better target metals such as platinum. However, X-rays cannot easily be focused or bent. They continue in the direction in which they were emitted originally until they are absorbed.

Nearly twenty years after Roentgen's discovery, another researcher, W. D. Coolidge, manufactured an even better tube. It had a true vacuum inside and was more stable and easier to control than the Crookes tube. Coolidge also found that using tungsten as the target produced more X-rays. Many improvements since those days have resulted in the manufacture of tubes that are smaller, more efficient, and produce more X-rays faster.[39]

2.6.3 Basic Principles of CAT

Computer Aided Tomography (CAT) is a technique using X-rays to photograph one specific plane of the body. A Computerised Tomography (CT) scanner is an X-ray machine that rotates through 180 degrees around a patient, taking measurements every few degrees.

X-rays or Roentgen rays are electromagnetic radiation of the same type as light but of much shorter wave length, in the range of $5x10^{-9}$ metre to $6x10^{-11}$.[39] Gamma rays are shorter and ultraviolet light rays are longer than X-rays. Electromagnetic (EM) radiation consists of waves of energy associated with electric and magnetic fields, resulting from the acceleration of an electric charge. These electric and magnetic fields, which require no supporting medium, can be propagated through space. These fields are at right angles to each other and to the direction of propagation. EM waves travel through space with a uniform speed of $2{,}997x10^{8}$ metres per second. The SI unit Photon is regarded as a quantum of EM radiation.

The absorption of the X-ray by matter depends upon the atomic number and the concentration of atoms of the material. The lower the density, the more transparent the material is to X-rays. Bone, for instance, is more opaque than the surrounding flesh. This makes it possible to take an X-ray photograph (radiograph, fluorescent screen) of the bones of a living person. [37]

A patient is scanned at a minimum of 3 mm thick slices and 3 mm intersections. A part or a fossil is preferably scanned at 1 mm or finer slices. It must be kept in mind that the patient needs to be subjected to the minimum amount of radiation. If the patient risks being exposed to more radiation, the risk of radiation could outweigh the benefit of the result by far. The data sheet needs to be completed on site for future reference.

X-ray film needs to be printed, representing the CAT 2D images. Orientation markings need to be made on the X-ray films, as well as the scanning parameters.

A certain amount of radiation may be tolerated by living beings. The unit for radiation is Sievert (Sv). It is the equivalent absorbed dosage of ionising radiation multiplied by a dimension-less factor equal to 1 joule per kilogram. The International Commission on Radiological Protection stipulates the dimension-less factors. The former unit of dose equivalent, the rem, is equal to (10 Milli Sv) 1×10^{-2} Sievert.[37] About 30% of radiation exposure in medicine is caused by CAT. The following measures can be taken to help reduce radiation exposure: [29]

- Reduction of energy by reducing the scanner current setting (mA) to the minimum level. This is achieved at the expense of increased image noise.
- Elevations of pitch factor (the ratio of table feed to slice thickness). A 50% increase of the table feed will reduce the radiation dose by 33%. The nominal slice thickness should be kept constant. At the same time, however, this measure also increases the effective section thickness up to 50%.
- Determination of the precise area to be examined. The use of pre-programmed spiral scans often yields unnecessary scans, as a spiral cannot be stopped before completion.
- Storage of raw data sets. Unfortunately, this requires considerable storage capacity. In unclear cases, a new reconstruction can be made from existing data sets.

Traditional X-rays combined with a computer makes CT scans valuable to doctors in diagnosing many different illnesses. A CT scanner is a huge, doughnut-shaped machine. The patient lies on a bed while the X-ray tube circles around the patient's body; taking a series of "slice" views that are then transmitted to a computer. The computer can combine many thin slices into one picture, stacking them to create a three-dimensional (3D) image. The image can be copied onto traditional X-ray film, or it can be stored in the computer for future use.

CT scanners, like the MRI, are very good at making images of soft tissue, such as the brain, but they are also excellent for making images of bones. Sometimes, when a bone has to be replaced with an artificial one, an engineer will use a 3D picture from a CT scan to build the artificial bone. The engineer first uses the images from a CT scan to build a plastic model of the bone to be replaced. The model is then used to make an artificial bone that replaces the deformed or diseased one. A surgeon removes the bone and installs the implant. [17]

2.6.4 Magnetic Resonance Imaging (MRI)

In this form of radiology, traditional X-rays are not used at all. Instead, a giant magnet is used along with a computer. A MRI machine looks like a narrow tunnel with the patient lying on a bed that moves into the tunnel until it stops. The magnet generates a magnetic field around the patient. This field causes the hydrogen atoms in the body to line up. A radio signal is sent out, knocking the hydrogen atoms off centre, so that they wobble like tops. A computer measures the speed with which the atoms return to the centre. This information is used to create an image of the inside of the body on a monitor similar to a television screen.

The body images can be created from front to back, from side to side, or in a cross section. The MRI is especially good at producing images of soft tissues, such as the brain and spinal cord, tendons, muscles, or arteries.

For example, if a person suddenly dropped to the floor due to a seizure, doctors would need to know what happened in the brain to cause the seizure. The MRI could be a lifesaver. A scan of the brain could show a tumour that no one had suspected was there. Such tumours can often be removed by means of brain surgery. [39]

2.6.5 Hounsfield Units

Godfrey N. Hounsfield received a Nobel Award in 1979 for his remarkable work in the radiology field. The Hounsfield system is based on a Grey-scale system. For instance, Denser material such as bone absorbs more X-rays than soft tissue. This can be seen on the printed film as well. On a X-ray film, the lighter areas represent bone, while the black areas represent air. It is actually a black and white image with variations of grey sections. With the development of the digital image, Hounsfield developed a system that allows one to distinguish between different sections. These sections are called pixels. One digital image can consist of a matrix of 512 horizontal pixels, and 512 vertical pixels. Each pixel can have a different grey scale or Hounsfield unit. The Hounsfield system ranges from -1000 to + 1000HU.

The following table shows the basic unit for various materials:

Table 2.5 Hounsfield Units of Materials

Description	Hounsfield Units (HU)
Fatty Tumour	-40HU to -80HU
Fat	-70HU to -90HU
Calcification Areas	> +200HU
Water	0HU
Air	-1000HU
Soft Tissue	+20HU to +70HU
Tumour	-100HU to +75HU
Lungs	-1000HU to -200HU
Brain	+10HU to +45HU
Liver	+10HU to +75HU
Contrast Agents in Vessels	+75HU to 300HU
Bone	+400HU to +900HU

2.7 Industrial CAT Apparatus of the C.S.I.R.

The C.S.I.R. has a high resolution and high-powered Phillips MG324 CAT scanner. The CAT scanning system is made up of an X-ray source, the CAT scanner and a computer with the ACTIS CAT scan imaging and control software installed in it as illustrated in Fig. 2.13 [18]

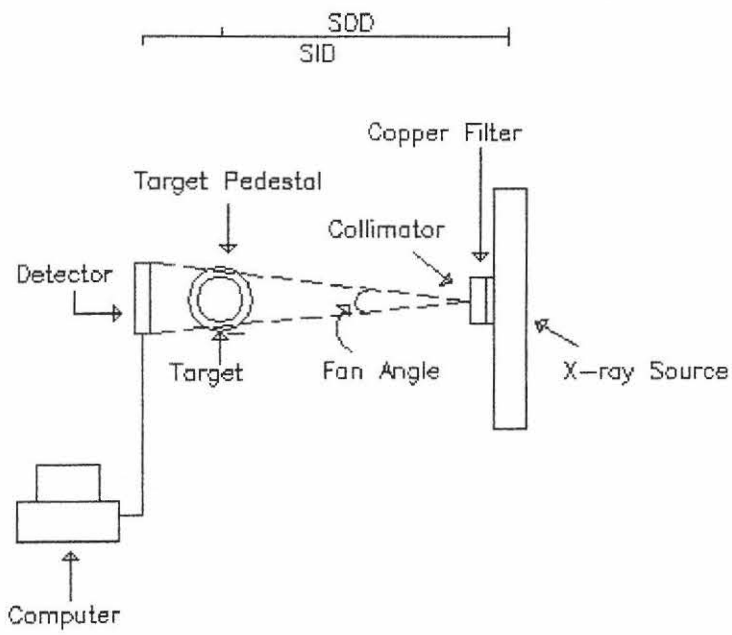

Figure 2.13 The CAT scanning equipment

<u>**The X-Ray Source**</u> - is a Philips MG 324 unit with a maximum power output of 320 kV at 5 mA corresponding to the large spot size of 1.8 mm by 1.8 mm. For the accurate CAT scanning to be done in this project, the smaller spot size of 0.8 mm by 0.8 mm, which has a maximum power output of 250 kV at 2.55 mA, was used.

<u>**The Collimator**</u> - attached to the front of the X-ray source, is a simple collimator fitted with a removable lead filter, as well as space for extra filters that can be added as required.

All this filter space is required when warming up the X-ray unit as it operates at maximum power in its warming-up cycle, producing dangerous levels of radiation.

The Fan Angle - is the angle at which the detector can pick up the X-rays from the X-ray source. It is the ratio between the width of the detector and the distance of the detector from the X-ray source (see Fig. 3.14). Although this is not a piece of apparatus, it is an important concept that should be understood when analysing the CAT scanning system.

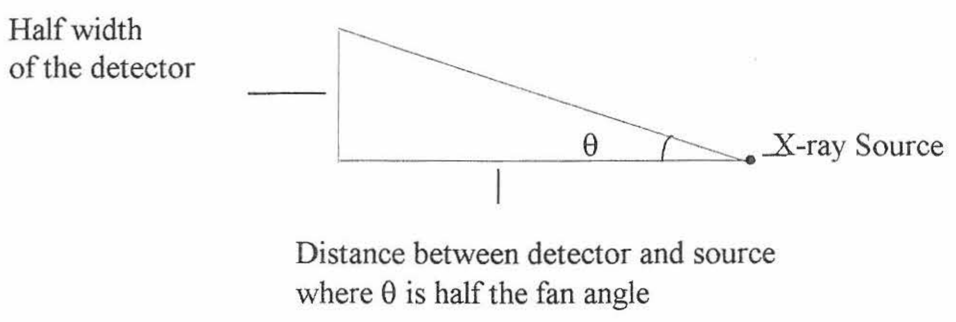

Figure 2.14 Explanation of fan angle

The Target - is the object that is being scanned. It is mounted on the revolving target pedestal. The pedestal is a raised Perspex pedestal with a diameter of 45 mm. Note that with this CAT scanner, instead of the X-ray source moving around the target as is normally the case, the target pedestal rotates which produces a similar effect.

The Detector - is a set of 2048 sensors that are arranged over a width of 45 mm. Thus, each sensor covers a width of 0.02 mm. This provides much greater accuracy than is achieved with the standard commercial scanner found in most hospitals.

The Computer - used in this application is a standard personal computer with an Intel 80486 DX processor with 48 megabytes of ram. It is equipped with a ¼" tape drive for bulk data storage. The computer is directly connected to the detector, controlling the motion of the detector and the target pedestal.

The ACTIS Software- is the software that controls the movement of the detector and the target pedestal. The software also reads in the data from the detector and converts this data from a raw image file to a CAT scan image. The conversion of the raw data into an image requires extensive mathematical manipulation by the software. A detailed study of these mathematical techniques will be laborious and complex and lies outside the scope of this project. The software is Windows (Microsoft or UNIX) based and is easy to use.

Functions of the CAT Scanning System- include the following:

- DR scanning (digital radiograph, the standard type of X-ray available at a hospital)
- CAT scanning
- Viewing of the scans on a multipurpose viewer
- Data storage
- Motion control

2.7.1 Data Collection Procedure

The part was fitted onto the high resolution Phillips CAT scanner.

The start-up procedure is as follows:

- Log into the computer as the manager user, using BIR as a password
- Fit all Cu and Pb filters to the collimator
- Close the aperture of the collimator
- Make sure that the power is on at the switch box, underneath the table and at the detector
- Exit the scanning area and close the gate
- Switch the mains on at the control box
- Turn the key clockwise to the ⬋ sign
- Set code to suit the downtime

Code	Warm-up Time	Downtime
103	Long (1 hour)	> 7 days
102	Medium (0.5 hour)	2 to 3 days
101	Short (20 min.)	1-5 hour

- Press the black No.1 starter button
- Automatic setting, could rise to a maximum of 250 kV
- Select small spot for CAT

Once the warm-up process is completed, the CAT scanner needed to be configured and calibrated. For the Actis software configuration settings, the following details are required:

- Source Image Distance (SID)
- Source Object Distance (SOD)
- D.A.S. Gain
- Focal Spot size - normally fine (0.8 x 0.8mm) for CT

  or else large (1.8 x 1.8 mm) for crystal orientation work.
- Integration time - normally 64 ms

The calibration procedure is as follows [18] p27, p28: The scanning procedure is methodical and the same method was followed each time. The CAT scanning system was calibrated, including:

- Detector alignment
- Offset
- Gain
- Central ray and Wedge

Detector Alignment - This calibration procedure aligns the X-ray detectors and finds the exact vertical midpoint of the X-ray stream. The detector alignment scan is performed at 250kV and 2.5mA or as set on the control box. Remove all the filters from the collimator. Set the values in the Actis software, start the process on the control box by pushing the black button No.1. Select the OK button on the Actis window to start the process. A variation of 0.1 should be acceptable.

Offset - This calibration procedure is performed to ensure that each detector has a zero reading at zero X-ray intensity (no X-rays are used in this calibration).

Gain - This calibration procedure is used to test the integrity of each of the 2048 detectors with respect to the selected gain setting. The source voltage can be set to 250kV and the source current to 2.5mA. Select a vertical table position for the following three tests.

Central Ray - This calibration procedure uses a 250-micron metal wire in the centre of a Perspex tube to find the exact transitional midpoint of the X-ray stream. The calibration is vital when large objects are to be scanned. The reason for this is that the CAT scanner "breaks" a large object into parts that are then scanned individually and added together by means of the processing unit. To do this reconstruction successfully, the scanner needs to have an exact centre reference point from which to work. The central ray calibration is also used with the detector alignment calibration to help focus the detector set. Set parameters to 250kV, 2.5mA, vertical table to 50mm. Start the process on the control box. Switch the control off when complete.

Wedge - This calibration procedure is usually done to help calibrate the CAT scanner for the specific substance being scanned. The procedure as specified by the handbook supplied by the scanner manufacturers requires that a wedge of the specimen be scanned. In the case of fossils, this is difficult to do, as one cannot cut a two and a half million-year-old fossil into a wedge for calibration purposes. However, it was decided just to let the system scan nothing. The 250kV test specimen was removed from the rotating table and the parameters were set as in the previous stage. Start the process on the control box by using button No.1. Switch controls off when completed.

Each element of the calibration routine must be carried out to fully calibrate the CAT scanning system. Whenever the system is turned on, it must be calibrated again and it was found in practice that the system should be recalibrate at least every 24 hours.

Radiograph - the next part of the procedure was to take a digital radiograph (DR) of the part that was to be scanned to judge its height and width and to optimise the scanning process. This helps to determine scanning parameters such as the following:

- the field of reconstruction
- how long it would take to scan

From the Actis software, select a new part and enter the information pertaining to the new part. Set the voltage, current, start and end positions, as well as the object width. The thin and thick Cu filters can be fitted to the collimator, if required. Start the process on the control box with button No.1, confirm the start with the Actis software.

CAT Scanning - After this, a single CAT scan image was taken to check that the parameters mentioned above had not been set too small and that all other parameters (e.g. SOD) were correct. The clarity of an image can be judged by looking at it and comparing it with other images of lower quality. Once this has been checked, the scanning starts, normally from about half a millimetre below the fossil to about half a millimetre above it. Set the CT scanning parameters, slice position, slice width, voltage and current. The number of slices can be determined by dividing the scanning height by the slice increment. Set the resolution to high and the process to continuous for automatic scanning or start for single scanning.

Data Transfer - Following the CT scanning stage, the data was archived onto tape and transferred by using File Transfer Protocol (FTP) to the computer with the conversion software on it. Keep a record of the name and number of the converted and transferred images.

System Shutdown - Exit the Actis software on the PC and select power down. Switch off the computer and screen. Switch the control box to ≈ position. Allow the system to cool down before final shutdown. Shutdown the collector box.

2.7.2 Data-processing Procedure

The conversion process entails the following:

- converting the CAT 2D data to Mimics 2D data and then into 3D images.
- converting the 3D images to 3D geometric computer models.
- converting the 3D geometric computer models to physical prototypes.

With the use of the CCUNF method, an option file was created containing all the required parameters in a text format. The 2D CAT scan images were then converted into a Mimics format using the options file while running the CCUNF command. The data conversion command is called CCUNF.

The conversion from the raw CAT scan images to the final STL file is also a methodical procedure.

- An option file is created to store certain characteristics of the scan.
- The option file is then used to convert the image data files to a format that the MIMICS software can read.
- The CAT scan slice data set is now converted to a 3D solid model using an option within the MIMICS package.

The next step is the one that requires the most time, effort and judgement, namely to manually remove the noise from the slice data images manually. This involves removing the tape and supports that hold the fossil while CAT scanning, from the image. This can become very difficult, as it is often hard to distinguish exactly where the tape ends and the very porous fossil starts. With experience one can begin to judge what the shape of the fossil at the joint should be and adjust the image accordingly. This is, however, not accurate and must be noted as a source of error. Although this sounds like a serious problem, it is not that grave, because the tape is not even a millimetre thick and only touches the fossil in a few places. This is shown below in the following Fig. 2.15

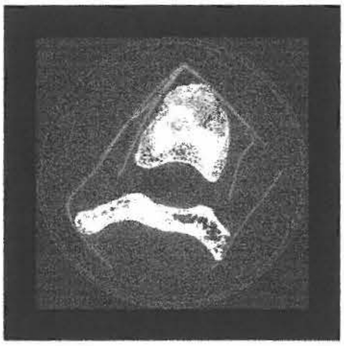

Figure 2.15 CAT image of a fossil.

Once a solid 3D model exists, the CTM software is applied to the 3D model to create a STL file. Again, a number of options are available to the user, mostly dealing with the resolution of the STL file that is to be created. It will indicate whether interpolation is required.

The conversion system is made up of an O2 Silicon Graphics computer and the Materialise software. The Materialise software consists of 2 sections, MIMICS, which converts the CAT scan images to 3D models and CTM, which converts the 3D model to the STL file format. The conversion from CAT scan data to an STL involves a number of steps. The first is from the ACTIS image data to an unheaded file format after the file has been exported from the ACTIS software. The next conversion is from this unheaded file format into the MIMICS software file format. The third conversion is to a .3dd file format, a specialised format within the MIMICS software that combines the slice files into a 3D solid model. The final conversion is done, using a further Materialise application, CTM, that converts the data from the .3dd file format to an STL file format.

The next link in the chain is to transfer the data files by means of File Transfer Protocol (FTP), from the computer with the ACTIS software, to the computer with the Materialise software. This is an easy exercise as the FTP goes through the internal network at speeds faster than 100 kilobytes per second. The conversion from the image data files to a format that can be read by the Mimics software is a two-step process. The first step requires setting the different scan parameters in an "option" file.

These options include:

- HIS = The image horizontal size (512)
- VIS = The image vertical size (512)
- Number of images per file (1)
- File swap format (3)
- FOR = Field of reconstruction (50)

Thus:

Pixel size = FOR/HIS = 50/512 = 0,097mm

Other parameters are also required to be put into the option file. Note that the numbers in brackets are standard inputs into the option file. Also note the pixel size is in millimetres. It is a size indication based on the horizontal image size of 512. The 512 unit is the number of pixels across the x- or y-axis (after averaging). The field of reconstruction is the diameter of the CAT scan image. The next step is to convert the image data files into data files that the MIMICS software can read.

The CAT scan slices must then be converted into a 3D solid model. In some cases the slice data must be edited to remove noise data. Very often the slice data must be edited to digitally erase the devices holding the fossil. In some cases, the fossil was placed in a Perspex dish and the Perspex had to be removed from the reconstruction.

Furthermore, the fossil is held down by using standard masking tape. This must also be removed from the slices before the solid model is made in order to preserve the correct surface finish of the original fossil.

The removal of the extra data is not difficult, but is rather time-consuming because each slice must be edited individually, which could amount to 200 individual edits, which must in some cases be edited pixel by pixel. If even one pixel is missed on any one slice and that pixel is not connected to other pixels directly, the software will not allow you to convert to a 3D model. This is because the conversion to a 3D model requires that there be only one object in the conversion from slice data to a solid model.

A solution was to scan the models in a different way; by closing the Perspex bowl with masking tape and scanning the fossil on top of the tape. This meant that a few images were blurred at the bottom of the fossil. The reason was the noise of the surrounding masking tape. The fossil presses slightly on the tape. Thus, between 400 and 600 microns (the bottom 2 or 3 slices) were inaccurate when converting to a solid model.

2.7.3 The Accuracy Testing Procedure

The accuracy of two sections of the process was checked. The accuracy of the CAT scan data was tested. This was done in the following way:

- An antelope vertebra was CAT scanned and a 3D solid model was generated.
- A maximum accuracy STL file was produced of the vertebra in two halves (top section and main section).
- The antelope vertebra was scanned on the CMM using a 1 mm-diameter probe.
- The STL file was converted to a point data file and correlated against the CMM point data using the Surfacer software package.

The next test for accuracy was done by comparing the STL file against the grown stereo lithography part, measured on the CMM machine of STS14D. This was done in the following way:

- STS14D was CAT scanned and a 3D solid model was generated.
- The solid model was turned into a STL file using a z accuracy of 0.2 mm (slice thickness) and a x-y accuracy of 0.25 mm (2 pixels).
- The STL file was used to grow a stereolithography part of STS14D.
- The stereolithography part was scanned on the CMM machine using a 2 mm diameter probe (the 1 mm probe was broken).
- The STL file was converted to a point data file and correlated against the CMM point data using the Surfacer software package.

2.7.4 Finding the Optimum Conditions

Before it was possible to analyse how accurate the data obtained from the CAT scanning was, it was necessary to measure a test set of data. A set of CAT scans was taken of a fossilised antelope vertebra (STS 2426). The spacing was at 200 microns over areas of detail (near the bottom and top) and at 500 microns over areas of less detail (the middle). The following image, Fig.2.16, shows a radiograph (ordinary X-ray) of the vertebra. Note that the bottom area is glue that was used to hold the vertebra to the revolving pedestal while scanning.

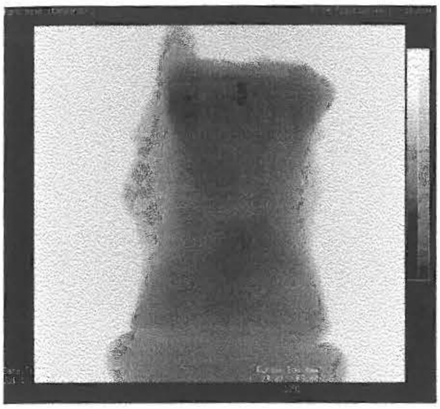

Figure 2.16 An X-Ray image of STS 2426, the antelope vertebra

The same vertebra was then measured using a co-ordinate-measuring machine (CMM) with a nominal accuracy of 3 microns. The CMM data can be output into an STL file format. The STL file can then be read by a CAD package called Surfacer. The CAT scan data was converted to a CAD solid model and then to an STL file format using the procedure described above. The two sets of data could now be compared to yield the differences between the CAT scan data and the CMM data to give an overall error. To do this it was accepted that the CMM error is, in reality, at about 10 microns (based on the experience of the operators using the equipment). The Surfacer package then has a function that will correlate the two sets of data and will give a mean and maximum error between the two sets. This mean and maximum error can then be used to help specify the overall accuracy of the replication process.

It was necessary to first find the optimum conditions for scanning. A number of factors can be varied to give different quality of scans. This was particularly necessary because there were some disturbing artifacts (disturbance features on the CAT scan image) coming through on the scans themselves. These included circular rings (as depicted below Fig. 2.17), as well as other general noise.

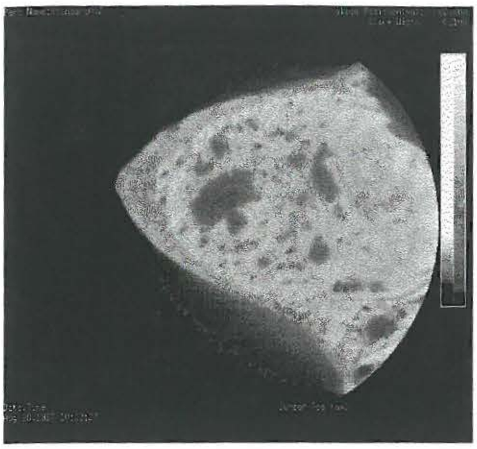

Figure 2.17 A CAT scan showing circular rings

The scan quality was determined by the clarity of the image. Although this sounds non-specific, it is important to note that this testing was done by comparing different scans visually and deciding which gave the best image. All scans were taken at two different places (62 mm and 75 mm) along the fossil so those two different images at varying density could be considered for each parameter test. Both physical and computer-based parameters were varied.

The following parameters were altered:

- Power (current and voltage)
- Source object distance (SOD)
- Source image distance (SID)
- Manual filters (Copper and Lead)

Power

Both the current and voltage were varied to try to find the best power settings to obtain artifact-free images. The X-ray source has the ability to output X-rays at a power of 320 kV at 5mA on a large spot size. For accurate CAT scanning, a small spot size is used and the maximum power under these conditions is 250 kV at 2.55 mA. Note that if the voltage is dropped when using the small spot size, a larger current can be used. The following conditions were used:

Table 2.6 Parameter Variation, Power

Test Number	Voltage (kV)	Current (mA)
1	150	2
2	200	2
3	150	3
4	200	3
5	100	1.5

Variation of the voltage and current in the manner mentioned above seemed to make no difference to the number and extent of the circular artifacts and other noise on the CAT scans.

Source Object Distance and Source Image Distance

These two parameters are dependent upon each other to a large degree therein that when the source is moved backwards, both the SOD and the SID change. The SID can be changed independently, but this was not considered since changing this would only result in a smaller or larger fan angle.

The results are shown in the following Table 2.7.

Table 2.7 Parameter Variation, SOD and SID

Test Number	SID (mm)	SOD (mm)
1	750	688
2	751	688
3	749	688
4	750	687
5	750	689
6	751	687
7	751	689
8	750	615

Note that the first test here (test 1) was measured to be the correct SID and SOD using a tape measure. There was no change to the noise artifacts because of changing the SID and the SOD. Further tests showed that the CAT scanning system is insensitive to small changes to the SID and SOD and that they need only be accurate to about 10 mm. Thus, a possible source of error had been eliminated.

Filters

The next parameter that was tested refers to the effect of manual filters. It was found quite early that the insertion of a lead filter (even a thin one) led to too great an attenuation in the X-rays, giving very poor results. For this reason, only copper filters of varying thickness were used. The first test required scanning of the antelope fossil at a SOD of 688 mm, a SID of 750 mm, voltage at 250 kV and current at 2 mA. First a 3 mm copper filter, and then a 5 mm copper filter, was used. It was found that the circles and other noise artifacts were greatly reduced and, in some cases, even disappeared. The reason for the great improvement in the image below Fig. 2.18 was that the copper filters removed a great deal of the lower energy radiation, which was obviously causing noise in the system.

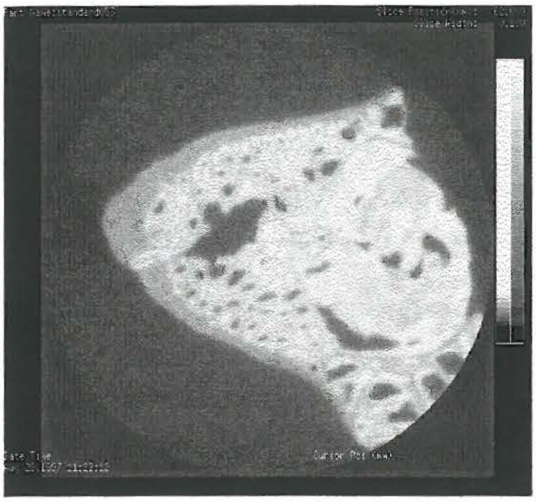

Figure 2.18 The image without rings using copper filters
(rings radiating from the centre have been eliminated)

Once the main problems had been removed (the low energy radiation causing the circular rings), it became necessary to find the optimal combination of variables to provide the best images. First a set of tests was done to find the optimal power settings using either the 3 mm or 5 mm copper filters. The results are given in Table 2.8.

Table 2.8 Parameter Variation, Filter Thickness

Test Number	Voltage (kV)	Current (mA)	Filter Thickness (mm)
1	250	2	3
2	250	2	5
3	300	2	5
4	300	2	3
5	250	2.5	3

These scans were done at a SOD of 688 mm and a SID of 750 mm. It seemed that at the lower powers, the images had fewer artifacts and noise, but if a 3 mm filter was used at low power, the X-rays were be too greatly attenuated, thereby giving "weak" images. If a high power setting and a thin filter were used, not enough of the low energy radiation was attenuated and again the image became prone to noise disturbance. A further factor affecting this was the SID and the SOD. The reason for this was that the X-rays became more scattered and thus attenuated when they were further away from the source, and became more concentrated when closer to the source. Thus, it was necessary to test the filters at different SODs and SIDs.

The next set of tests was done with the SID at 600 mm and the SOD at 545 mm. The results are given in Table 2.9.

Table 2.9 Parameter Variation, Filter Thickness at New SOD and SID

Test Number	Voltage (kV)	Current (mA)	Filter Thickness (mm)
1	250	2	3
2	250	1.5	3
3	250	1.5	5
4	250	2	5
5	250	2.5	5

It was found that test number 5 yielded the best resolution and quality of image.

The computer-based parameters that had to be tested:

- Integration time
- Gain
- Computerised Filters

Integration Time

Integration time is the time that the detectors are given to absorb the X-rays. A longer integration time means that a greater number of X-rays are absorbed by the detectors, but on the other hand, the detectors may become saturated. A low integration time means that fewer X-rays, and thus less information, is passed to the detectors, but there is less chance of saturation. The problem of saturating the detectors cannot be taken lightly. It can result in very inaccurate readings.

The main problem arises in the situation shown below:

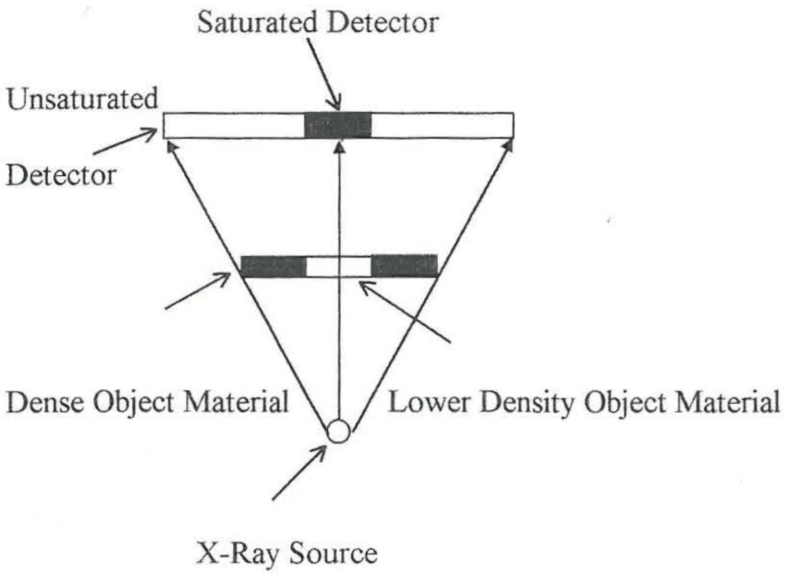

Figure 2.19 The problem of saturating the detectors

If the object that is being scanned is of varying density and the integration time is calibrated for the dense area, then the area of the object that is less dense causes the detector to become saturated. Alternatively if the calibration is done for the less dense area, the detectors sensing the denser area do not get enough information and an incomplete image is produced. Thus in the context of this project, it was decided to test different integration times and their effects on the final CAT images.

The results of these tests are given in Table 2.10.

Table 2.10 Parameter Variation, Integration Time

Test Number	Voltage (kV)	Current (mA)	Filter Thickness (mm)	Integration Time (ms)
1	250	2	5	64
2	250	2	3	64
3	250	2	5	128

The reason that the filter thickness was changed is that the filter lowers the density of X-rays leaving the X-ray source. Thus for a thicker filter it is necessary to have a longer integration time. It was found that the setting of 64 ms resulted in the best images being produced.

Gain

Gain is a parameter that affects the processing and reconstruction of the CAT scan image. It affects a multiplier within the reconstruction mathematics. Since the documentation provided with the ACTIS CAT scanning system does not include the reconstruction mathematics and algorithms, it was impossible to tell what exactly was affected. However, tests were done, varying the gain, in order to see whether a better image could be obtained. The software allows the gain to be varied between 1 and 8 in square increments (1, 2, 4, and 8) with a default value of 8. It was found that by lowering the gain, the image became slightly less clear and so the gain was left at the default value of 8.

Computerised Filters

The ACTIS software allows four different reconstruction filters to be applied to the CAT image.

The result of each filter is shown in Fig 2.20.

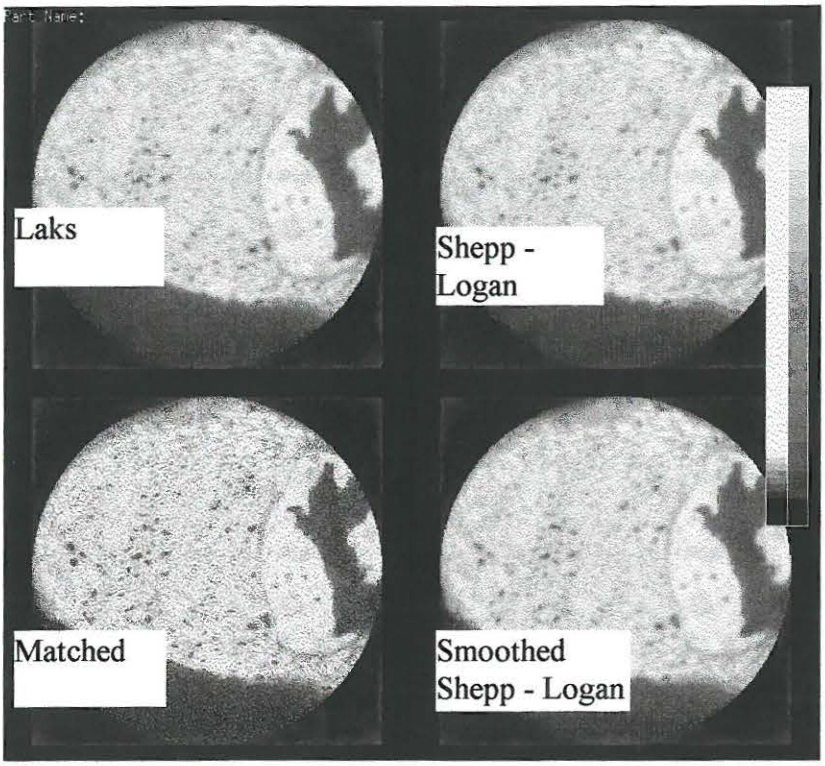

Figure 2.20 Comparing the same image using different filters

The documentation provided with the software does not accurately describe the effect of each filter physically or mathematically. The same antelope vertebra image was compared using the different filters and it was decided that the Shepp-Logan was the most effective.

Final Parameters

Once the best computer filter had been chosen, a final scan was done to check all the parameters that had been selected by taking a final scan. The final parameters chosen were:

- Voltage : 250 kV
- Current : 2.5 mA
- SID : 600 mm
- SOD : 525 mm
- Copper Filter Thickness : 5 mm
- Integration Time : 64 ms
- Gain : 8
- Computerised Filter : Shepp-Logan

The yield of these parameters is shown in the following CAT scan image.

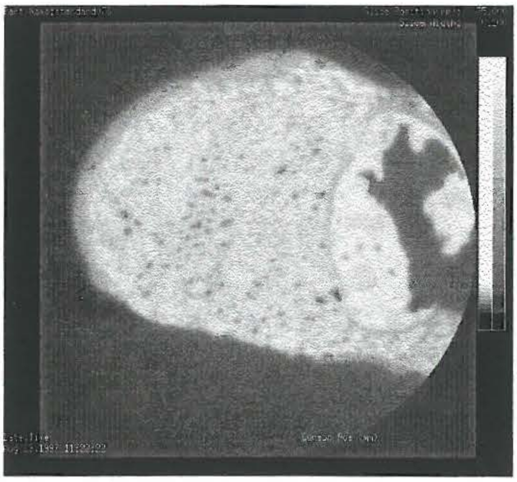

Figure 2.21 Confirmation of final parameters.

2.8 Medical Apparatus

This section will deal with scanners used for medical case studies.

2.8.1 Krugersdorp Private Hospital

The Elscint 2400 Elect CAT scanner was used. They also have a Siemens MRI system, but no method of retrieving data from that MRI system.

2.8.1.1 Data Collection Procedure

Data was stored by the radiology technician in sets of about 30 slices. This was done to allow the X-ray tube to cool down during scanning and storing stages. It also allowed a time delay for the computer to process the data. The data was stored on 1.4 Mb stiffies. The READELSC command was used to retrieve the data from the stiffie and to number the 2D CAT scan images sequentially. This data were then transferred to the Silicon Graphics O2 Computer, called LANCRE, hosting the Materialise software, with the aid of File Transfer Protocol (FTP).

2.8.1.2 Data-processing Procedure

The Materialise command, called CCELSC, automatically converts the Elscint 2D CAT scanned images into the Mimics CAT image format.

2.8.2 Hydromed Hospital

Hydromed has state-of-the-art GE spiral CAT scanner and Siemens MRI equipment.

2.8.2.1 Data Collection Procedure

Data was stored by the radiographer in sets of approximately 45 slices. This was done to allow the X-ray tube to cool down during scanning and storing stages. It also allowed a time delay for the computer to process the data. The data was stored on a 4 mm DAT cartridge by the GE technicians, as part of a backup procedure.

The data was then loaded on the C.S.I.R. HP computer, called FATHOM, the only DAT drive that could read the 4 mm DAT tape. The HP computer also had limited disk space and only part of the data could be retrieved at a time. This data were then transferred to the Silicon Graphics O2 Computer, called LANCRE, hosting the Materialise software, with the aid of File Transfer Protocol (FTP). Once the data was transferred to LANCRE, it was deleted from the hard drive to make space for the new data set. This process was repeated until all the data was retrieved from the 4 mm DAT tape. The external SCSI DAT drives were not compatible. A compatible external SCSI DAT drive was later borrowed, and made the transfer of data effortless. The general UNIX tar command was used to retrieve the data from the 4 mm DAT tape.

2.8.2.2 Data Processing Procedure

Various manual and automatic conversion methods were experimented with, and the only successful conversion command proved to be the CCGEADVA command. This automatic conversion command can be used to convert General Electric Hi-speed and Hi-light Advantage CAT images to a Mimics CT image format. It is best to group the various sets of one patient or part together, otherwise the sets should be handled separately without reference to the other sets during the 3D imaging and part creation phases.

2.8.3 Morningside Clinic and Pretoria East Hospital

Morningside Clinic and the Pretoria East Hospital have state-of-the-art Toshiba spiral CAT scanner and X-vision series.

2.8.3.1 Data Collection Procedure

The radiology departments were very helpful and contributed to the success of this case study. The owners' greatest concern was that the CAT scanner would be down for at least 3 hours during the data transfer process.

A qualified Toshiba technical supervisor was contracted to retrieve the CT data. The spiral data was converted or reconstructed into slice data by the radiographer. Two sets of data were prepared with different slice parameters. A laptop was connected to the scanner. A ¼" data cartridge tape streamer was connected to his laptop. The data was stored on the data cartridge as part of a maintenance programme.

The ¼" data cartridge (Dysan DC6250 - 250Mb- 1020 ft.) was subsequently inserted in the C.S.I.R.'s tape streamer that is connected to a Clipper system, Intergraph IPRO 6700 computer. The data were then stored on the hard drive in a temporary directory. Thereafter data was transferred via a local area network (LAN) with the aid of file transfer protocol (FTP) to the computer hosting the Materialise software.

2.8.3.2 Data-processing Procedure

The data was again stored in a temporary directory. The CCUNF command was used to import the CAT-scanned slices. This command is described in the Materialise software manual in detail. The parameters used during this conversion are listed in the data sheet. Materialise, a Belgium-based company, assisted in the first file conversion process. The author was also supplied with more information on the conversion of CAT images. The latest Mimics software version converts the data automatically.

2.8.4 Medical Apparatus Summary:

Table 2.11 Summary of the Medical CAT Scanners used in this study.

	Krugersdorp Private Hospital	**Hydromed Hospital**	**Morningside Clinic**	**Pretoria East Hospital**
Scanner Type	Elcint 2400 Elect	G.E. SPIRAL	Toshiba X-Vision SPIRAL	Toshiba X-Vision SPIRAL
Data Media	1.4Mb Stiffies	4 mm DAT	1/4" DATA CARTRIDGE	1/4" DATA CARTRIDGE
Conversion Commands	READELSC FTP CCELSC	FTP CCGEADVA	FTP CCUNF	FTP CCUNF

2.8.5 Other Potential Medical Apparatus

Table 2.12 Summary of the Medical Apparatus

• The Willows Hospital • Siemens MRI	• Bell Street Hospital • Siemens CT
• Universitas Academic • Siemens MRI • G.E. Spiral CT	• National • Siemens CT
• Entambeni Hospital • ElCint Spiral CT	• St. Augustus • Siemens & G.E. Sprial CT
• Montana Hospital • G.E. Spiral CT	• Robinson Hospital • Phillips CT

3 ANTHROPOLOGICAL CASE STUDIES

3.1 Lystrosaurus Skull - Anthropological

Lystrosaurus - A Therapsid (mammal-like reptile can be seen in Fig. 3.1) that was present in very large numbers (running into the millions) in Gondwana during the Triassic period. (Gondwana was the supercontinent consisting of the landmasses of South America, Africa, Antarctica, Australia and India that split and drifted apart during the periods following the Triassic).

3.1.1. Background

It is a member of a group of therapsids called Dicynodonts, characterised by their horny beaks and only two teeth - the canines, which grew quite large and appeared like tusks. They lived in sizable herds beside water sources (rivers and lakes), and were herbivorous. Probably the major component of their diet consisted of plants called horsetails, which grew more than a metre tall. *Lystrosaura* are particularly interesting because they were among the few Dicynodonts to appear in the fossil record after the great extinction event at the end of the Permian period, which wiped out 95 percent of all life on earth. In fact, the *Lystrosaurs* were present together with the first dinosaurs. There were at least two species of *Lystrosaur*, namely a very large one with a flat-fronted face that grew to the size of a big Brahman bull, and a smaller one with a more rounded snout. They were sprawling animals, chunky and lumbering and probably incapable of any great burst of speed. They would not have been scaly or furry, but would have had tough leathery skins. *Lystrosaura* are creatures that inhabited the ancient Karoo area of South Africa.[15]

The Permian period started approximately 286 million years ago and ended with the start of the Triassic period about 248 million years ago. The first dinosaurs therefore appeared almost in the middle of the Triassic period (220 million years ago).

The Materialise software was applied extensively during the conversion process. Fig. 3.3 shows a 2D cross section produced by the CAT scanner. The black regions in this figure represent the fossil where the white region represents the rock formation. This was a very interesting case study. What made it so interesting was that the fossil's skull was and is still encapsulated in rock, as Fig. 3.2 shows. The big advantage is that the rock could be electronically removed to display the fossil, with the aid of CAT and 3D computer image processing as can be seen in Fig. 3.4, 3.5, and 3.6. The saving in cost and time is astronomical. Imagine an archeologist spending months to grind the rock away, compared to this new process that will take less than a week to complete.

This fossil was scanned at two hospitals, namely at Hydromed and Krugersdorp Private Hospitals. Different apparatus was used, as the technicians hoped to achieve better results by using the more recent spiral CAT scanners.

3.1.2 Images

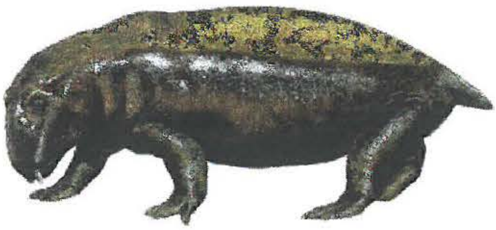

Figure 3.1 The Lystrosaurus.

Figure 3.2 The Lystrosaurus encapsulated in rock.

Figure 3.3 2D CAT-scanned slice No. 138

Figure 3.4 3D rendering of the top twenty slices

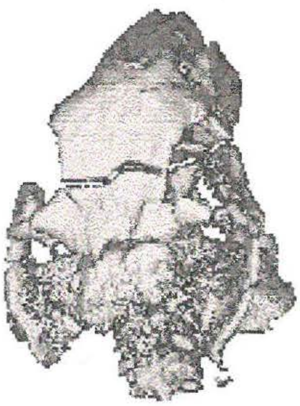

Figure 3.5 3D rendering of the skull, top-righthand view of skull.

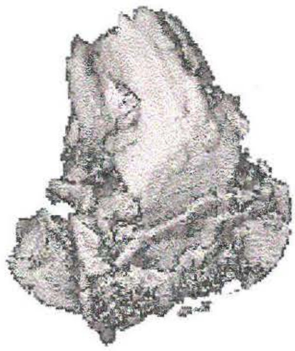

Figure 3.6 3D rendering of the skull, top-lefthand view of skull.

3.1.3 Lystrosaurus Data Sheet:

	Description	Options/Units	Data K'dorp	Data Hydromed
	CT Image Names		fos.xxx	4s4I
	Patient/Project Name		fos.pat	4s4i.pat
	Number of First Input Image		27/01	68
	Number of Last Input Image		157/99	133
	Number of First Output Image		000	000
	CT or MRI	CT, MRI	CT	CT
	Horizontal No. of Image Pixels	0 to 65535 (265,512,1024)	512	512
	Vertical No. of Image Pixels	0 to 65535 (265,512,1024)	512	512
	Number of Images per File	(1)	1	1
	File Swap Format (0,3)	0,3	CCELSC	CCGEADVA
	Pixel Type	B,UB,S,US,L,UL,F	-	-
	Inter Image Header Size	0	-	-
	Add Value	0 to 4095	-	-
	Scale Value	0 to 4095	-	-
	Table Position	(mm)	0	0
	Distance Between Slices	(mm)	1	1
	Slice thickness	(mm)	1	1
	Pixel Size SQ.	F.O.R./No. Hor. Pixels (mm)	0.47	0.43
	Gantry Tilt Angle	Degrees	0	0
	Field of Reconstruction/View	(mm)	240	220
	Number of Images		130	65
	File Size of CAT Image	Kb	270-280	270-280
	File Size of Converted Image	Kb	135	135
	.3dd file size	Mb	1.4 (X.srf)	1.4 (X.srf)
	.STL file size	Mb	not grown	not grown
	RP Method	(SLA,FDM,OTHER)	-	-
7	.IGS file size	Mb	-	-
	RP Slice file size	Mb	-	-
	RP Download File size	Mb	-	-
	Grow Time	Hour	-	-
1	Tip size	(T12, T25)	-	-
2	Slice Thickness	(0.01", 0.014")	-	-
3	Finishing Time	Hour	-	-
4	Processing Time	Hour	5	10
5	Data Retrieval Time	Hour	4	4
6	Total Cost	Rand		=14*150+300 =2400

3.2 *Thrinaxodon* - Anthropological

Thrinaxodon - A late Permian period mammal-like reptile that came very close to being a mammal. It was a carnivorous little creature that grew to about the size of a small dog. It's needle-sharp teeth were classic indications of its meat diet, being present in even the smallest (youngest) of specimens. It has been suggested that *Thrinaxodon* was an insect-eater, as well as a scavenger and a hunter of smaller animals. This interesting animal was a burrower.

3.2.1 Background

Many fossils of *Thrinaxodon* have been found that died in their sleep when their tunnels obviously collapsed in on them. They curled up just as a cat would when sleeping. There is disagreement between South African and American scientists about reconstruction of *Thrinaxodon*. Americans persist in putting fur on them as seen in Fig. 3.8, while South African scientists are adamant that fur had not evolved as a body covering 230 million years ago when these creatures were around. American scientists have also speculated that *Thrinaxodon* were territorial animals that scent-marked their territories. [15]

A plastic resin print was made from the original fossil. A great deal of rock was still inside the fossil. This rock was generally not removed, as it was too difficult to do and not easily accessible. The greyish resin fossil shown in Fig. 3.7, was CAT-scanned at Krugersdorp

Private Hospital. The data was retrieved and converted according to the procedure mentioned earlier.

This particular case study seemed to be uncomplicated and very exciting. The data was converted with great ease in a very short period. The next stage, namely converting into 3D imaging, also proceeded rapidly and effortlessly. A 3D model was created and a STL model was exported with the aid of the Materialise CTM software.

The STL file was imported into the QuickSlice software and processed. The processing took place on a Silicon Graphics Indy computer, called INDY1. The data processing failed miserably after two trials. The computer could not manage the large data files. The Quick Slice software was installed on the Silicon Graphics O2 computer, called LANCRE.

Various grow parameters were selected, and the data processing was started again. This computer processed successfully, generating the horizontal slice, SSL file as well as the machine language, SML file. The SML file was then transferred, via the LAN, with the aid of FTP, to INDY1 as it was connected directly to the FDM machines. The red ABS plastic prototype, shown in Fig. 3.7, was removed from the working envelope and the support structure was removed and cleaned.

3.2.2 Images

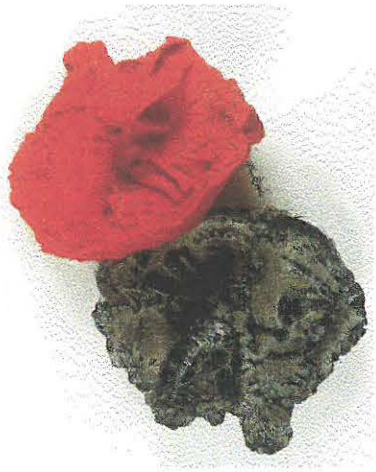

Figure 3.7 The Thrinaxodon Fossil (grey) and ABS Plastic Prototype (red)

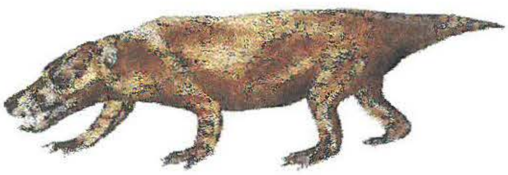

Figure 3.8 An artistic impression of the Thrinaxodon

3.2.3 *Thrinaxodon* Data Sheet:

	Description	Options/Units	Data
1	CT Image Names		bpi2.001
2	Patient/Project Name		bpi2.pat
3	Number of First Input Image		1
4	Number of Last Input Image		99
5	Number of First Output Image		000
6	CT or MRI	CT, MRI	CT
7	Horizontal No. of Image Pixels	0 to 65535 (265,512,1024)	512
8	Vertical No. of Image Pixels	0 to 65535 (265,512,1024)	512
9	Number of Images per File	(1)	1
10	File Swap Format (0,3)	0,3	CCELSC
11	Pixel Type	B,UB,S,US,L,UL,F	-
12	Inter Image Header Size	0	-
13	Add Value	0 to 4095	-
14	Scale Value	0 to 4095	-
15	Table Position	(mm)	0
16	Distance Between Slices	(mm)	1
17	Slice thickness	(mm)	1.2
18	Pixel Size SQ.	F.O.R./No. Hor. Pixels (mm)	0.47
19	Gantry Tilt Angle	Degrees	0
20	Field of Reconstruction/View	(mm)	240
21	Number of Images		99
22	File Size of CAT Image	Kb	75
23	File Size of Converted Image	Kb	60
24	.3dd file size	Mb	25
25	.STL file size	Mb	26.75
26	RP Method	(SLA,FDM,OTHER)	FDM
27	.IGS file size	Mb	-
28	RP Slice file size	Mb	9
29	RP Download File size	Mb	10.8
30	Grow Time	Hour	41.4
31	Tip size	(T12, T25)	T12
32	Slice Thickness	(0.01”, 0.014”)	0.01”
33	Finishing Time	Hour	4
34	Processing Time	Hour	2
35	Data Retrieval Time	Hour	4
36	Total Cost	Rand	=41.4*100+6*150+4*55+500 =5760

3.3 Cango Cave Buck - Anthropological

This fossil-related case study was selected, as there is very little chance that the fossil would be damaged during the process of capturing data by means of non contact RE methods. The fossil's geometry also challenged conventional RE methods in terms of material density and wall thickness variations as well as geometric complexity.

3.3.1 Background

The electronic data, as well as the final product, a prototype, would also be used to verify this archaeological finding. The National Museum requested that the geometry be captured, so that it can be used during discussions with other specialists. This buck fossil was found in the Cango caves near Oudtshoorn, Western Cape. This fossil was scanned at the Hydromed Hospital in Bloemfontein. The data transfer process is describe in section 2.8.2.

Fig. 3.9 shows more superior surface smoothness and detail than Fig. 3.10 due to finer scanning slices and 3D reconstruction parameters. The staircase ripple effect is clearly visible on the fossil in Fig. 3.10. Detail was also captured as can be seen in Fig. 3.9.

3.3.2 Images

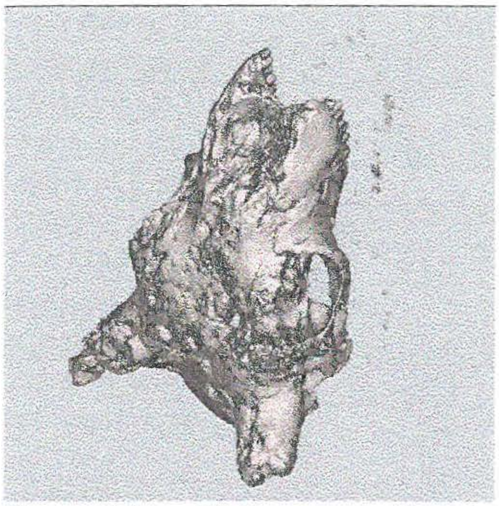

Figure 3.9 3D Reconstruction-1mm thick slices
(of the Cango Fossil- scanned at top right-hand view.)

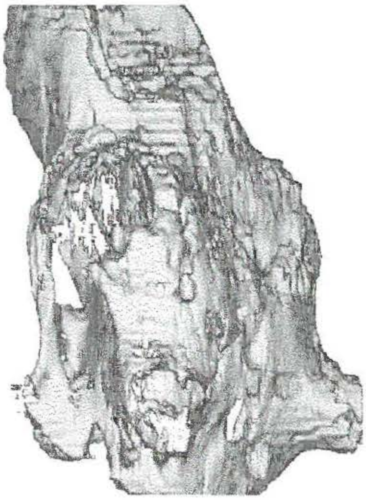

Figure 3.10 3D Reconstruction-3mm thick slices
(of the Cango Fossil scanned at top left-hand view.)

3.3.3 Cango Cave Buck Data Sheet:

	Description	Options/Units	Data
	CT Image Names		E6282S10I*.CT
2	Patient/Project Name		2S10I.pat, kbok.pat
3	Number of First Input Image		1/21
4	Number of Last Input Image		288/306
5	Number of First Output Image		000
6	CT or MRI	CT, MRI	CT
7	Horizontal No. of Image Pixels	0 to 65535 (265,512,1024)	512
8	Vertical No. of Image Pixels	0 to 65535 (265,512,1024)	512
9	Number of Images per File	(1)	1
10	File Swap Format (0,3)	0,3	CCGEADVA
11	Pixel Type	B,UB,S,US,L,UL,F	-
12	Inter Image Header Size	0	-
13	Add Value	0 to 4095	-
14	Scale Value	0 to 4095	-
15	Table Position	(mm)	0
16	Distance Between Slices	(mm)	1
17	Slice thickness	(mm)	1
18	Pixel Size SQ.	F.O.R./No. Hor. Pixels (mm)	0.47
19	Gantry Tilt Angle	Degrees	0
20	Field of Reconstruction/View	(mm)	240
21	Number of Images		288
22	File Size of CAT Image	Kb	270-280
23	File Size of Converted Image	Kb	20-35
24	.3dd file size	Mb	10.56 (.srf)
25	.STL file size	Mb	-
26	RP Method	(SLA,FDM,OTHER)	-
27	.IGS file size	Mb	-
28	RP Slice file size	Mb	-
29	RP Download File size	Mb	-
30	Grow Time	Hour	-
31	Tip size	(T12, T25)	-
32	Slice Thickness	(0.01", 0.014")	-
33	Finishing Time	Hour	-
34	Processing Time	Hour	3
35	Data Retrieval Time	Hour	4
36	Total Cost	Rand	=2*7*150+1166 =3266

3.4 Sea-horse - Anthropological

Resource Recovery Systems (Pty.) LTD, specialising in electro-forming, presented a nickel-plated sea-horse. This was made from an original sea-horse. The focus of this case study was to capture the geometry from the actual specimen, a sea-horse, and use it in the jewellery industry.

3.4.1 Background

The freeform geometric complexity made it difficult to use other RE methods. The C.S.I.R.'s high-resolution scanner later proved to be very effective during the RE process.

Fig. 3.11, 3.12 and 3.13 show 3D reconstructions of the 2D scanned data. Fig. 3.14 shows a photograph of the seahorse prototype, produced at twice the scale with the aid of FDM.

The C.S.I.R.'s high resolution Phillips CAT scanner was used. The sea-horse was fitted into the rotary table and secured with putty. CAT images were taken at 0,2 mm thick and at 0,2 mm intersections. Despite the thin slices, the staircase effect is still evident as can be seen in Fig. 3.11 and 3.12. This data were stored on the UNIX-based computer. Section 2.7 describes the process in more detail.

3.4.2 Images

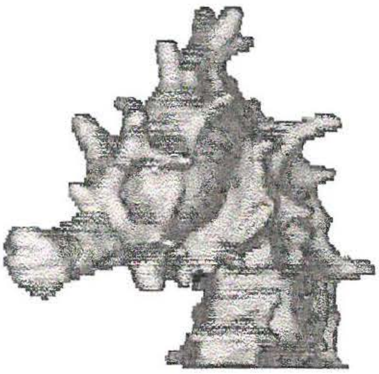

Figure 3.11 Frontal left hand view of the 3D reconstructed Sea-horse.

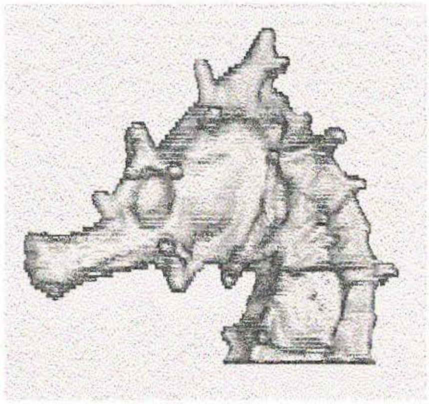

Figure 3.12 Left hand view of the 3D reconstructed Sea-horse.

Figure 3.13 Bottom view of the 3D reconstructed Sea-horse.

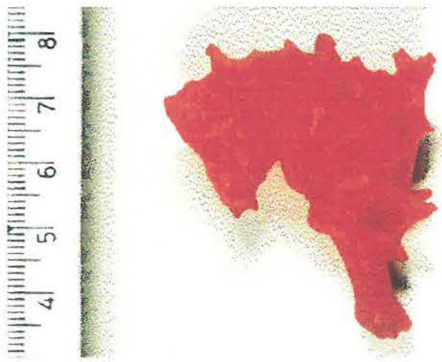

Figure 3.14 FDM Prototype of the Sea-horse

(scale 2:1. Material - Investment Casting Wax ICW06)

3.4.3 Sea-horse Data Sheet:

	Description	Options/Units	Data
	CT Image Names		shorse_1.01
	Patient/Project Name		sea-horse.pat
	Number of First Input Image		sea-horse00
	Number of Last Input Image		sea-horse85
	Number of First Output Image		000
	CT or MRI	CT, MRI	CT
	Horizontal No. of Image Pixels	0 to 65535 (265,512,1024)	512
	Vertical No. of Image Pixels	0 to 65535 (265,512,1024)	512
	Number of Images per File	(1)	1
0	File Swap Format (0,3)	0,3	3,CCUNF
1	Pixel Type	B,UB,S,US,L,UL,F	US
2	Add Value	0 to 4095	DEFAULT
3	Scale Value	0 to 4095	DEFAULT
4	Table Position	(mm)	30.2
5	Distance Between Slices	(mm)	0.2
6	Slice thickness	(mm)	0.2
7	Pixel Size SQ.	F.O.R./Nr. Hor. Pixels (mm)	0.078125
8	Gantry Tilt Angle	Degrees	0
9	Field of Reconstruction/View	(mm)	40
0	Number of Images		85
1	File Size of CAT Image	kb	315
2	File Size of Converted Image	kb	265
3	.3dd file size	Mb	0.198
4	.STL file size	Mb	14.31
5	RP Method	(SLA,FDM,OTHER)	SLA
6	.IGS file size	Mb	-
7	RP Slice file size	Mb	12
8	RP Download File size	Mb	13
9	Grow Time	Hour	4
0	Tip size	(T12, T25)	T12
1	Slice Thickness	(0.01", 0.014")	0.01"
2	Finishing Time	Hour	1
3	Processing Time	Hour	5
4	Data Retrieval Time	Hour	6
5	Total Cost	Rand	=11*150+ =1650

3.5 Meerkat Skull - Anthropological

The skull of a Meerkat was glued to an aluminium fixture. The fixture was designed to be used with both the CAT scanner and CMM and manufactured by a precision toolmaker. The fixture has three cylindrical pins used to register the two data sets. See figure 3.15. The aim of this study was to compare the accuracy of the two different RE systems.

3.5.1 Background

The case study was used to evaluate the accuracy of the CAT scanner. A certain area of the skull was selected to perform the dimensional tests. The area had to be easily accessible by the CMM touch probe. The curvature of the selected area also had to be constant to simplify the probe compensation.

The fixed skull was placed in the CAT scanner and a series of images was taken. The fixture had to be lifted by about 10 mm to fit into the vertical workspace. The region of interest was scanned to obtain the same cross section in the same orientation as with the CMM. The 2D CAT scanned data was retrieved and converted by using the Materialise software.

The next step was to sample 3D point data of the skull, at the area of interest. ASCII data of the 3D co-ordinate points was then transferred to the HP computer with the aid of FTP.

The Surfacer software package was used to import the CMM point co-ordinate data and to place splines through the selected points. A series of axial sections was produced.

Both CAT and CMM data sets were exported to IGES format. Intergraph EMS software was used to import the data sets into one file. The CMM data set was rotated by 90 degrees and moved to match the CAT-scanned data set. A surface was placed through the CAT-scanned spline data set. A parametric point language programme was used to determine the variation between the two systems of approximately 0.2mm.

3.5.2 Images

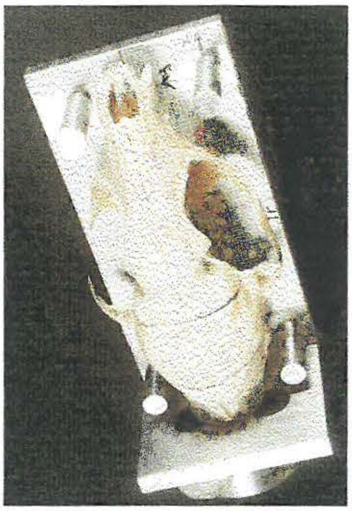

Figure 3.15 Meerkat Skull mounted onto the aluminium fixture.

3.5.3 Meerkat Skull Data Sheet:

	Description	Options (Default)	Data
1	CT Image Names		fos.00
2	Patient/Project Name		fos.pat
3	Number of First Input Image		27/01
4	Number of Last Input Image		157/99
5	Number of First Output Image		000
6	CT or MRI	CT, MRI	CT
7	Horizontal No. of Image Pixels	0 to 65535 (265,512,1024)	512
8	Vertical No. of Image Pixels	0 to 65535 (265,512,1024)	512
9	Number of Images per File	(1)	1
10	File Swap Format (0,3)	0,3	0
11	Pixel Type	B,UB,S,US,L,UL,F	US
12	Inter Image Header Size	0	-
13	Add Value	0 to 4095	-
14	Scale Value	0 to 4095	-
15	Table Position	(mm)	0
16	Distance Between Slices	(mm)	1
17	Slice thickness	(mm)	0.2
18	Pixel Size SQ.	F.O.R./No. Hor. Pixels (mm)	0.13
19	Gantry Tilt Angle	Degrees	0
20	Field of Reconstruction/View	(mm)	69
21	Number of Images		99
22	File Size of CAT Image	kb	265
23	File Size of Converted Image	kb	215
24	.3dd file size	Mb	4
25	.STL file size	Mb	17
26	RP Method	(SLA,FDM,OTHER)	FDM
27	.IGS file size	Mb	4
28	RP Slice file size	Mb	12
29	RP Download File size	Mb	14
30	Grow Timc	Hour	4
31	Tip size	(T12, T25)	T12
32	Slice Thickness	(0.01", 0.014")	0.01"
33	Finishing Time	Hour	2
34	Processing Time	Hour	5
35	Data Retrieval Time	Hour	4
36	Total Cost	Rand	=11*100=1100

3.6 Taung Child Skull - Anthropological

Australopithecus Africanus

TIME: Tertiary (Late Pliocene)

LOCALITY: Africa (Ethiopia, Kenya, South Africa and Tanzania)

SIZE: 4 ft 4 in/1.3 m tall

The skull of an infant specimen of A. Africanus--"southern ape of Africa"--was unearthed in the Transvaal in 1924. It was largely disregarded by anthropologists of the time, who thought that human origins lay with another fossil found some years earlier in Piltdown in Southern England. This latter fossil, which appeared to possess a large brain, was later proved a fake.

3.6.1 Background

A. Africanus is now rightly regarded as a hominid; one which lived from about 3 million to about 1 million years ago. Even if A. Africanus was not our direct ancestor, it was certainly very close. The brain was small by modern standards, being about the same size as a chimpanzee's (up to 400 cc), and the face still had heavy, apelike jaws. The canines were reasonably large, but in other respects, the teeth were quite human. Like A. Afarensis, it was a slightly built creature, weighing about 65lb/30 kg, which walked upright, see Fig. 3.16.

More important than its overall appearance though, was its lifestyle. Some have claimed that it had moved from woodland to open savannah. Tools and co-operative hunting techniques were already developed. To such a gang of individuals, hunting down and killing a single animal or chasing away another animal from its kill. Others argue that the evidence is equivocal. The bone "tools" are so ill-formed that they are probably nothing more than the remains of a hyena's meal. Although hunting was probably significant in human evolution, it is likely that plants--including seeds, nuts, fruit, leaves, stems and roots--formed the major part of the diet.[16]

The skull of a Taung child fossil, shown in Fig. 3.17, 3.18 and 3.19, was used in the process to evaluate the system further. This fossil consists of three parts, the brain area, the front facial section and part of the lower jaw. Anthropologists used this fossil to reconstruct a complete skull of the Taung child. The reconstructed skull and jaw were also scanned in order to capture the geometry as can be seen in Fig. 3.20 and Fig. 3.21.

New computer technologies allows sculptors to digitally sculpt. This RE method can be used to capture the geometry of an existing fossil, convert it for the sculptor who can in turn use it to build-up the flesh, muscle and skin around the bone structure.

Hydromed Hospital at Bloemfontein scanned these parts. The data was retrieved and converted according to the data retrieval procedure section 2.8.2.

3.6.2 Images

Figure 3.16 Representation of the Australopithecus Africanus

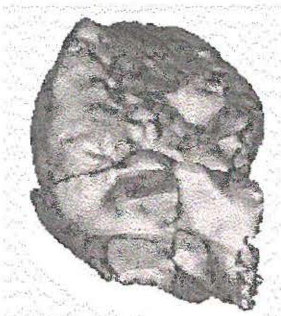

Figure 3.17 3D Image of the Taung Child fossil's skull

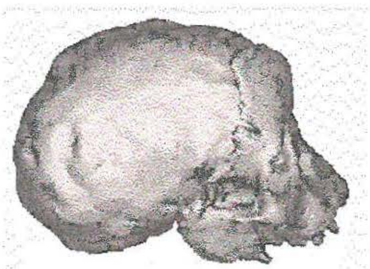

Figure 3.18 The three parts of the Taung Child fossil, side view.

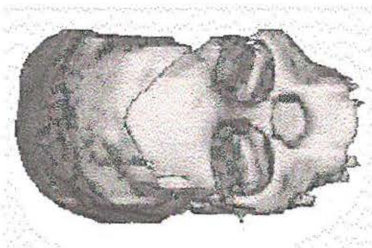

Figure 3.19 CAT-scanned 3D reconstructed image, frontal top view.

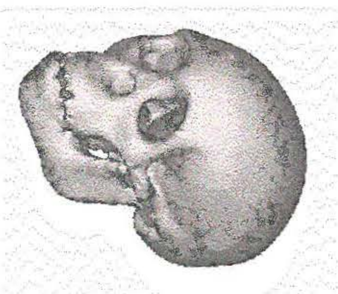

Figure 3.20 3D image of the complete reconstructed skull, frontal side view.

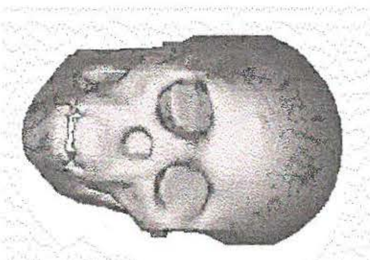

Figure 3.21 Another representation of the reconstructed skull, frontal top view.

3.6.3 Taung Child Skull Data Sheet:

	Description	Options/Units	Data
1	CT Image Names		Taung.00
2	Patient/Project Name		Taung.pat
3	Number of First Input Image		34.5
4	Number of Last Input Image		133.5
5	Number of First Output Image		000
6	CT or MRI	CT, MRI	CT
7	Horizontal No. of Image Pixels	0 to 65535 (265,512,1024)	512
8	Vertical No. of Image Pixels	0 to 65535 (265,512,1024)	512
9	Number of Images per File	(1)	1
10	File Swap Format (0,3)	0,3	0
11	Pixel Type	B,UB,S,US,L,UL,F	GEADVA
12	Inter Image Header Size	0	-
13	Add Value	0 to 4095	-
14	Scale Value	0 to 4095	-
15	Table Position	(mm)	34.5
16	Distance Between Slices	(mm)	3
17	Slice thickness	(mm)	3
18	Pixel Size SQ.	F.O.R./No. Hor. Pixels (mm)	0.36
19	Gantry Tilt Angle	Degrees	0
20	Field of Reconstruction/View	(mm)	185
21	Number of Images		33
22	File Size of CAT Image	kb	270-285
23	File Size of Converted Image	kb	11-55
24	.3dd file size	Mb	1.2,1.4
25	.STL file size	Mb	9.4, 12.5
26	RP Method	(SLA,FDM,OTHER)	-
27	.IGS file size	Mb	-
28	RP Slice file size	Mb	-
29	RP Download File size	Mb	-
30	Grow Time	Hour	-
31	Tip size	(T12, T25)	-
32	Slice Thickness	(0.01", 0.014")	-
33	Finishing Time	Hour	-
34	Processing Time	Hour	-
35	Data Retrieval Time	Hour	-
36	Total Cost	Rand	=33*100=3300

3.7 Discussion of Anthropological Case Studies

3.7.1 Advantages

3.7.1.1 Non-destructive Analysis

Referring to the *Lystrosaurus* data sheet, the fossil could be digitally retrieved from the rock in about 14 hours, which costs about R2 400, excluding the CAT scanning. 3D reconstructed renderings of the fossil hidden in the rock can be produced at this stage. True 3D data can be generated. One can only appreciate the benefit of this new process when it is compared with the old manual method of rock removal, taking several weeks to extract the fossil from the rock. There may not be a great cost saving at this stage. However, with this method, one can very quickly determine what is inside the rock, the position and orientation of the fossil in the rock. Several weeks may be spent extracting the fossil from the rock and the fossil may not be of great value or importance. It will therefore streamline the process. Making use of this technology will enable the anthropologist to be more productive and efficient. The internal geometry of the fossil can also be visualised. The conventional manual method very often only succeeds in removing the rock from the outer boundary.

3.7.1.2 Geometric Complexity

This is the ideal method for capturing complex, low-tolerance and detailed geometry. Virtual reality and digital sculpting programmes can be used to realistically visualise the fossil. The nature of the geometry is extremely complex and free form in nature. The fossils featured have many undercuts and hard-to-reach areas. No conventional 3- or 4-axis scanning system can be used to capture this geometry successfully. CAT scanning is the only method to reverse engineer these parts. The X-rays penetrated the hard-to-reach areas and undercut sections very easily and cost-effectively. Again accuracy was not of great importance which made this reverse engineering technique ideal to use.

3.7.1.3 The Digital Format

The RE method was used to capture the geometry and convert it into a digital format so that it could be used in other post-processes such as virtual reality, rapid prototyping and animation applications. This process provided the possibility of the 3D data of rare and fragile fossils being shared and distributed internationally.

3.7.2 Process Limitations

3.7.2.1 Slice Interval

The Cango Buck fossil was scanned twice. The first time the fossil was scanned, the data was reconstructed at 3 mm thick slices and 3 mm thick intervals. The 3D reconstruction resulted in a staircase effect and produced a poor surface finish. The staircase effect could be reduced by increasing the smoothing factor, one of the software features. A great deal of data was so lost due to the coarse scanning reconstruction. The second scan was reconstructed to 1 mm thick slices and 1 mm intervals. This 3D reconstruction clearly showed better results. Bone detail was missing, most probably due to the thin bone sections and low bone density. The small sea-horse specimen needed to be scanned at a minimum of 0,2 mm slices and intervals to capture the fine, detailed geometry. It could only be done by using a high-resolution industrial CAT scanner. Medical CAT scanners can scan with a minimum slice thickness of 0,5 mm thick.

3.7.2.2 Data Storage and Processing

The data was often stored in three sets of about 45 slices each during the CAT scanning stage. This was also done to allow the X-ray tube to cool down during scanning and storing stages. It also allowed a time delay for the computer to process the data. The data was stored on the computer's hard drive in different directories and processed separately. Surface files were generated (.srf) from the 2D CAT-scanned images. The various .srf files could not be joined at a later stage for 3D image processing, as they were stored in different directories. Moving the files into one directory did not solve the problem. The original CAT 2D images were copied to a new directory where the data was converted and processed again, in order to view it as one entity.

The one 486 UNIX-based computer (C.S.I.R. Apparatus) needs to be upgraded to accommodate larger sets of data storage and processing. It requires a larger hard drive and more RAM capacity, as well as a faster processor unit. CAT scanning can be done overnight if properly planned. Only sets of maximum 16 images could be converted simultaneously with this particular system. Better planning will reduce the time to manipulate the two data sets to place them in the same co-ordinate system.

3.7.2.3 Storage Media

Varieties of CAT-scanning systems were used. The standard media for data storage of medical CAT-scanning devices is called a magnetic optical disk (MOD). Each system, however, has its own type of MOD. The method of storing the data to the MOD also varies with the different types of CAT-scanning machines.

4 mm DAT and 1/4" data cartridges or magnetic tape drives are also available in some cases. Data can also be stored on a laptop computer when it is connected to the CAT scanner. Another alternative storing system can be via the local area network (LAN) to another computer. Siemens and G.E. offered to assist in converting the data from MOD to compact disk (CD) with the aid of a CD writer.

The variety of storing devices and systems makes it difficult and expensive to make provision for the whole range. One should at least be able to read CDROM, DAT and 1/4" tape media.

3.7.2.4 Material Properties

A wide variety of different materials were scanned during the case studies. The following material properties affected the CAT-scanning results:

- Material Density
- Material Wall Thickness
- Material Magnetic Properties

A great deal of data was also lost due to low bone density and thin bone sections. A good example of this is the lack of detail captured in the cartilage region of the Cango Buck fossil. A substantial difference of density variation is also required to digitally separate some of the sections from one part, as described in the *Lystrosaurus* case study. A variety in material properties affects the accuracy dramatically. The average deviation was less than 0,2 mm. The pixel size was 0,13 mm. In the case of the Lystrosaurus, the fossil and the rock densities were almost similar. This made the process more complicated and required a lot of manual editing to obtain reasonable results. Density variation in one item can also complicate the process.

4 Medical Case Studies

4.1 Human Maxilla and Mandible - Medical

The maxillary bone, or maxilla, of the skull holds the upper teeth and encloses the opening for the nasal passage. The upper part of the bone meets the parietal and nasal bone between the eyes. The maxilla also meets the zygomatic bone (cheekbone) below the eye. The lower part of the maxilla has sockets for the eight teeth of one side of the upper jaw, shown in Fig. 5.1. Behind this, the maxilla also forms the front part of the roof of the mouth, or hard palate, which creates a firm resistance when the tongue is manipulating food in the mouth. This palate also separates the mouth from the air passage that leads from the nose to just above the windpipe at the back of the throat. [13], [14]

The mandible (jawbone), shown in Fig. 4.2 and 4.3, is connected to the upper part of the skull, or cranium, at a joint in the temporal bone. It contains the sockets for the 16 lower teeth. Like some of the bones of the skull, it first appears in the developing baby, or fetus, as a pair of bones, but these later fuses together to make the mandible stronger.

The mandible has to be strong, since strong muscles are connected to it.

The temporal muscle is attached to part of the front of the jaw joint, known as the coronoid process. The masseter muscle is attached to the angle of the jaw. Both of these muscles are used when chewing or closing the mouth. The mouth is opened by using the digastric muscle. It is connected to the back of the mandible under the chin, and the lateral pterygoid muscle, which runs from the inner side of the jaw to the underside of the skull.

Adults have eight teeth in each quarter of the mouth - two incisor teeth, one canine tooth, two premolar teeth and three molar teeth, totalling 32 teeth in the whole of the mouth. This adult set of teeth is unlike the first set of baby teeth, called "milk teeth." Milk teeth do not include any molar teeth, so children only have five teeth in each quarter of the mouth, and therefore have only 20 teeth altogether.

Both adult and milk teeth are sunk into sockets in the bones that hold them - the upper teeth are held in the maxilla (a bone of the skull), and the lower teeth are held in the mandible (jawbone). The roots of the teeth are up to twice as long as the part of the tooth that can be seen above the gum.

4.1.1 Background

A 41-year-old female patient required a dental implant. The prostodontist was contacted and it was agreed that it would be of great value to capture the geometry of the maxilla and mandible to determine if there was sufficient bone structure required for an operation of this nature. The patient was scanned at Morningside Clinic with the aid of their Toshiba Spiral X-Vision/GX CAT Scanner. From the spiral data, sagittal and coronal multi-planar reconstruction images were made. The CAT-scanned film was used to verify the converted data. This was useful. However, the film did not represent the axial CAT scan images that were used to reconstruct the 3D data. Reference [29] p. 44, recommended a 1.5 mm slice thickness with a 1 mm table feed. The X-ray energy should not exceed 100 mA per section. The patient's head needs to be fixed securely.

Permission was granted for retrieving this patient's data from the CAT scanner.

4.1.2 Images

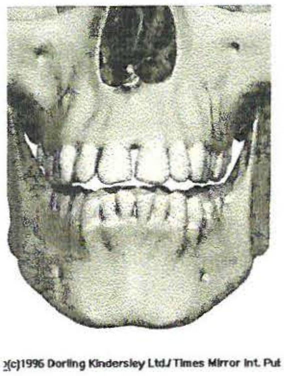

Figure 4.1 The Human Maxilla and Mandible.

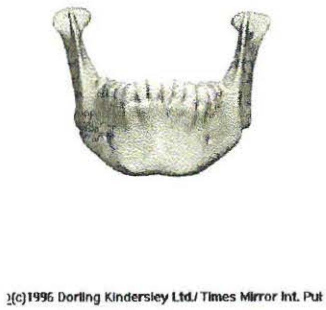

Figure 4.2 The Human Mandible, front view.

Figure 4.3 The Human Mandible, side view.

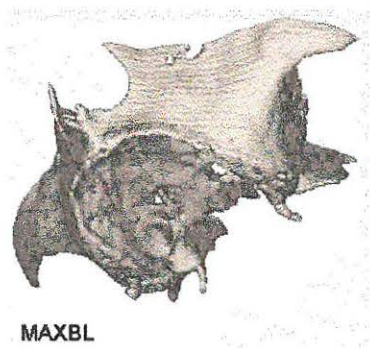

Figure 4.4 The patient's reconstructed Maxilla.

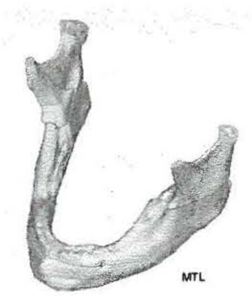

Figure 4.5 The patient's reconstructed Mandible

Figure 4.6 FDM Prototypes

(The patient's Mandible and Maxilla with dental implants fitted.)

4.1.3 Maxilla and Mandible Data Sheet:

Description	Options (Default)	Data Maxilla	Data Mandible
CT Image Names		cruz	cruz
Patient/Project Name		cruz.pat	cruz.pat
Number of First Input Image		1:643:9/-19.5	1:643:9/-19.5
Number of Last Input Image		1:643:155/53.5	1:643:155/53.5
Number of First Output Image		000	000
CT or MRI	CT, MRI	CT	CT
Horizontal No. of Image Pixels	0 to 65535 (265,512,1024)	512	512
Vertical No. of Image Pixels	0 to 65535 (265,512,1024)	512	512
Number of Images per File	(1)	1	1
File Swap Format (0,3)	0,3	0	0
Pixel Type	B,UB,S,US,L,UL,F	S	S
Header Size		8704	8704
Inter Image Header Size	0	0	0
Add Value	0 to 4095	2048	2048
Scale Value	0 to 4095	1.8	1.8
Table Position	(mm)	0	0
Distance Between Slices	(mm)	0.5	0.5
Slice thickness	(mm)	3	3
Pixel Size SQ.	(mm)	0.2598	0.2598
Gantry Tilt Angle	Degrees	0	0
Field of Reconstruction/View	(mm)	133	133
Number of Images		146	146
File Size of CAT Image	kb	252	252
File Size of Converted Image	kb	180	180
.3dd file size	Mb	15	13
.STL file size	Mb	26.37	32
RP Method	(SLA,FDM,OTHER)	FDM	FDM
.IGS file size	Mb	-	-
RP Slice file size	Mb	6.79	3.7
RP Download File size	Mb	5.9	7.6
Grow Time	Hour	18.25	23.75
Tip size	(T12, T25)	T12	T12
Slice Thickness	(0.01", 0.014")	0.01"	0.01"
Finishing Time	Hour	8	6
Processing Time	Hour	6	6
Data Retrieval Time	Hour	2	2
Total Cost	Rand	=1500+330+ 1825 = 3655	=8*150+6*55+ 2375 = 3905

4.2 Human Pelvis - Medical

The hipbone is attached to the vertebral column (backbone) by the five sacral vertebrae, which fuse together in the adult to form the sacrum.

The hip joint is on the side of the hipbone, rather than underneath it . There is a deep socket for the head of the femur (thighbone) at the hip joint. This provides more space for the muscles on the inner side of the thigh. See Fig. 4.7 and 4.8.

The knee joints are closer to a middle line drawn vertically through the body. This means the knees are closer to the centre of gravity of the body and give more stability. The femur, therefore, has to run inward, as well as downward, to meet the knee joint.

The femur forms the upper part of the leg. It not only supports the body when standing, but is also used when walking, running, jumping, climbing or squatting. Therefore, it is the largest and strongest bone in the body.

The femur is also the longest bone, making up over a quarter of a human being's total height. The size of the femur makes it prone to injury.

The rounded upper end of the femur meets the hipbone at the hip joint, which is a ball-and-socket joint. A narrower neck runs sideways and downward to meet the shaft of the bone. Near the upper end of the femur are two projections, and it is here that muscles are attached to the bone. At the lower end of the bone, two rounded surfaces fit into two small hollows on the upper end of the tibia (main shinbone). This forms the knee joint. [13], [14] Reference [29] p. 20, recommended scanning parameters of 10 mm slice thickness with 10 mm table feed. Reconstruction to thinner slice thickness was required for realistic imaging. CAT parameters such as 300 mm F.O.V., 120 kV and 50 to 100 mA can be used.

4.2.1 Background

A male patient required a hip transplant. The orthopaedic surgeon was contacted and it was suggested that it would be of great value to capture the geometry of the pelvis to determine if there was sufficient bone structure as required for an operation of this nature.

The patient was scanned at Morningside Clinic with the aid of their Toshiba Spiral X-Vision/GX CAT Scanner. Permission was granted that this patient's data could be retrieved from the CAT scanner. Morning Side Clinic prepared a 3D visualisation of the scanned area. The spiral data were prepared in two sets to evaluate the difference. The radiologist firstly prepared one set of 33 mm thick slices and 3 mm intervals or spacing. The finest possible slice thickness and slice spacing were requested to achieve the best results. In this case it was considered better to sample more data than required.

The right-hand pelvis and femur were in a developed state of deterioration. The orthopaedic surgeon was particularly interested in the left-hand pelvis. For a successful hip replacement, sufficient bone structure is required at the back of the pelvis. It was quite clear that the front side of the pelvis did not have sufficient bone structure. The most probable cause of the poor state of the pelvis could be a form of osteoporosis. The data processing of this case was particularly difficult. The fibre, soft tissue and muscle suspended bone particles. The pelvis needed to be separated from the other bone and soft tissue. The pelvis and femur were hardly recognisable in certain areas. It was therefore difficult to decide what bone structure formed part of the pelvis and what part was suspended by soft tissue.

The orthopaedic surgeon provided the left-hand side of a real human pelvis for reference. CAT-scanned film was also provided with 2D-slice information, as well as 3D rendering to be used for verification, as shown in Fig. 4.9 and 4.10. The data were then processed and a meeting was arranged with the orthopaedic surgeon to verify the results of the computer screen. He was pleased with the results and requested continuation to the next phase of the project.

The next stage was to create a prototype of the pelvis. The 3dd file was used with the Materialise CTM software to generate a STL format file. The STL file was then used with the Stratasys QuickSlice software. Horizontal slices were created. The software automatically performed support generation. The SML file was created. The prototype was grown with the red ABS plastic material, shown in Fig. 4.11 and 4.12, and finished by removing the support structure generated by the FDM process.

The prototype of the pelvis was supplied to the orthopaedic surgeon. Later he temporarily fitted a cup to the pelvis prototype, with the aid of bonding putty, to display the principle of fitting the cup into the pelvis, as shown in Fig 4.11 and 4.12. Areas where bone and bone cement would normally be filled in with bone cement were left out to view the detail of the pelvis's condition.

4.2.2 Images

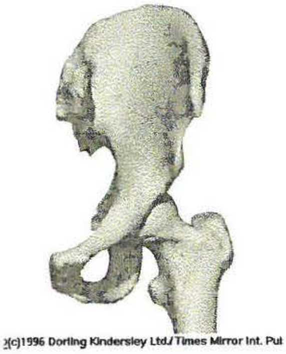

Figure 4.7 The Human Pelvis and Femur.

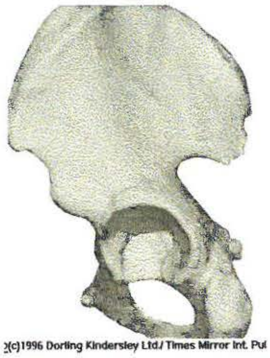

Figure 4.8 The Human Pelvis.

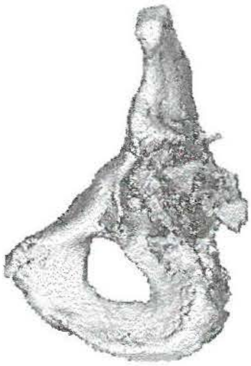

Figure 4.9 3D reconstruction of the patient's Pelvis.

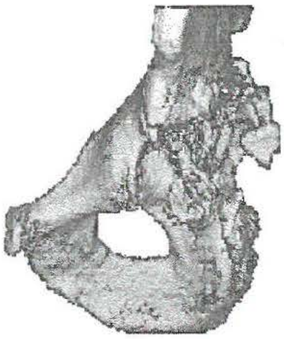

Figure 4.10 3D reconstruction of the patient's Pelvis.

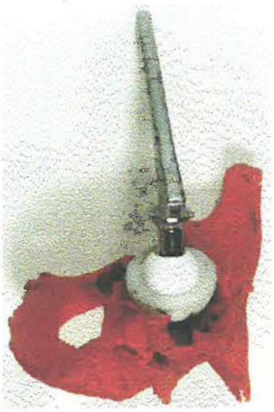

Figure 4.11 FDM prototype of the patient's Pelvis with prosthesis fitted.

Figure 4.12 FDM prototype of the patient's Pelvis with prosthesis fitted.

4.2.3 Pelvis Data Sheet:

Description	Options/Units	Data
CT Image Names		566:227 - 527
Patient/Project Name		hip3
Number of First Input Image		566:227
Number of Last Input Image		566:526
Number of First Output Image		hip3.000
CT or MRI	CT, MRI	CT
Horizontal No. of Image Pixels	0 to 65535 (265,512,1024)	512
Vertical No. of Image Pixels	0 to 65535 (265,512,1024)	512
Number of Images per File	(1)	1
File Swap Format (0,3)	0,3	0
Pixel Type	B,UB,S,US,L,UL,F	S
Header Size		8704
Inter Image Header Size	0	0
Add Value	0 to 4095	2048
Scale Value	0 to 4095	1.1
Table Position	(mm)	0
Distance Between Slices	(mm)	0.5
Slice thickness	(mm)	3
Pixel Size SQ.	F.O.R./No. Hor. Pixels (mm)	0.71
Gantry Tilt Angle	Degrees	0
Field of Reconstruction/View	(mm)	364
Number of Images		257
File Size of CAT Image	Kb	215
File Size of Converted Image	Kb	215
.3dd file size	Mb	0.742 *.3dd
.STL file size	Mb	34.62 , pellft.stl
RP Method	(SLA,FDM,OTHER)	FDM
.IGS file size	Mb	-
RP Slice file size	Mb	34.19, pellft.ssl
RP Download File size	Mb	34.46
Grow Time	Hour	109.9
Tip size	(T12, T25)	T12
Slice Thickness	(0.01", 0.014")	0.01"
Finishing Time	Hour	6
Processing Time	Hour	5
Data Retrieval Time	Hour	4
Total Cost	Rand	=109.9*100+6*55+9*150 =12670

4.3 Human Brain - Medical

The brain is encased in the bony skull and floats in a pool of cerebrospinal fluid, which protects the brain from shock waves. The brain is divided in several regions, each with its own important functions.

The brain monitors and regulates many unconscious bodily processes, as well as being the site of conscious and intellectual memory and emotions. The brain weighs about 1,3 kg and contains over 100 billion nerve cells and millions of supporting cells.

Although the brain accounts for only 2 % of a person's body weight, it requires 20 % of the body's blood.

Humans have the most complex brain of all animals. It provides humans with the power of original thought as well as communication by means of speech and writing. [14], [2]

5.3.1 Background

Data were retrieved from the General Electric MRI scanner at Hydromed Hospital, Bloemfontein. The 2D CAT-scanned images were imported by using the GE ADVANTAGE program. The Materialise Mimics software was used during this phase. The cerebellum was separated from the rest of the body by using a mask command. This case study was performed to investigate the method of data retrieval and conversion on a MRI scanner.

4.3.2 Images

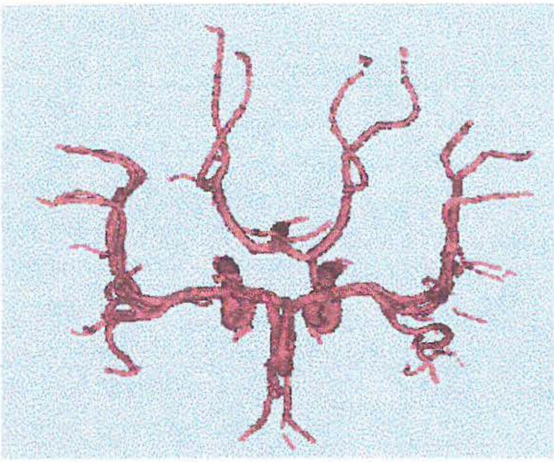

Figure 4.13 Human Brain artery network, top view.

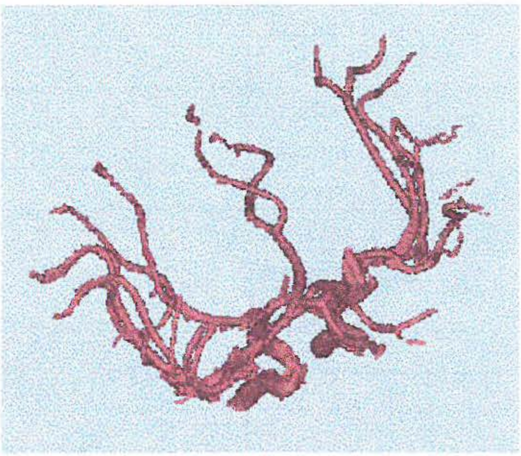

Figure 4.14 Human Brain artery network, top right hand view.

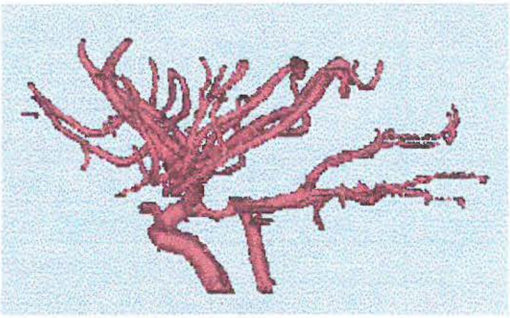

Figure 4.15 Human Brain artery network, frontal left hand view.

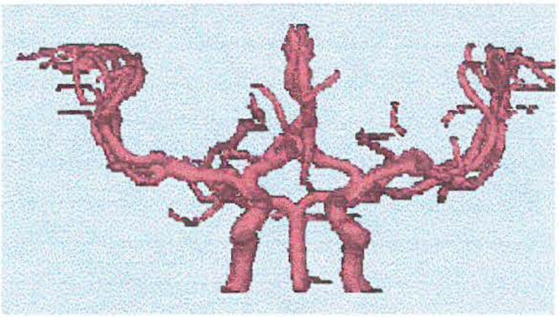

Figure 4.16 Human Brain artery network, frontal view.

4.3.3 Brain Data Sheet:

Description	Options/Units	Data
CT Image Names		brain
Patient/Project Name		brainm
Number of First Input Image		brainm_1.000 @ -26.5
Number of Last Input Image		brainm_1.060 @ 32.5
Number of First Output Image		brainmri.000
CT or MRI	CT, MRI	MRI
Horizontal No. of Image Pixels	0 to 65535 (265,512,1024)	512
Vertical No. of Image Pixels	0 to 65535 (265,512,1024)	448
Number of Images per File	(1)	1
File Swap Format (0,3)	0,3	CCGEADVA
Pixel Type	B,UB,S,US,L,UL,F	-
Inter Image Header Size	0	-
Add Value	0 to 4095	-
Scale Value	0 to 4095	-
Table Position	(mm)	-
Distance Between Slices	(mm)	1
Slice thickness	(mm)	3
Pixel Size SQ.	F.O.R./No. Hor. Pixels (mm)	0.39
Gantry Tilt Angle	Degrees	0
Field of Reconstruction/View	(mm)	200(150)
Number of Images		60
File Size of CAT Image	Kb	265
File Size of Converted Image	Kb	203-227
.3dd file size	Mb	6.7-17
.STL file size	Mb	-
RP Method	(SLA,FDM,OTHER)	-
.IGS file size	Mb	-
RP Slice file size	Mb	-
RP Download File size	Mb	-
Grow Time	Hour	-
Tip size	(T12, T25)	-
Slice Thickness	(0.01", 0.014")	-
Finishing Time	Hour	-
Processing Time	Hour	2
Data Retrieval Time	Hour	2
Total Cost	Rand	600

4.4 Maxilla Cranio Facial – Medical

This case study again shows the necessity of rapid prototyping in medicine.

4.4.1 Background

The patient, a three-year-old boy, was scanned at the Pretoria East Hospital Clinic with the aid of their Toshiba Spiral X-Vision/GX CAT Scanner. The 2D CAT slices were again stored on ¼" data cartridge magnetic tape. 2D CAT images of various positions were stored on film for record-keeping purposes.

The patient required maxilla cranio-facial surgery. Maxilla-Facial specialists from the University of Pretoria requested a prototype of the patient's skull. The skull was required for pre-surgical planning.

Permission was granted so that this patient's data could be retrieved from the CAT scanner. Pretoria East Hospital prepared a 3D visualisation of the scanned area. The spiral data were prepared in one set. The radiology team prepared one set of 3 mm thick slices and 3 mm intervals or spacing. The finest possible slice thickness and slice spacing were again requested to obtain the best results. In this case it would be better to sample more data than required. The CAT scanner parameters were restricted to scanning distance and slice thickness. The surgeon was particularly interested in the frontal or facial area of the skull. For a successful facial reconstruction, the facial geometry had to be known.

The data were then processed and a meeting was arranged with the surgeons to verify the results on the computer screen. They were pleased with the results and requested that we continue with the next phase of the project.

The next phase was to create a prototype of the skull. The 3dd file was used with the Materialise CTM software to generate a STL format file. The STL file was then used with the Stratasys QuickSlice software. Horizontal slices were created. The software performed support generation, automatically. The SML file was created. The FDM machines require this data to build a prototype. The prototype was grown with the red ICW06 wax material and finished by removing the support structure generated by the FDM process. The skull was grown in two sections to simplify the prototyping process. The removal of the support structure was made easier by growing the skull in two sections.

The prototype of the skull was supplied to the maxilla-facial surgeons. This prototype could only be used for visual inspection. Wax prototypes are very fragile and can break easily when handled. It also does not machine easily. A bronze casting was made from this wax skull with the aid of the investment casting process. A second skull prototype was produced by a group in Holland. The skull was produced in the glass-filled nylon material with the aid of SLS rapid prototyping technology.

Figures 4.17 and 4.18 shows axial CAT scan cross sections of the patient's skull. These black and white images represent the grey scale principle earlier discussed in section 2.6.6. Fig. 4.19 and 4.20 shows the prototypes grown with the aid of the SLS rapid prototype technology. Fig. 4.22 clearly shows the metal brace fitted to the skull above the left eyebrow and the eye cut out section as the surgeons later performed the operation. Fig.

4.21 shows the wax prototype grown with the aid of the FDM rapid prototyping technology. This wax prototype was then later converted to the bronze investment cast model shown in figure 4.20. Fig. 4.23 and 4.24 shows digital images of the 3D reconstructions generated from 2D CAT axial slices. Fig. 4.23 shows the combination of soft tissue, digitally made slightly transparent and the skull, bone section colored green. Fig. 4.25 and 4.26 shows photographs taken during the complex operation.

4.4.2 Images

Figure 4.17 2D CAT scan slice at the 1100 position

Figure 4.18 2D CAT scan slice at the 1080 position

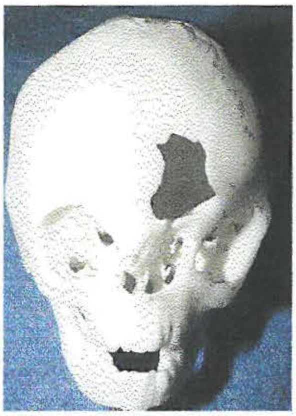

Figure 4.19 SLS skull prototype in GF nylon

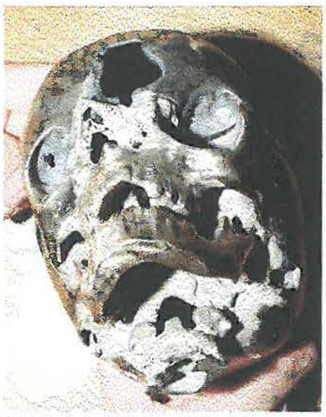

Figure 4.20 Bronze casting of the skull

Figure 4.21 FDM skull prototype in ICW06 wax.

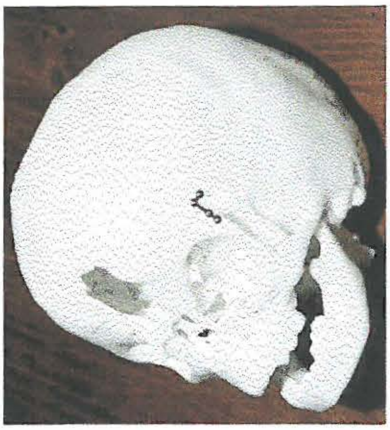

Figure 4.22 Surgical Reconstructed SLS prototype.

Figure 4.23 3D Image of skull, combines soft and hard tissue.

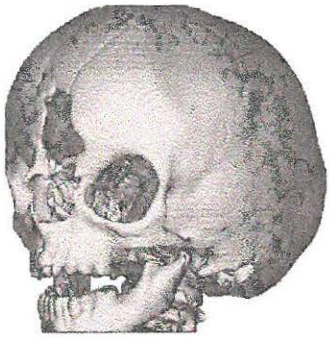

Figure 4.24 3D Image of skull, bone structure only.

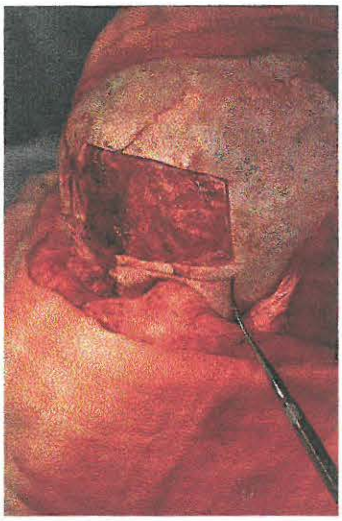

Figure 4.25 Skull sections already cut and removed.

Figure 4.26 The metal brace fitted.

4.4.3 Maxilla Cranio Facial Data Sheet:

Description	Options/Units	Data
CT Image Names		seun.00
Patient/Project Name		seun.pat
Number of First Input Image		1.6912.2
Number of Last Input Image		1.6912.319
Number of First Output Image		seun.00
CT or MRI	CT, MRI	CT
Horizontal No. of Image Pixels	0 to 65535 (265,512,1024)	512
Vertical No. of Image Pixels	0 to 65535 (265,512,1024)	512
Number of Images per File	(1)	1
File Swap Format (0,3)	0,3	Toshiba
Pixel Type	B,UB,S,US,L,UL,F	-
Inter Image Header Size	0	-
Add Value	0 to 4095	-
Scale Value	0 to 4095	-
Table Position	(mm)	-1021.5
Distance Between Slices	(mm)	3 recon to 1
Slice thickness	(mm)	3 recon to 1
Pixel Size SQ.	F.O.R./No. Hor. Pixels (mm)	0.39
Gantry Tilt Angle	Degrees	0
Field of Reconstruction/View	(mm)	200
Number of Images		154
File Size of CAT Image	Kb	521
File Size of Converted Image	Kb	76-131
.3dd file size	Mb	6*.srf
.STL file size	Mb	96, 17.9 with filter
RP Method	(SLA,FDM,OTHER)	FDM, SLS
.IGS file size	Mb	-
RP Slice file size	Mb	28.9+19.4
RP Download File size	Mb	12.1+13.9
Grow Time	Hour	132.9
Tip size	(T12, T25)	T12
Slice Thickness	(0.01", 0.014")	0.01"
Finishing Time	Hour	8
Processing Time	Hour	16
Data Retrieval Time	Hour	3
Total Cost	Rand	=27*250+7500=14250

4.5 Discussion of Medical Case Studies

4.5.1 Advantages

4.5.1.1 Pre-operative Planning

The Selective Laser Sintering (SLS) System proved to be the best rapid prototyping (RP) system to produce prototypes for this application. It is of great use to produce prototypes without the generation of a support structure. The support structure always needs to be removed and very often causes problems to such an extent that the prototype is damaged. Stratasys has been performing research and material development in this field. Stratasys plans to have a soluble support material on the market. This support structure can then be dissolved in order to ease the support removal procedure.

The surgeons worked with ease using the nylon prototype during the pre-operative planning stage. The skull prototype was marked and cut in sections as the surgeons planned the operation. A brace was also fitted to reposition the eye socket section. Both the maxilla cranio-, facial- and neuro-surgeons frequently referred to the nylon skull prototype in theatre during the extremely complex eight-hour operation.
The bronze casting was made from the wax prototype. It proved to be useful for preserving the wax prototype. Casting imperfections such as pit holes were evident.

The reproduction of the pelvis enabled the orthopaedic surgeon to select the correct size of cup and prosthesis. The polypropylene cup and the metal prosthesis were fitted to the

ABS plastic pelvis. The orientation of these components could be determined prior to the operation. The finest resolution was often selected to produce a prototype with superb definition. It was the first series of medical case studies and it was necessary to capture and produce as much detail as possible to demonstrate the technology. The time of 110 hours taken to build a pelvis prototype can be reduced to a third. The cost of this phase will then drop accordingly. The total project time of 126.7 hours, for a pelvis case study, can be reduced to only 53.3 hours in future.

By supplying the prostodontist with a plastic maxilla and mandible enabled him to actually fit the metal implants, called abutments. These prototypes were used to confirm the prostodontist's diagnosis regarding the lack of bone in the maxilla region, making dental implants impossible in this region.

The brain study confirmed the usage of MRI scanning technology that can be included and combined with existing rapid prototyping technologies.

4.5.1.2 Virtual Reality Interface

This skull data was supplied to the C.S.I.R. Virtual Reality Centre. Initially they struggled to retrieve the data due to a lack of computer power. This skull is now used to demonstrate the virtual reality surgery concept to be used by medical students with the aid of a force feedback system. Some of the operation tools can be fitted to the force feedback device.

4.5.2 Process Limitations

4.5.2.1 Cost and Delivery

Both CAT scanning and RP processes are layer-based systems. More layers will take longer and cost more, but will result in improved detail. Similarly, less layers will also cost less, but will result in less detail. A fine balance needs to be obtained between the amount of detail and the cost involved, in order to achieve success.

It was suggested that surgeons would be very keen to obtain prototypes on a routine basis if the cost was in the region of several hundred Rand. Once a larger market is established, the cost can be reduced. Some of the patients can afford to pay for the cost of this technology themselves, but others are not so fortunate.

Delivery or turn-around time and cost are the most important factors for the medical specialists. The acceptable delivery time for a pelvis case study would be 3 to 5 days.

This can only be achieved by having a tape streamer fitted to the CAT scanner, so that data storage can take place without interrupting the radiologist's normal workflow. This would also require a dedicated RP system. Data retrieval should be more automated or should be performed after hours to avoid any interference with the radiology team's daily workload.

4.5.2.2 Dimensional Verification

Several measurements were taken at a particular slice regarding the maxilla case study. The dimensions varied from 0,46 mm in the z-axis to 1,48 mm in the xy-axis. If the pixel size was 0,26 mm, a tolerance of ±0.26 mm should be acceptable. The measurements in the 3D Mimics software were larger in both cases. It was very difficult to determine the accuracy as the printed 2D CAT scan images (multi-planar reconstruction) did not correlate with the axial CT images that were used to reconstruct the 3D model. In this particular case, the deviation might have been due to the thin bone section in the maxilla. The threshold may be set too low to obtain a full maxilla 3D image, but will result in an oversize mandible. It is mainly due to the large difference in bone density between the teeth and jawbone.

2D CAT images were compared with the Mimics images. CAT-scanned images were printed on film and were also provided with 2D slice information as well as 3D reconstructed rendering to be used for verification purposes. The window and threshold settings were optimised on the CT computer for each specific case study. It was of great value to have the 2D and 3D CAT-scanned film printouts for verification. It was also used for determining the patient's orientation, as well as dimensional inspection.

Regarding the pelvis case study, measurements in the xy-axis, from the CAT scan film at the -133 mm position were compared with the converted Mimics slice at approximately the same position. Measurements that were taken with the aid of a caliper, from the CAT scan film, and with the aid of the mouse position from the Materialise software were compared. The scale was determined for the CAT film images to be 4,35:1, thus 1 mm on the film, which actually represented 4,35 mm. Measurements were compared and varied 1 mm in 45 mm or about 2 %. A second measurement provided better results, 3,13 mm over a 280 mm distance, or a deviation of 1,1 %.

Measurements were also taken in the z-axis. A new scale was determined and the deviation proved to be 3,33 mm for a distance of 17,53 mm, or 19 %. It was not easy to find the same position to compare the dimensions and the variation could be due to that. It would also be due to the overlap of the scanned slice data. A comparison of the measurements was taken from the 3D constructions made by Morningside Clinic and compared to the 2D-slice position of the converted Mimics Data.

5 INDUSTRIAL CASE STUDIES

5.1 Internal Combustion Engine Piston - Industrial

5.1.1 Background

It was required to capture the internal geometry of a internal combustion engine (ICE) piston. This data would then be used to create the multiple split cores for a low-pressure casting process. A typical study where the geometry of an existing part needs to be used to create tooling for a manufacturing process. The plan was to capture the piston's inner geometry, produce the five multiple split core sections, build them on the SLA500 stereolithography machine in Quick Cast format, cast the core sections by using the investment casting process, and then do the final machining.

The CMM was also used to capture some of the piston's geometry. Another identical piston was cut in sections to display some of the hidden areas that could not be reached. The piston was not symmetrical and it was therefore necessary to capture the entire geometry of the complete piston. At that stage, the C.S.I.R.'s CAT scanner could not be used as it was still being repaired. The only other option was to scan it at one of the local hospitals.

Most medical CAT scanners are not capable of scanning metal materials. Only some materials can be CAT-scanned, such as Stainless Steel, Molybdenum, Titanium, Copper alloys and Aluminium. Most ICE pistons have a metal ring encased at the compression and oil ring region, during the casting process. This Aluminium reinforced metal ring provides the strength in a specific region where it is most required. Engineers apply this design technique so that both a strong and lightweight component can be produced. Other materials normally cause a scatter of X-rays and may result in artifacts or noise, which could have happened during this case study. The X-ray power also plays a large role. It was decided that the only option, at the time, was to manufacture a print of the inside of the piston.

Room Temperature Vulcanizing (RTV) rubber was poured into the piston after the section had been sealed at the gudgeon pin. The rubber print was removed after it had stabilized and hardened. The rubber print was hollowed out to allow the print to collapse and then it was removed from the piston.

The rubber print was then taken to Krugersdorp Hospital to be CAT-scanned. The 2D CAT-scanned data was again stored on microfloppies as part of a routine backup procedure. A lot of time was spent on touching up the 2D CAT-scanned images, since the rubber print had been hollowed out and displayed some casting flaws. More detail than required was also displayed on the rubber print, which was later removed. The 2D editing were necessary to obtain a usable 3D representation.

5.1.2 I.C.E. Piston Data Sheet:

	Description	Options/Units	Data
1	CT Image Names		Piston.001
2	Patient/Project Name		kolben.pat
3	Number of First Input Image		000
4	Number of Last Input Image		030
5	Number of First Output Image		000
6	CT or MRI	CT, MRI	CT
7	Horizontal No. of Image Pixels	0 to 65535 (265,512,1024)	512
8	Vertical No. of Image Pixels	0 to 65535 (265,512,1024)	512
9	Number of Images per File	(1)	1
10	File Swap Format (0,3)	0,3	CCELSC
11	Pixel Type	B,UB,S,US,L,UL,F	-
12	Inter Image Header Size	0	-
13	Add Value	0 to 4095	-
14	Scale Value	0 to 4095	-
15	Table Position	(mm)	0
16	Distance Between Slices	(mm)	1
17	Slice thickness	(mm)	1.2
18	Pixel Size SQ.	F.O.R./No. Hor. Pixels (mm)	
19	Gantry Tilt Angle	Degrees	0
20	Field of Reconstruction/View	(mm)	0.6
21	Number of Images		30
22	File Size of CAT Image	Kb	75
23	File Size of Converted Image	Kb	60
24	.3dd file size	Mb	4
25	.STL file size	Mb	4 & 36
26	RP Method	(SLA,FDM,OTHER)	SLA & FDM
27	.IGS file size	Mb	-
28	RP Slice file size	Mb	34
29	RP Download File size	Mb	32
30	Grow Time	Hour	6
31	Tip size	(T12, T25)	T12
32	Slice Thickness	(0.01", 0.014")	0.01"
33	Finishing Time	Hour	2
34	Processing Time	Hour	10
35	Data Retrieval Time	Hour	3
36	Total Cost	Rand	1950+500=2450

5.2 Motor Car Door Mirror Rubber Seal - Industrial

The geometry of a motor car door mirror rubber seal was required to produce injection mould tooling.

5.2.1 Background

The rubber seal was taken to Krugersdorp Hospital to capture the geometry. One millimetre thick slices were required to obtain sufficient detail of the seal's geometry. Three data sets of sixty slices each were made since this was the maximum number of slices that could be scanned at one time. The limitations were related to the computer processing capability, hard drive space and X-ray tube cooldown periods. The seal was aligned in two axes with the visual aids available on the CAT scanner. A flat section of foam was used to suspend and separate the seal from the scanner's table. This would be of help later during the data conversion and processing stages. CAT scanning was done at 130 kV.

The 2D CAT scanned data was processed and 3D reconstructions were made. The 1mm thick slices proved to be useful in producing smooth surface geometry, during the 3D-reconstruction process. Fig. 5.1, 5.2, 5.3 and 5.4 shows the 3D reconstructed images.

5.2.2 Images

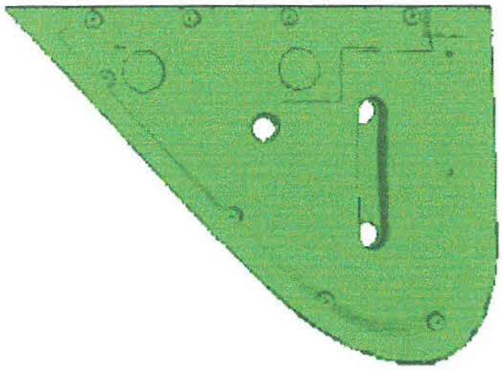

Figure 5.1 Motorcar door window rubber seal, rear view.

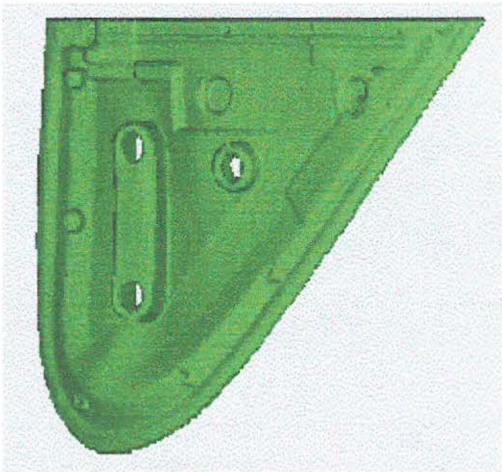

Figure 5.2 Motorcar door window rubber seal, frontal-right-hand view.

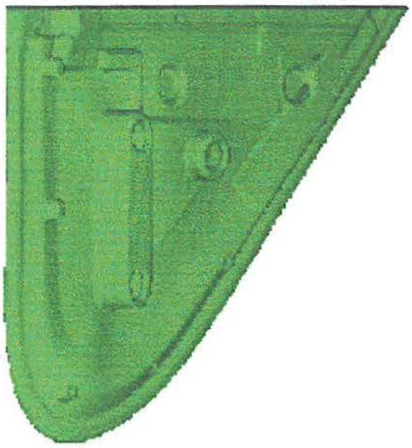

Figure 5.3 Motorcar door window rubber seal, frontal-left-hand view.

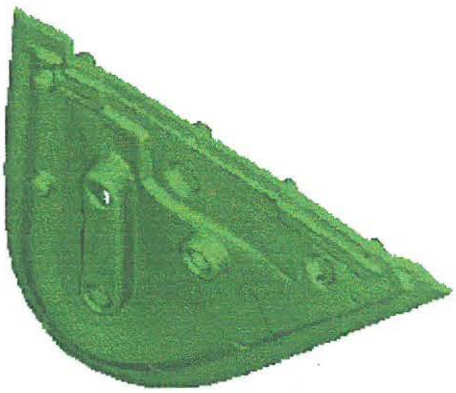

Figure 5.4 Motorcar door window rubber seal, frontal-top view.

5.2.3 Rubber Seal Data Sheet:

	Description	Options (Default)	Data
	CT Image Names		mirror.00
	Patient/Project Name		spiel.pat
	Number of First Input Image		mirror1.000 @ 34.5
	Number of Last Input Image		mirror1.147 @ 179.8
	Number of First Output Image		000
	CT or MRI	CT, MRI	CT
	Horizontal No. of Image Pixels	0 to 65535 (265,512,1024)	512
	Vertical No. of Image Pixels	0 to 65535 (265,512,1024)	512
	Number of Images per File	(1)	1
0	File Swap Format (0,3)	0,3	CCELSC
1	Pixel Type	B,UB,S,US,L,UL,F	-
2	Inter Image Header Size	0	-
3	Add Value	0 to 4095	-
4	Scale Value	0 to 4095	-
5	Table Position	(mm)	34.5
6	Distance Between Slices	(mm)	1
7	Slice thickness	(mm)	1.2
18	Pixel Size SQ.	F.O.R./No. Hor. Pixels (mm)	0.684
19	Gantry Tilt Angle	Degrees	0
20	Field of Reconstruction/View	(mm)	350
21	Number of Images		147
22	File Size of CAT Image	Kb	27
23	File Size of Converted Image	Kb	19-22
24	.3dd file size	Mb	0.234
25	.STL file size	Mb	8.9
26	RP Method	(SLA,FDM,OTHER)	-
27	.IGS file size	Mb	-
28	RP Slice file size	Mb	-
29	RP Download File size	Mb	-
30	Grow Time	Hour	-
31	Tip size	(T12, T25)	-
32	Slice Thickness	(0.01", 0.014")	-
33	Finishing Time	Hour	-
34	Processing Time	Hour	1
35	Data Retrieval Time	Hour	3
36	Total Cost	Rand	600+800=1200

5.3 Gearbox Housing - Industrial

Capturing the geometry of an existing part can play a critical role if this data can successfully be used for a finite element modelling (FEM) and casting simulation process analysis. The computer modelling and analysis method can thus be applied to assist in optimising the manufacturing process. A computer 3D model of the part, a gearbox housing, was required to perform an analysis and process modelling of a casting process. 3D CAD and STL files existed, but these files proved to be unacceptable for FEM and process analysis. The STL file was generated from the 3D CAD file. A new STL file generated from the CAT-scanning data could possibly solve the problem of the STL file generated from CAD data.

5.3.1 Background

The quarter scale SLA prototype was CAT-scanned by using the GE. CAT scanner at Hydromed Hospital, which is based in Bloemfontein. The 2D CAT slices were again stored on 4 mm DAT magnetic tape. 2D CAT images of various positions were stored on film for record-keeping purposes.

Fig. 5.5 shows a bottom view of the gearbox casing. Fig. 5.6 and 5.7 shows two different elevated views of the 3D reconstructed model. From these figures, one can clearly see the problems experienced by capturing insufficient geometry.

5.3.2 Images

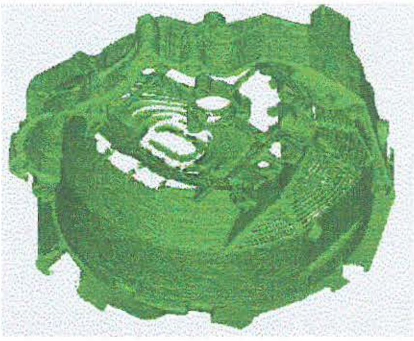

Figure 5.5 Gearbox housing, bottom view.

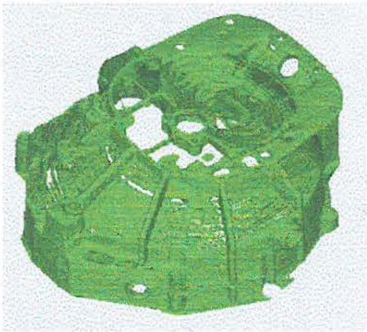

Figure 5.6 Gearbox housing, elevated frontal view.

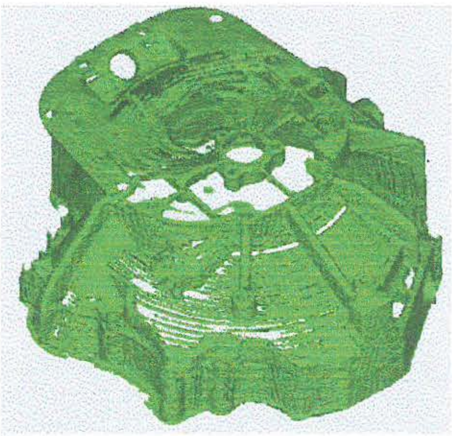

Figure 5.7 Gearbox housing, elevated rear view.

5.3.3 Gearbox Housing Data Sheet:

	Description	Options (Default)	Data
	CT Image Names		1s6I.*
	Patient/Project Name		1s6I
	Number of First Input Image		E6281S6I1.CT
	Number of Last Input Image		E6281S6I79.CT
	Number of First Output Image		1S6I1_1.000
	CT or MRI	CT, MRI	CT
	Horizontal No. of Image Pixels	0 to 65535 (265,512,1024)	512
	Vertical No. of Image Pixels	0 to 65535 (265,512,1024)	512
	Number of Images per File	(1)	1
0	File Swap Format (0,3)	0,3	CCGEADVA
1	Pixel Type	B,UB,S,US,L,UL,F	-
2	Inter Image Header Size	0	-
3	Add Value	0 to 4095	-
4	Scale Value	0 to 4095	-
5	Table Position	(mm)	0
6	Distance Between Slices	(mm)	1
7	Slice thickness	(mm)	1
8	Pixel Size SQ.	F.O.R./No. Hor. Pixels (mm)	0.47
9	Gantry Tilt Angle	Degrees	0
0	Field of Reconstruction/View	(mm)	240
1	Number of Images		79
2	File Size of CAT Image	kb	270-280
3	File Size of Converted Image	kb	11-23
4	.3dd file size	Mb	3.2 *.srf
5	.STL file size	Mb	17
6	RP Method	(SLA,FDM,OTHER)	SLA
7	.IGS file size	Mb	-
8	RP Slice file size	Mb	19
9	RP Download File size	Mb	16
0	Grow Time	Hour	6
1	Tip size	(T12, T25)	-
2	Slice Thickness	(0.01", 0.014")	0.01"
3	Finishing Time	Hour	3
4	Processing Time	Hour	2
5	Data Retrieval Time	Hour	2
6	Total Cost	Rand	=8*250=2000

5.4 Aluminium Foam - Industrial

This project was performed for a German engineering student who was completing his doctorate in engineering. The project was automotive-related. The aim of the project was to determine the geometry of the foam structure and relate it to the mechanical properties of the material.

5.4.1 Background

Exciting technological advances often first appear in the form of raw materials - the matter from which either components or entire future systems will be made. This is also true for a new type of rigid polyurethane foam developed at Sandia National Laboratories in Albuquerque, and it appears to be the case for the products of a new manufacturing process developed by scientists at the Office of Naval Research (ONR). In a programme sponsored by the ONR, researchers have come up with a low-cost method for manufacturing two types of ultra-light porous metals. The lightweight closed-cue and open-cue materials, which reportedly demonstrate excellent strength, heat dissipation, and blast-suppression properties, could end up some day be found in products ranging from critical aircraft components to bridges and buildings.

Work on lightweight metals is not something new. German and Japanese automobile manufacturers, such as Audi, are already using them in components that add structural strength to those products, and concept cars with frames and fenders made from these exotic materials have been seen at automobile shows. However, ONR researchers are probing new frontiers, both in the structural composition of their porous metals and in the range of their potential applications.

The closed-cell porous metals resemble an ordinary sponge. The cells are evenly sized and holes are spaced at regular intervals. The open-cell materials have an appearance similar to the randomly sized and spaced holes found in a sponge. The size of the holes can be varied to suit the intended use of the material. They actually have very different properties. The closed-cue foams would be very good to use for thermal insulation; measurements have shown a 400°C drop across an inch of foam. Potential uses are protecting ammunition magazines or to act as a flame retardant. The open-cell foams are actually useful for heat dissipation.

The Aluminium foam samples were prepared in Germany by the University of Erlangen. Two types of samples were prepared; cubical type shown by Fig. 5.10 and 5.11 and cylindrical type. The cylindrical foam samples were encased by 3mm thick, open-ended, Aluminium tube.

It was envisaged that this reverse engineering technology could be used to inspect the inner structure of the samples. The size and geometry of the inner pores or holes needed to be established. This geometric data could then be referenced with the mechanical properties of the specific samples, as the various samples were prepared with different hole size foam.

Images of the 3D reconstructed data are displayed in the following figures. Fig. 5.8 shows a section of three cylindrical samples with the difficulties experienced in this case study regarding the varying wall thickness. Fig. 5.9 shows a 2D CAT scanned image of 18 different cubical samples.

All the samples were scanned using three different CAT scanners with varying results as discussed in section 5.7.

5.4.2 Images

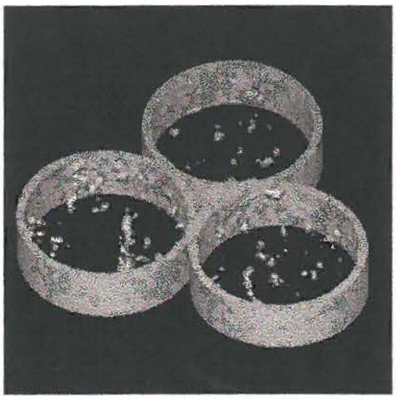

Figure 5.8 Aluminium foam suspended in a tube.

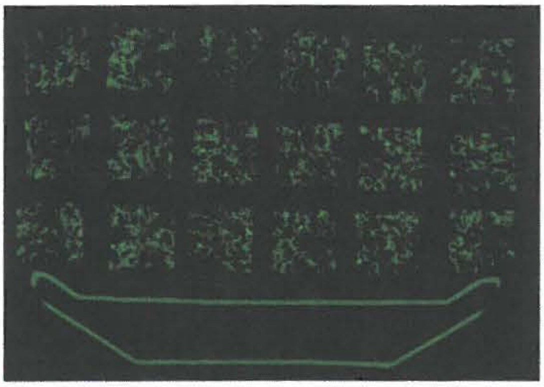

Figure 5.9 2D CAT-scanned image of Aluminium foam.

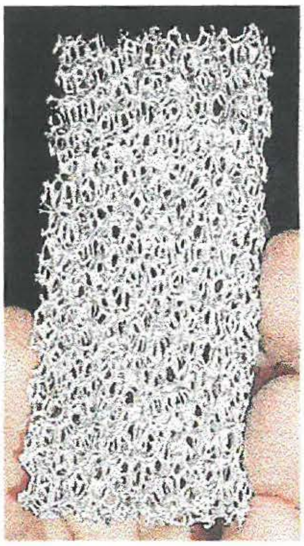

Figure 5.10 Image of the cubical Aluminium foam.

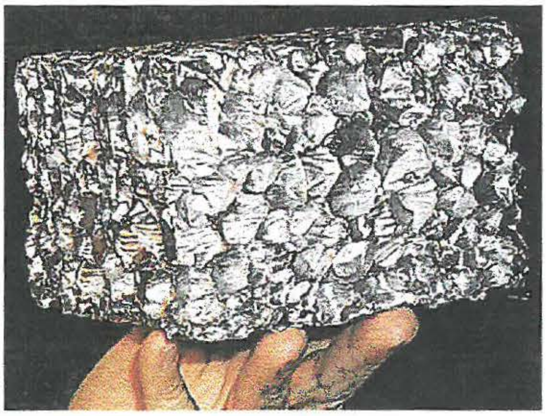

Figure 5.11 Image of the cubical Aluminium foam.

5.4.3 Aluminium Foam Data Sheet:

	Description	Options/Units	Data
	CT Image Names		Alfaom.00
	Patient/Project Name		Alfoam.pat
	Number of First Input Image		00
	Number of Last Input Image		50
	Number of First Output Image		Alfoam.00
	CT or MRI	CT, MRI	CT
	Horizontal No. of Image Pixels	0 to 65535 (265,512,1024)	512
	Vertical No. of Image Pixels	0 to 65535 (265,512,1024)	512
	Number of Images per File	(1)	1
0	File Swap Format (0,3)	0,3	Ccelcint
1	Pixel Type	B,UB,S,US,L,UL,F	-
2	Inter Image Header Size	0	-
3	Add Value	0 to 4095	-
4	Scale Value	0 to 4095	-
5	Table Position	(mm)	0
6	Distance Between Slices	(mm)	1
7	Slice thickness	(mm)	1
8	Pixel Size SQ.	F.O.R./No. Hor. Pixels (mm)	0.39
9	Gantry Tilt Angle	Degrees	0
0	Field of Reconstruction/View	(mm)	200
1	Number of Images		50
2	File Size of CAT Image	Kb	265
3	File Size of Converted Image	Kb	215
4	.3dd file size	Mb	7,*.srf
5	.STL file size	Mb	75
6	RP Method	(SLA,FDM,OTHER)	-
7	.IGS file size	Mb	-
8	RP Slice file size	Mb	-
9	RP Download File size	Mb	-
0	Grow Time	Hour	-
1	Tip size	(T12, T25)	-
2	Slice Thickness	(0.01", 0.014")	-
3	Finishing Time	Hour	-
4	Processing Time	Hour	16
5	Data Retrieval Time	Hour	3
6	Total Cost	Rand	=3500

5.5 Oxygen Face Mask - Industrial

5.5.1 Background

An industrial designer needed to design a new facemask with some features of an existing facemask. The aim of this study was to capture the geometry of an existing facemask and apply it in the design of a new oxygen face mask with additional features.

Krugersdorp Private Hospital was again approached to perform the CAT scanning. A series of coronal sections was produced. The data was retrieved and converted according to the data conversion procedure. The next step was to supply the data to the designer so that it could be used during the design process of the oxygen facemask.

This study shows a typical application of the technology where the geometry of an existing item can be used to produce a new superior product.

Fig. 5.12 shows an isometric view of the CAT scanned slices in IGES format. Fig. 5.13 shows an isometric view of the 3D reconstructed data but in STL format. Fig. 5.14 and 5.15 shows 2D CAT scanned images as the oxygen facemask was placed on the CAT scanner's table. Fig. 5.16 shows an auxiliary view to explain the type of undercut and thin sections in the nose region. The difficulties experienced are discussed in section 5.6.

5.5.2 Images

Figure 5.12 Cross sections of the mask.

Figure 5.13 CAT-scanned 3D reconstruction.

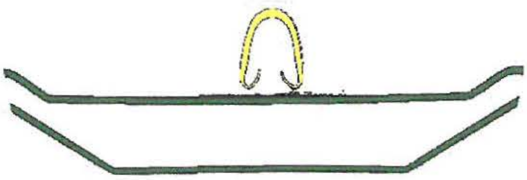

Figure 5.14 2D CAT-scanned Slice 119 of the face mask (yellow section)

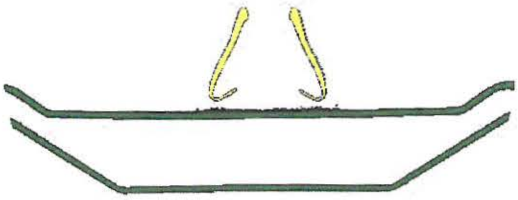

Figure 5.15 2D CAT-scanned Slice 89 of the face mask (yellow section)

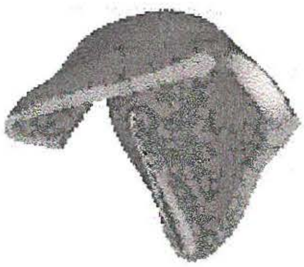

Figure 5.16 Face mask undercut section.

5.5.3 Oxygen Face Mask Data Sheet:

	Description	Options/Units	Data
	CT Image Names		CT1-60
	Patient/Project Name		mask.pat
	Number of First Input Image		1
	Number of Last Input Image		60
	Number of First Output Image		000
	CT or MRI	CT, MRI	CT
	Horizontal No. of Image Pixels	0 to 65535 (265,512,1024)	512
	Vertical No. of Image Pixels	0 to 65535 (265,512,1024)	512
	Number of Images per File	(1)	1
0	File Swap Format (0,3)	0,3	0
1	Pixel Type	B,UB,S,US,L,UL,F	Ccelcint
2	Inter Image Header Size	0	-
3	Add Value	0 to 4095	-
4	Scale Value	0 to 4095	-
5	Table Position	(mm)	0
6	Distance Between Slices	(mm)	3
7	Slice thickness	(mm)	3
8	Pixel Size SQ.	F.O.R./No. Hor. Pixels (mm)	0.3
9	Gantry Tilt Angle	Degrees	0
0	Field of Reconstruction/View	(mm)	150
1	Number of Images		60
2	File Size of CAT Image	Kb	55-60
3	File Size of Converted Image	Kb	16
4	.3dd file size	Mb	0.645
5	.STL file size	Mb	4.6
6	RP Method	(SLA,FDM,OTHER)	-
7	.IGS file size	Mb	-
8	RP Slice file size	Mb	-
9	RP Download File size	Mb	-
30	Grow Time	Hour	-
31	Tip size	(T12, T25)	-
32	Slice Thickness	(0.01", 0.014")	-
33	Finishing Time	Hour	-
34	Processing Time	Hour	5
35	Data Retrieval Time	Hour	2
36	Total Cost	Rand	=7*100+2500=3200

5.6 Discussion of Industrial Case Studies

5.6.1 Advantages

5.6.1.1 Geometric Complexity

This reverse engineering (RE) method was successfully applied, in the case of the oxygen facemask, to supply the industrial designer with unique results. Again, this method proved to be the only RE method to capture the particular geometry. The mask was made of Silicon elastomer. No contact type reverse engineering method could be used to capture the mask's geometry without compromising spatial accuracy due to the surface displacement. The mask would have deformed under the touch probe during sampling of 3D co-ordinate points. 3- and 4-axis laser-scanning devices could also not be used due the facemask's geometry. The facemask geometry featured a deep undercut where the laser would not be able to enter. Accuracy again did not prove to play a critical role in the project, which made the CAT- scanning method the ideal method for reverse engineering.

The ICE piston geometry was also of such a nature that the normal touch probe or laser scanning methods could not be used. A flexible elastomer core was made of the internal geometry to simplify the reverse engineering process.

In the case of the Aluminium foam, the CAT scanning reverse engineering technique is the only non-destructive method that can easily capture the internal geometry. Another method is by using acoustic sound techniques, but this process poses complications of its own where the internal and external surface geometry should preferably be similar to be successful.

5.6.2 Process Limitations

5.6.2.1 RE Process Selection

Proper project planning is required for successful reverse engineering. Proper planning could make the difference between the possibility of capturing data and actually making the data work. Planning allows one to capture the correct data required for the applicable downstream process.

Various reverse engineering methods exist as described in section 2.5. It is very important to determine the full requirements in order to select the appropriate RE method. Another important factor is the type and form of input and output that is required. The old cliché can be applied in this case, namely "Horses for Courses".

If data manipulation is required for a certain part, a different route and method may be followed, compared to the normal data-capturing method. The two main applications of reverse engineering are direct copy-related work or a modified copy of the original. Other downstream applications of the results of RE could be a finite-element modelling (FEM) analysis, a casting or manufacturing process simulation, an identical scaled prototype, tooling or a modified copy of the original.

It may be better to scan the manufacturing tool, if it is available and if it is the final product required. If the tool itself is not available, proper planning is required to achieve the final product. Tooling often incorporates fine and subtle detail required for successful manufacturing, which may be critical to capture.

5.6.2.2 Material Properties

The material densities and atomic numbers are important factors that could affect the CAT-scanning process. During the image processing stage, the grey scale tolerance band, or threshold, can be adjusted. In this instance, the threshold setting, type of material and material cross-sectional wall thickness play a cardinal role. The threshold can easily be adjusted to vary the wall or cross section during the image-conversion process. The threshold can be increased to such an extent that the 3,5 mm wall thickness can be reduced to 2 mm. It is therefore important that some form of reference or verification is implemented.

Any imperfection in the sample will also be captured with this method. A fair amount of editing can be applied to solve this problem. If the material cross section is too thin or if the material density is too low, a poor CAT image will be generated. To improve poorly captured data, the threshold could be increased.

It is again clear that the material used to make the part plays a major role. The SLA gearbox prototype was made of an epoxy polyester. Measurements were taken of the part's wall thickness and these were compared to measurements taken from the CAT scan images. In general, the CAT scan images proved to be 0,4 to 2 mm thinner than the actual part. Again, the threshold was set to the optimum. Clearly, the CAT scanner settings (kVA & mA) were not optimised for the gearbox prototype, being made of SLA material. A lot of detail can be lost at the thinner wall sections, as can be seen from the generated 3D images during the gearbox case study. Sections of the part being scanned can become invisible to the CAT scanner if the (mA) setting is too high, especially when the part's material density is low. The motorcar mirror rubber seal study confirms this.

The Aluminium foam materials were prepared in cubes and cylindrical volumetric shapes. The cylindrical shapes were suspended in a cylindrical tube. The tube thickness was about 3 mm. Some of the foam sections were less than 0,3 mm thick. Due to the great variation in wall thickness, the cylindrical sections could not be processed successfully.

5.6.2.3 Software & Hardware

STL data manipulation tools are required that can perform Boolean operations, section 3D STL geometry, fix and verify STL data, as well as tools that can generate machine tool paths from STL data. STL format is the most common data format obtainable from RE, and it is therefore important to have the correct software programs that can manipulate STL format files.

The STL file size was again not manageable by lower-level PC hardware. Only a 5mm thick section of one cubic Aluminium foam sample was used to generate a STL file size of 25Mb.

5.6.2.4 CAT-scanning Settings

The CAT-scanning settings play a critical role in the generation of successful results. The Aluminium foam was scanned at three different venues, with varying results. 2D CAT images were checked during scanning. The window settings were optimised on the CT computer. The kVA and mA settings play an even larger role with regard to penetration and differentiation. The CAT scanner's type of sensors also affects the image quality during the scanning process.

During the Aluminium foam study, the CAT scanner settings were satisfactorily set to penetrate the thicker tube, but were too high to capture the thinner internal thin walled sections. It appeared almost like an over-exposed photograph. Fig. 5.8 shows this clearly. The cubical sections were scanned and processed successfully. One cube was selected and a STL file was generated.

CAT scanner settings should be considered with regards to the material properties and geometry. Methods of determining the optimal scanning settings are not always possible with medical CAT scanners as with industrial CAT scanners.

6 BIOLOGICAL CASE STUDIES

6.1 Avocados - Industrial/Biological

6.1.1 Background

This case study was performed for a group of C.S.I.R. food technologists. The study was based on a similar case that had been performed with nuts in the USA. The aim of this study was to separate the fat-rich areas from the water-rich areas within the avocado, as an indication of the stage of the ripening process. The separation is normally done by destroying the avocado in order to determine the stage of ripeness. The C.S.I.R.'s food technologists hoped to develop a non-destructive evaluation method to determine the ripeness of the avocado. This same technique would then be used to analyse other fruit such as mangos. The avocados were marked and placed in a fixture. Three ripe avocados were placed in the right hand column. Twelve avocados at different stages of ripeness were selected. Refer to Fig. 6.1 and 6.2.

Pretoria East Hospital was again approached to perform the CAT scanning. A series of axial sections were produced. The data were retrieved and converted. The next step was to separate the fat-rich areas from the water-rich areas. The water-rich areas were the regions of interest.

Digital images produced as a result of CAT scanning consist of pixels. Each pixel represents a part of the component that is scanned. The pixels are also made up of different Grey scale values, better known as a Hounsfield Unit (HU). This phenomenon was used to separate the water-rich areas from the fat-rich areas. The Hounsfield Unit for pure water is 0, while that of air is -1000. The Hounsfield theory is described in section 2.6.5. Isolation of the water-rich area was achieved by setting the threshold bandwidth to only include pixels with approximately 990 to 1010 Materialise Units, listed in Table 6.1. The Materialise software's units are 1000 units more than the normal Hounsfield Unit. A 20-units tolerance band was used. The avocado's total volumes were determined when the threshold setting was 957 units.

6.1.2 Conclusion

This unique method was successfully applied to supply the food technologists with the required results. The method proved to be the only non-destructive method known to perform the analysis.

The volumes and areas of dispersion of the water-rich areas, as well as of the entire avocado were determined for every avocado. The food technologists further manipulated the data that showed a clear trend. This process proved to be helpful towards solving the prediction regarding the avocado's ripeness stage. Avocados could be scanned on a routine basis in order to predict the ideal ripeness stage. Environmental conditions influence the ripening process and complicate the ripening prediction. This case study opened a brand new field of application for this unique combination of technologies. Biological applications can now be added to the medical, industrial and fossil-related fields of applications.

In the following table the mass and volumetric data are listed:

Table 6.1 Avocado Mass & Volumetric Data

Avocado Reference	Original Mass (Gram)	Total Volume (mm^3)	Water-rich Volume (mm^3)
2 (green) row 2 column 1	299.13	285196	32736
3 (green) row 3 column 1	303.65	283934	22351
4 (green) row 1 column 2	277.85	280365	17893
5 (green) row 2 column 2	290.17	278140	14342
6 (green) row 3 column 2	311.41	293161	27504
8 (green) row 1 column 1	336.50	355902	12883
10 (green) row 1 column 3	256.02	282911	21972
12 (green) row 2 column 3	272.72	257097	14684
13 (green) row 3 column 3	217.72	207626	8024
14 (ripe) row 1 column 4	265.02	230853	26589
15 (ripe) row 2 column 4	272.72	230994	21502
16 (ripe) row 3 column 4	217.72	278660	72146

6.1.3 Images

Figure 6.1 Isometric view of several avocados' water-rich areas.

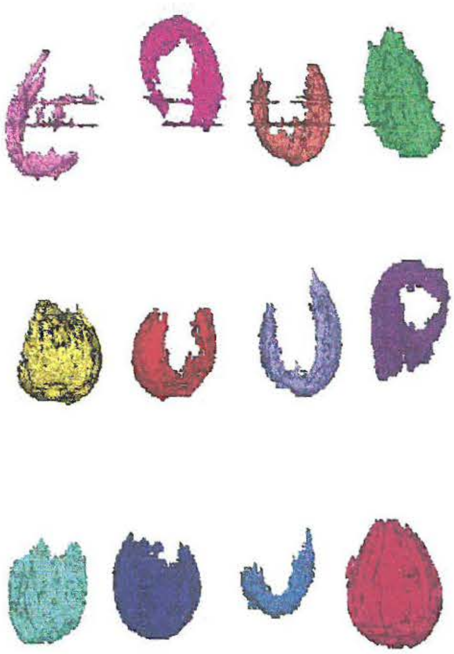

Figure 6.2 Front view of several avocados' water-rich areas.

6.1.4 Avocado Data Sheet:

	Description	Options/Units	Data
	CT Image Names		Avos.00
2	Patient/Project Name		Avos.pat
3	Number of First Input Image		212
4	Number of Last Input Image		-254
5	Number of First Output Image		000
6	CT or MRI	CT, MRI	CT
7	Horizontal No. of Image Pixels	0 to 65535 (265,512,1024)	512
8	Vertical No. of Image Pixels	0 to 65535 (265,512,1024)	512
9	Number of Images per File	(1)	1
10	File Swap Format (0,3)	0,3	0
11	Pixel Type	B,UB,S,US,L,UL,F	Toshiba
12	Inter Image Header Size	0	-
13	Add Value	0 to 4095	-
14	Scale Value	0 to 4095	-
15	Table Position	(mm)	-254
16	Distance Between Slices	(mm)	3
17	Slice thickness	(mm)	3
18	Pixel Size SQ.	F.O.R./No. Hor. Pixels (mm)	0.7
19	Gantry Tilt Angle	Degrees	0
20	Field of Reconstruction/View	(mm)	380
21	Number of Images		150
22	File Size of CAT Image	Kb	521
23	File Size of Converted Image	Kb	10-40
24	.3dd file size	Mb	2.5 ea.
25	.STL file size	Mb	-
26	RP Method	(SLA,FDM,OTHER)	-
27	.IGS file size	Mb	-
28	RP Slice file size	Mb	-
29	RP Download File size	Mb	-
30	Grow Time	Hour	-
31	Tip size	(T12, T25)	-
32	Slice Thickness	(0.01", 0.014")	-
33	Finishing Time	Hour	-
34	Processing Time	Hour	5
35	Data Retrieval Time	Hour	4
36	Total Cost	Rand	=9*100+300=1200

7 FUTURE APPLICATIONS AND RECOMMENDATIONS

7.1 Technology Transfer to Industry

The reaction of all the people involved in the project was overwhelming. National and Transvaal Museums, Krugersdorp Private Hospital, Southern Implants, SGI representatives and visitors to C.S.I.R., TCT Centre showed great interest in this technology.

South Africa has about 122 CAT- and 39 MRI-scanning devices. The scanning infrastructure is therefore already in place and some are accessible. The market must however still realise the need for and benefits of this technology. The benefit of this technology is obvious, but the market must still be educated for this first-world product. The market target area will be anthropology- and mostly medical-oriented.

The results of this project open brand new market opportunities in South Africa:

1. The application of this product will reduce the risk factor related to the planning of surgical operations and other medical procedures.
2. The application of this product will be to replicate valuable fossils to be used for educational purposes. Another output of this project was to establish a nation-wide network and to set up scanners to effectively convert the scanned data. This network will be crucial for the successful exploitation and application of the technology.

7.2 Commercialisation

A four-pronged approach should be followed.

1. Firstly, the approval of bodies such as the Representative Association of Medical Schemes (RAMS), SANLAM, Old Mutual and the Medical Research Council (MRC) would be of great value.
2. The second part of the approach should be to form alliances with the major medical product or equipment manufacturers such as TECMED, GE, Siemens and Toshiba. Support from their side can lead to the establishment of a full-time medical service centre.
3. The third part of the approach should be to obtain the support and recommendations of the various medical specialists and their professional bodies. Specialist input is highly regarded by the bodies mentioned in Point 1. and they often drive the decision-making process.
4. The fourth part of the approach should be to present this technology to the various educational institutions. This technology will very quickly and easily be accepted by the newer generation.
5. The following factors will play a large role in the technology transfer and commercialisation phases:

- MRC backing and process approval.
- RAMS coding for the procedure called pre-operation hard modelling for surgical planning or simply pre-operation hard modelling scanning.
- Presentations at related departments at technikon and university level.
- Local and international publications in various magazines and media.

7 REFERENCES

[1] 3D Systems Internet - http://www.3dsystems.com

[2] Brewer, Dr S. Body Facts, 1996.

[3] Brown, D. Image3 LLC, Velocity TM V2.0.

[4] Chartoff, R. P., Lightman, A.J., Schenk, J.A., Comb, J.W., Priedman, W.R. & Turley, P.W. The Fifth International Conference on Rapid Prototyping, Control Parameters and Material Selection for Fused Deposition Modelling, 163-170, 1995.

[5] Chartoff, R. P., Lightman A.J., Schenk, J.A., Swaelens, B. & Kruth, J.P. The Fourth International Conference on Rapid Prototyping. Medical Applications of Rapid Prototyping Techniques, 107-120, 1993.

[6] Chartoff, R.P., Lightman, A.J. The Sixth International Conference on Rapid Prototyping. Applications of Rapid Prototyping to Surgical Planning: A Survey of Global Activities, 43-50, 1995.

[7] Chartoff, R.P., Lightman, A.J., Schenk, J.A., Adachi, J., Hara, T., Kusu, N. &. Chiyokura, H. The Fourth International Conference on Rapid Prototyping. Surgical Simulation-using Rapid Prototyping, 135-142, 1995.

[8] Chartoff, R. P., Lightman, A.J., Schenk, J.A. &. Rovic, J.S. The Fifth International Conference on Rapid Prototyping, an Additive Fabrication For High Speed Production of Artificial Limbs, 47-56, 1995.

[9] Chartoff, R. P., Lightman, A.J., Schenk, J.A., Jacob, A.L., Hammer, B., Niegle, G., Lambrecht, T., Schiel, H., Steinbrich, W. & Hunzicker, M. The Fourth International Conference on Rapid Prototyping. First Experience in the Use of Stereolithography in Medicine, 121-134, 1993.

[10] Chartoff, R. P. & Lightman, A.J.. The Sixth International Conference on Rapid Prototyping. Ct-assisted Solid Free-form Fabrication, 267-274. 1995.

[11] Crech-Cumbo, R. RGC Engineering Sales Div. (Pty.) Ltd.

[12] Desk Artes – Software Package.

[13] Dorling Kindersley Ltd., The Ultimate 3D Skeleton, 1996

[14] Dorling Kindersley Ltd., The Ultimate Human Body 2.0, 1996.

[15] Duncan, M. Thrinaxodon and Lystorsaurus introduction, E-mail, 1998.

[16] Grollier, Prehistoria Multimedia CD, 1998.

[17] Hesse, Y. & Oware, J. ALIAS WAVEFRONT.

[18] Machet, A. Fossil Replication using CAT scanning, CAD and Stereo Lithography, 1996.

[19] Proceedings of the Industry of Mechanical Engineering, Journal of, Vol. 206h1, P43-P46, 1992.

[20] Raindrop Geometry – Software Package.

[21] Rapid News TCT North American version, Vol.2, No.7, P52, P53, Dec.1997.

[22] Rapid News TCT North American version, Vol.2, No.5, P46-P51, July/Aug.1997.

[23] Rapid News TCT North American version, Vol.2, No.3, P34-P39, May 1997.

[24] Rapid News TCT UK version, Vol.4, No.6, P32-P39.

[25] Rapid News TCT North American version, Vol.2 No.2, P27,29,51, March 1997

[26] Rapid News TCT North American version, Vol.2, No.6, Oct.1997.

[27] Rapid Prototyping Association of the Society of Manufacturing Engineers, Dr K. T. McAloon, Rapid Prototyping Technology: A unique approach to the diagnosis and planning of medical procedures, 1997.

[28] Rapid Prototyping Report, Cad/cam Publishing Inc., Vol.7, No.2, P4, P5

[29] Drs Rogalla, P., Mutze, S. & Hamm, B. Body CT, State of the Art, p.IX-XI, 1996.

[30] Rowe, T., Carlson, W. & Bottorff, W. Thrinaxodon: Digital Atlas of the Skull, The University of Texas Press. CD-ROM, 1993.

[31] Schenker, R. Report on the Step Proposal for Rapid Prototyping and Reverse Engineering, 1996.(C.S.I.R. Internal Report)

[32] SGI COSMOS- http://www.cosmos.com

[33] Solid View – Software Package

[34] Stratasys Internet - http://www.stratasys.com

[35] Swaelens, B. &. Boeykens, L., Materialise, User's Guide CT- Modeller System, version 5., 1997.

[36] The Edge, Vol. iv, No. 4, 3D Systems, P3-P9, 1996.

[37] Uvaron, E.B. & Isaacs, A. Dictionary of Science, 7th. Edition, P241, 367, 452, 486, 487, 510,.1993.

[38] Venter, M. Hydro CAD-CAM, Matra Datavision.

[39] Winkler, K. Inventions & Inventors - Radiology, 1996.

[40] Young, C.E. Rapid News - North America, Time-Compression Technologies - the Competitive Edge, Volume 1, Number 1, 6-10, 1996.

APPENDIX 1

Journal of Science publication

Novel combination of reverse engineering and rapid prototyping in medicine

R. Schenker[a*], D.J. de Beer[b], W.B. du Preez[c], M.E. Thomas[c] and P.W. Richter[c]

The technologies of reverse engineering and rapid prototyping are emerging as useful new tools in medicine. One application is of particular interest in orthopaedic, dental and reconstructive surgery. It involves the imaging, modelling and replication (as a physical model) of a patient's bone structure. The models can be viewed and physically handled before surgery, which is of great benefit in evaluation of the procedure and implant fit in difficult cases. The technology promises lessened risk to the patient and reduced cost through saving in theatre time. A case study is presented, involving hip replacement in a patient who had experienced severe bone loss through osteoporosis. Such applications are a further step towards the development of a new generation of customized bone implants.

The technologies respectively labelled reverse engineering and rapid prototyping have developed rapidly in recent years.[1] While the major applications are found in the fields of engineering and design, these technologies are emerging as useful new tools in medicine.[2–6] Reverse engineering and rapid prototyping are of particular interest in skeletal repair, where physical models of bone structure are produced for planning surgical procedure and evaluation of implant fit. The process typically involves imaging bone structure using computer axial tomography (CAT) scans, conversion of the two-dimensional slice data to three-dimensional computer-aided design (CAD) models and manufacture of physical models using any of a number of rapid prototyping (RP) technologies. The primary concerns at present include interpretation of images, discrimination of tissue types and dimensional accuracy. This article describes current capability through a case study involving hip replacement in a patient who had experienced severe bone loss through osteoporosis.

Capturing geometric shapes of existing physical parts or components in a format that can be used for further engineering is the basis of reverse engineering. Two- or three-dimensional data are subsequently used with some form of post-processing. There are at present some 30 shape-digitising methods that can be broadly grouped as contact or non-contact. The contact group includes touch probe and destructive methods, whereas the non-contact group includes laser, computer axial tomography, optical and ultrasonic methods. For medical applications, CAT (X-ray) and magnetic resonance imaging (MRI) are particularly important as data acquisition methods for reverse engineering.

The two-dimensional CAT or MRI slice images are converted to three-dimensional data, in the case described here as Stereolithography type (STL) files for rapid prototyping purposes. The STL file is a triangulate surface wire mesh of the CAD model and is the basis of subsequent rapid prototyping. The accuracy of models generated from CAT or MRI data is subject to the interpretation of images, discrimination between tissue types, dimensional accuracy and spacing of slices.

Various rapid prototyping systems have been developed in recent years, with regular improvements in quality and production speed. Most systems involve deposition or machining of material in sequential, patterned layers gradually to build a structure. The benefits of rapid prototyping include enhanced visualization capability, reduced development cost, early detection of design flaws and limited part testing prior to conventional prototyping. In the medical field, early applications centred on models of bone or other tissue which are used by surgeons to plan and perform complex procedures before actual surgery. Apart from obvious benefits to the patient, the approach promises significant savings through reduced theatre time and risk. Areas where this technology has been successfully applied include maxillofacial reconstruction, pelvic fractures, spinal trauma, orthodontic surgery, nose reconstruction and models of soft tissue structures such as cardiovascular systems.

For the work reported here, a commercial Stratasys fused deposition modelling machine was used to produce models in ABS polymer. The RP process normally starts with a three-dimensional solid or surface CAD model, or in this case two-dimensional CAT or MRI images, converted to STL type format. The STL model is sliced into horizontal layers and parameterized. Parameters include road width, slice thickness, fill type, and start and end positions.[1] Construction of the model then proceeds according to these criteria. Temporary structures are sometimes added to the model during manufacture to allow deposition of unsupported or suspended sections. These are removed on completion of the model.

Case study: hip replacement

A patient required replacement of the left hip joint. The procedure was complicated by the fact that the bone had deteriorated badly as a result of osteoporosis. A study was conducted with the orthopaedic surgeon to capture the bone structure of the hip region to facilitate assessment of the viability of the procedure.

The patient was examined using a Toshiba Spiral X-Vision/GX CAT scanner. The clinic then prepared a three-dimensional rendering of the scanned area. The information was prepared in two forms, as 3-mm-thick slices at 3 mm and 0.5 mm spacing, respectively, to evaluate the difference. The surgeon was particularly interested in the left side of the pelvis. For a successful hip replacement, sufficient bone structure is required at the posterior side of the acetabulum. It was clear from the CAT scan that the anterior side of the pelvis did not have sufficient bone structure.

The two-dimensional slice information, three-dimensional rendering and film images were supplied to verify mutual consistency. In the x-y (slice) plane, dimensional agreement between film and images after scaling was approximately 1–2 %. Along the z-axis the uncertainty was greater, approaching the slice thickness in magnitude.

Bone particles were incorporated in the soft tissue at the site and discrimination between viable and suspended bone was difficult, even using a cadaver left side pelvis as reference. The pelvis and femur

[a] Mandi's Technologies, P.O. Box 2715, Rant en Dal, Krugersdorp, 1740 South Africa.
[b] Department of Mechanical Engineering, Free State Technikon, Bloemfontein, South Africa.
[c] Manufacturing and Materials Division, CSIR, P.O. Box 395, Pretoria, 0001 South Africa.
*Author for correspondence. E-mail: rudis@ibi.co.za

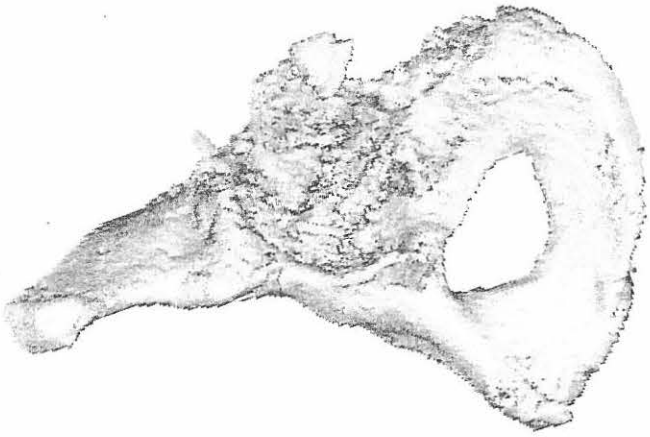

Fig. 1. Rendering of viable bone structure of the damaged pelvis following data reduction.

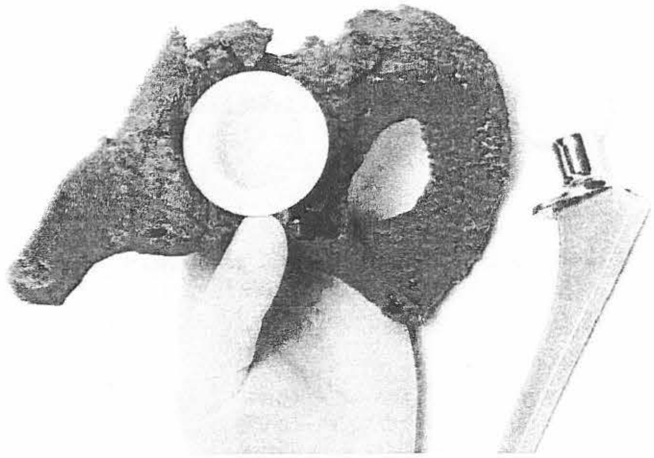

Fig. 2. Completed model with acetabular cup and femoral component to give scale.

were hardly recognizable in certain areas. The data were processed and subsequently reviewed with the surgeon prior to replica production. A rendering of the viable bone structure is shown in Fig. 1, indicating the extent of osteoporotic bone loss.

Data were converted to STL format and used with Stratasys QuickSlice™ software to generate horizontal slices with automatic support generation in an SML (machine control) file. The structure was grown in ABS polymer at 0.25-mm layer thickness and finished by removing supports (Fig. 2). The model was delivered to the orthopaedic surgeon, who used it for detailed planning and verification of the surgical procedure.

Implication for new generation implants

Applications beyond bone modelling are already envisaged. While present work is focused on the replication of bone structure as physical models, it is possible to produce not only such models but also custom implants to fit the modelled defects. This requires incorporation of a further new technology, that of prototyping directly in bioceramic material. Early work in this regard is described in a companion article.[6] The primary concern here is the internal design of the bioceramic structure, which has to meet biological rather than dimensional requirements for bone and tissue ingrowth.[7,8] The achievement of external dimensional accuracy is a matter of engineering.

At a more advanced level is the loading of biologically active molecules such as bone morphogenetic proteins onto implants.[9] This technology is not yet commercially available but holds the promise of greatly promoting healing of skeletal defects. In combination, the various technologies described here represent a comprehensive advance in bone tissue engineering.

The accuracy of conversion of two-dimensional image slices to three-dimensional CAD models is a limitation at present. The use of dense scan spacing, in this case 0.5 mm as opposed to 3 mm spacing, was considered beneficial in this regard. Film images were captured along with digital scan data and these were used to verify the accuracy and dimensions of rendered images. Access to scanning equipment for data retrieval requires careful management, as these instruments are in great demand, and data should ideally be captured in a parallel system or retrieved during off-peak hours. The turnaround time and cost are still high, due mainly to the absence of automated procedures, but a significant reduction in both turnaround time (about three days) and cost appears possible in routine application.

The studies reported to date indicate that although the application of rapid prototyping technology in medicine is relatively underdeveloped, it is already justified in certain cases.

We wish to acknowledge contributions from the following: A.N. Kirkbride, I. Dymond, M. Fox, M. Botma, R. Beyer, B. Swaelens, F. Mosweu, P.S. Maswanganye, L. Maphoso and U. Ripamonti.

1. Jacobs P.F. (1996). *Stereolithography and other RP&M Technologies: from Rapid Prototyping to Rapid Tooling*. Society for Manufacturing Engineers, Dearborn, Mich.
2. Chartoff R.P. and Lightman A.J. (1995). Applications of rapid prototyping to surgical planning: a survey of global activities. *Proceedings of the Sixth International Conference on Rapid Prototyping*, pp. 43–50. University of Dayton, Ohio.
3. Chartoff R.P., Lightman A.J., Schenk J.A., Adachi J., Hara T., Kusu N. and Chiyokura H. (1993). Surgical simulation using rapid prototyping. *Proceedings of the Fourth International Conference on Rapid Prototyping*, pp. 135–142. University of Dayton, Ohio.
4. Chartoff R.P., Lightman A.J., Schenk J.A., Jacob A.L., Hammer B., Niegle G., Lambrecht T., Schiel H., Steinbrich W. and Hunzicker M. (1993). First experience in the use of stereo lithography in medicine. *Proceedings of the Fourth International Conference on Rapid Prototyping*, pp. 121–134. University of Dayton, Ohio.
5. Chartoff R.P., Lightman A.J., Schenk J.A., Swaelens B., Kruth J.P. (1993). Medical applications of rapid prototyping techniques. *Proceedings of the Fourth International Conference on Rapid Prototyping*, pp. 107–120. University of Dayton, Ohio.
6. Richter P.W., Thomas M.E. and Van Deventer T. (1999). Macroporous hydroxyapatite bioceramics by solid freeform fabrication: towards custom implants. *S. Afr. J. Sci.* **95**, 325–326.
7. Thomas M.E., Richter P.W., Van Deventer T., Crooks J. and Ripamonti U. (1999). Macroporous hydroxyapatite bioceramics for bone substitute applications. *S. Afr. J. Sci.* **95**, 359–362.
8. Ripamonti U., Crooks J. and Kirkbride A.N. (1999). Sintered porous hydroxyapatites with intrinsic osteoinductive activity: geometric induction of bone formation. *S. Afr. J. Sci.* **95**, 335–343.
9. Ripamonti U., Ma S. and Reddi A.H. (1992). The critical role of geometry of porous hydroxyapatite delivery system in induction of bone by osteogenin, a bone morphogenetic protein. *Matrix* **12**, 202–212.

The world is too big for us. Too much is going on, too many crimes, too much violence and excitement. No matter how hard you try, you get behind in the race. It's a strain to keep pace. Science empties its discoveries on you so fast that you stagger beneath them.
Atlantic Journal (June 1833)